

Aalborg Universitet



**AALBORG UNIVERSITY**  
DENMARK

## Integration of Large-scale Consumers in Smart Grid

Rahnama, Samira

*Publication date:*  
2015

*Document Version*  
Accepted author manuscript, peer reviewed version

[Link to publication from Aalborg University](#)

*Citation for published version (APA):*  
Rahnama, S. (2015). *Integration of Large-scale Consumers in Smart Grid*. Department of Electronic Systems, Aalborg University.

### General rights

Copyright and moral rights for the publications made accessible in the public portal are retained by the authors and/or other copyright owners and it is a condition of accessing publications that users recognise and abide by the legal requirements associated with these rights.

- Users may download and print one copy of any publication from the public portal for the purpose of private study or research.
- You may not further distribute the material or use it for any profit-making activity or commercial gain
- You may freely distribute the URL identifying the publication in the public portal -

### Take down policy

If you believe that this document breaches copyright please contact us at [vbn@aub.aau.dk](mailto:vbn@aub.aau.dk) providing details, and we will remove access to the work immediately and investigate your claim.

Samira Rahnama

# Integration of Large-scale Intelligent Consumers in Smart Grid



**AALBORG UNIVERSITY**  
DENMARK



Integration of Large-scale Intelligent Consumers in Smart Grid  
Ph.D. Thesis

ISBN: 978-87-7152-062-0  
April 2015

Copyright 2012-2015 © Samira Rahn timer

# Contents

<b>Contents</b>	<b>III</b>
<b>Preface</b>	<b>V</b>
<b>Abstract</b>	<b>VII</b>
<b>Synopsis</b>	<b>IX</b>
<b>Thesis Details</b>	<b>XI</b>
<b>1 Introduction</b>	<b>1</b>
1.1 Motivation . . . . .	1
1.2 Background and State of the Art . . . . .	3
1.3 Objectives . . . . .	11
1.4 Contributions . . . . .	11
1.5 Outline of the Thesis . . . . .	13
<b>2 Aggregator Design</b>	<b>15</b>
2.1 Hierarchical Setup . . . . .	15
2.2 Model of Consumers and Constraints . . . . .	17
2.3 Objective Function at the Aggregator . . . . .	24
2.4 Information Flow . . . . .	27
2.5 Interactions Between the Aggregators and the Grid Operator . . . . .	28
2.6 Summary . . . . .	28
<b>3 Proposed Robust Design</b>	<b>31</b>
3.1 Model Predictive Control . . . . .	31
3.2 Feedback Mechanism . . . . .	33
3.3 Two-stage Optimization . . . . .	36
3.4 Summary . . . . .	40
<b>4 Case Studies</b>	<b>43</b>
4.1 Supermarket Refrigeration System . . . . .	44
4.2 HVAC Chiller with an Ice Storage . . . . .	46
4.3 Summary . . . . .	50
<b>5 Simulation Results</b>	<b>51</b>

## CONTENTS

---

5.1	Power Distribution . . . . .	51
5.2	Heterogeneous vs. Homogeneous Aggregation . . . . .	57
5.3	Evaluation of Aggregator . . . . .	64
5.4	Robust Setup . . . . .	68
5.5	Indirect Control . . . . .	73
5.6	Summary . . . . .	80
<b>6</b>	<b>Experimental Verification</b>	<b>81</b>
6.1	Experimental Setup . . . . .	81
6.2	Sequence of Operations . . . . .	83
6.3	Aggregator Design for the Experimental Setup . . . . .	86
6.4	Danfoss Supermarket Refrigeration System . . . . .	88
6.5	Grundfos Chiller System with Ice Storage . . . . .	93
6.6	SYSLAB Test Facility at Risø . . . . .	96
6.7	Experimental Results . . . . .	96
6.8	Summary . . . . .	104
<b>7</b>	<b>Conclusion</b>	<b>105</b>
7.1	Concluding Remarks . . . . .	105
7.2	Future Work . . . . .	107
	<b>References</b>	<b>109</b>

# **Preface and Acknowledgements**

This thesis is submitted in partial fulfilment of the requirements for the degree of Doctor of Philosophy at the Section of Automation and Control, Department of Electronic Systems, Aalborg University, Denmark. The work has been carried out in the period January 2012 to May 2015 under the supervision of Professor Jakob Stoustrup, Associate Professor Henrik Rasmussen and Associate Professor Jan Dimon Bendtsen. The work is supported by Danish government via the Strategic Platform for Innovation and Research in Intelligent Power, iPower project.

I would like to express my special thanks to my supervisors for their invaluable support, guidance and encouragement during the course of this project. I am grateful to my industrial collaborators, Torben Green from Danfoss and Casper Hillerup Lyhne from Grundfos for providing me the great opportunity to work on their systems and test facilities. I would also like to thank Oliver Gehrke and Anders Thavlov from Technical University of Denmark for their help in the experimental part of the project.

Last but not least, I would like to express my deepest gratitude to my family and my friend, Maryam Soleimanzadeh.



# | Abstract

The current power grid is increasingly facing major changes. Traditional resources in power generation are gradually replaced with renewable energy such as wind and solar due to the lack of fossil fuel resources and the increase in CO<sub>2</sub> emissions. Furthermore, growing use of distributed energy resources (DER) such as photovoltaic panels etc changes the central topology of the grid to the distributed form. These changes have created new challenges for the power grid. Unlike the traditional resources, wind and solar energy are notoriously difficult to both control and store. Thus, establishing a balance between production and consumption is becoming more challenging as the share of intermittent resources increases. Likewise, with the emergence of new DER types, congestion management will become more challenging at the distribution grid level. The future power grid, known as “smart grid”, will enable us to tackle the new challenges and enhance the reliability of the power grid by taking advantage of modern technologies, communication links and control strategies.

A prominent feature of the smart grid is to involve the consumer side in balancing effort, rather than placing the entire burden of maintaining this balance on the producers. This can be done by advancing or postponing the consumption units when there is power surplus or power deficit in the power grid. Flexible consumption can contribute to providing ancillary services along with the generation side. This thesis investigates the utilization of flexible consumers in the future grid.

The focus of this work is on industrial consumers. We propose a three-level hierarchical control framework, in which a so-called “Aggregator” is located between a number of flexible industrial demands and a grid operator. The aggregator is the heart of this setup, with the task of handling the energy/power services can be derived from the demand that these consumers represent. The exact responsibility of the aggregator, however, can vary depending on several factors such as control strategies, demand types, provided services etc. This thesis addresses the aggregator design for a specific class of consumers. The work involves selecting an appropriate control scenario, formulating the optimal objective function at the aggregator, modeling the flexibility of our specific case studies and determining the required information flow. This thesis also investigates different types of aggregation, when we have different types of consumers or the consumers are of a same type. we provide a comparison between heterogeneous and homogeneous aggregation of the consumers. Eventually, this thesis describes an industrial scale experimental setup for evaluating the proposed aggregator. The aggregator aims to provide a distribution grid service from the industrial thermal loads. Our case studies are a supermarket refrigeration system and an HVAC chiller in conjunction with an ice storage which are virtually connected to the aggregator. Practical results obtained from testing on real industrial consumers demonstrate the theoretical studies to a satisfactory level.



# Synopsis

Det nuværende elnet er på vej imod store forandringer. På grund af mangel på fossile brændstoffer og stigende CO<sub>2</sub>-udledning erstattes traditionelle energikilder indenfor elproduktion gradvist af vedvarende energikilder som vind og sol. Voksende brug af distribuerede energiresourcer (DER) som solcellepaneler etc. ændrer endvidere nettets topologi fra en overvejende centraliseret form til en mere distribueret form. Disse ændringer skaber nye udfordringer for elnettet. I modsætning til de traditionelle energikilder er vind- og solenergi notorisk vanskelige både at kontrollere og lagre, hvilket giver nye udfordringer med hensyn til at opretholde balance mellem produktion og forbrug. Indførelse af nye DER typer vil ligeledes med stor sandsynlighed føre til overbelastning på distributionsnet-niveau og heraf følgende udfordringer på mellem- og lavspændingsnettet. Det fremtidige elnet, kendt under betegnelsen "smart grid", vil stå os i stand til at tackle disse nye udfordringer og forbedre pålideligheden af elnettet ved at udnytte moderne teknologi, kommunikationsforbindelser og kontrolstrategier.

Et vigtigt aspekt ved smart grid er at forbrugersiden inddrages i den overordnede balance-strategi, fremfor at hele ansvaret lægges på produktionssiden. Dette kan gøres ved at fremrykke eller udskyde forbrug, når der er over- eller underskud af produceret effekt i elnettet. Fleksibelt forbrug kan også samarbejde med produktionssiden om at levere hjælpetjenester. Denne afhandling undersøger udnyttelsen af fleksible forbrugere i fremtidens elnet.

Dette arbejde fokuserer på industrielle forbrugere. Vi foreslår en tre-lags hierarkisk kontrolstruktur, hvor en såkaldt "Aggregator" er placeret mellem en række fleksible industrielle forbrugere og en elnetsskoper. Aggregatoren har den centrale opgave at håndtere tjenester i form af bestemte energi- og effektforbrugsmønstre, som de underliggende forbrugere kan tilbyde. Hvad aggregatoren præcist kan tilbyde, kan imidlertid variere afhængigt af flere faktorer, som kontrolstrategier, efterspørgsel, udbudte tjenester mv.

I denne afhandling designes en aggregator for en bestemt klasse af forbrugere, herunder valg af et passende kontrol-scenarie, formulering af en performance-funktion for aggregatoren, modellering af fleksibilitet for et specifikt udvalg af case-studier, og det nødvendige dataflow mellem de enkelte enheder bestemmes. Endvidere studeres forskellige typer af aggregering, når forskellige typer af forbrugere er tilgængelige, eller forbrugerne er af samme type (heterogene og homogene forbrugere). Til sidst beskrives forsøg udført på en forsøgssætning involverende termiske last-enheder af industriel mælestok; mere specifikt et supermarkeds-køleanlæg og et ventilationssystem med islagere, der begge er forbundet til den designede aggregator via internet. De praktiske forsøgsresultater viser god overensstemmelse med de teoretiske bidrag.





# Thesis Details

<b>Thesis Title:</b>	Integration of Large-scale Intelligent Consumers in Smart Grid
<b>PhD Student:</b>	Samira Rahn timer
<b>Supervisors:</b>	Assoc. Prof. Jan Dimon Bendtsen Prof. Jakob Stoustrup Assoc. Prof. Henrik Rasmussen
<b>Industrial Collaborators:</b>	Torben Green, Research Engineer, Danfoss Casper Hillerup Lyhne, Development Engineer, Grundfos

The main body of this thesis is based on the following papers and parts of the papers are used directly or indirectly in the thesis:

- 1) Samira Rahn timer, Jakob Stoustrup and Henrik Rasmussen, “Model Predictive Control for Integration of Industrial Consumers to the Smart Grid Under the Direct Control Policy”, *In Proceedings of IEEE Conference on Control Applications (CCA), Hyderabad, India, 2013.*
- 2) Samira Rahn timer, Jakob Stoustrup and Henrik Rasmussen, “Integration of Heterogeneous Industrial Consumers to Provide Regulating Power to the Smart Grid”, *In Proceedings of IEEE Conference on Decision and Control (CDC), Florence, Italy, 2013.*
- 3) Samira Rahn timer, S. Ehsan Shafei, Jakob Stoustrup, Henrik Rasmussen and Jan Dimon Bendtsen, “Evaluation of Aggregators for Integration of Large-scale Consumers in Smart Grid”, *In Proceedings of 19th IFAC World Congress, Cape Town, South Africa, 2014.*
- 4) Samira Rahn timer, Jan Dimon Bendtsen, Jakob Stoustrup and Henrik Rasmussen, “Power Balancing Aggregator Design for Industrial Consumers Using Direct Control”, *In Proceedings of IEEE European Control Conference (ECC), Austria, July, 2015.*
- 5) Samira Rahn timer, Jan Dimon Bendtsen, Jakob Stoustrup and Henrik Rasmussen, “Aggregation of Industrial Thermal Loads in Smart Grid”, *Submitted to IEEE Transactions on Smart Grid.*
- 6) Samira Rahn timer, Torben Green, Casper Hillerup Lyhne and Jan Dimon Bendtsen, “Industrial Demand Management Providing Ancillary Services to the Distribution

Grid: Experimental Verification”, *Submitted to IEEE Transactions on Control System Technology*.

# 1 | Introduction

## 1.1 Motivation

Environmental concerns together with decreasing fossil fuel resources have driven many countries to increase the share of renewable energy in power generation. Traditional resources are gradually replaced with renewable energies such as wind and solar to reduce CO<sub>2</sub> emission and overcome depletion of fossil fuel resources (see Figure 1.1-top). As of the time of this writing, approximately 20% of the Danish electric energy supply is covered by wind energy (on a yearly average), and all political indications point in the direction of more wind energy in the future. The target is to obtain 50% of electricity consumption from wind by 2020. Unlike the traditional resources, wind and solar power are intermittent and notoriously difficult to both control and store, which implies that as the penetration of them increases, it will become more difficult to maintain balance between production and consumption. Thus more sophisticated control strategies are needed to stabilize the frequency of power grid [1]. Moreover, the current power grid is changing from the centralized topology to the distributed form with growing use of distributed energy resources (DER) such as small-scale combined heat and power (MicroCHP) plants, electric vehicles (EV), rooftop solar panels ( photovoltaic or PV ) etc [2] (see Figure 1.1-bottom). This also adds new requirements for congestion management and safe operation of the distribution grid [3].

At the same time, modern sensors and advanced communication technologies enable two-way and automated data exchange between the grid operators, generation side and intelligent consumers [4]. The current power grid requires a fundamental change in infrastructure to meet the future challenges and to take full advantage of modern technologies. The future power grid, known as Smart Grid, utilizes modern technologies and control strategies to overcome the new challenges and consequently, enhance the reliability, efficiency and sustainability of the power grid [5].

Rather than placing the entire burden of maintaining balance between the production and consumption of electricity on the producers, it has relatively recently been proposed to involve the consumer side in the balancing task as well which leads to demand side management (DSM). A more intelligent demand response is an inseparable part of the Smart Grid solutions. One of the key components of a smart grid is a flexible consumption. In this context, flexible demand refers to those consumers that can advance or postpone their consumption in response to a grid operator command or incentive signals to help the grid [6]. For example, when there is power surplus or power deficit in the power grid, we can increase or decrease the consumption instead of decreasing or increasing the

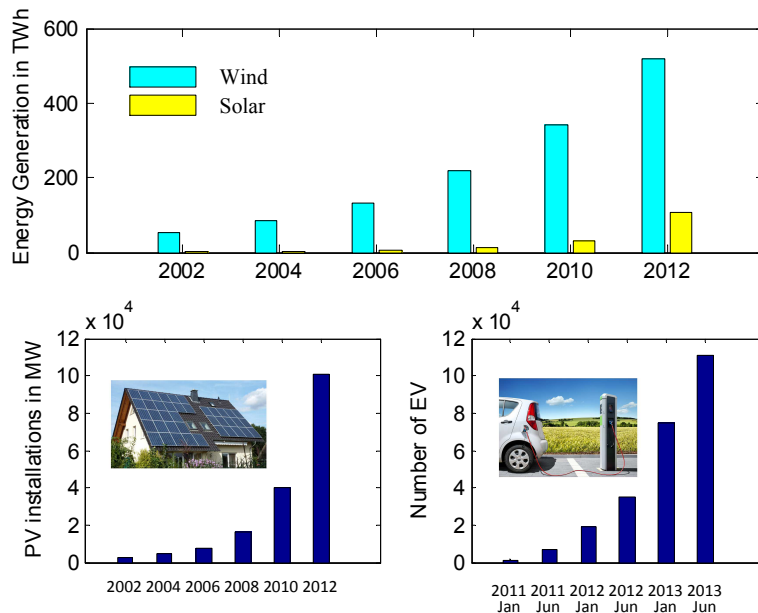


Figure 1.1: Worldwide electricity generation from renewable resources over 10 years (top plot). Worldwide PV installations and cumulative EV sales (bottom plots).

power generation. The notion of a smart grid gives consumers the opportunity to evolve from a mere consumption unit to an active player in the electricity market [7].

The flexible consumers will be able to offer their flexibility to the main grid operators such as Balance Responsible Party (BRP), Transmission System Operator (TSO), Distribution System Operator (DSO) etc [8]. BRPs are trading companies, which have the responsibility of supplying energy to a number of consumers under their jurisdiction during a given period of time. They trade power in different markets. For example, in the day-ahead market, BRPs bid their power schedules a day before the actual consumption/production based on the anticipated consumption. By utilizing the flexibility of consumers, BRPs will be able to reduce the cost of deviation between the power which is bought/sold one day ahead and the actual consumption/ production. In other words, the actual consumption is becoming closer to the anticipated consumption which prevents trading power at a higher price in the balancing power market [9].

TSO is a non-commercial organization, which is responsible for reliable and secure operation of the whole power grid. To maintain the balance between production and consumption at all times, the TSO procures ancillary services. According to United states FERC (Federal Energy Regulatory Commission), ancillary services are “those services necessary to support the transmission of electric power from seller to purchaser given the obligations of control areas and transmitting utilities within those control areas to maintain reliable operations of the interconnected transmission system.” They are required during both normal conditions and system contingencies. [10] has defined six generic groups of ancillary services, involving continuous regulation and energy imbalance management (for correcting fluctuations with a minute to an hour time schedule), instantaneous con-

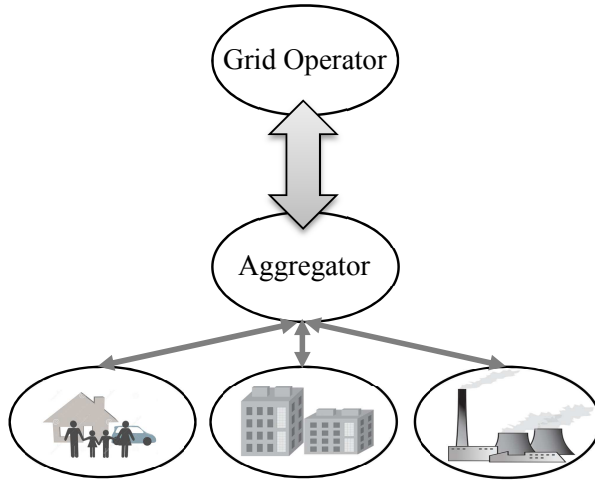


Figure 1.2: Aggregator as a new market player between the grid operator and the residential, commercial or industrial consumers.

tingency reserve and replacement reserve (for restoring system stability in response to a contingency event), voltage control (for maintaining transmission system voltage within the limits with absorption or injection of reactive power) and black start (for restarting the power system after a major blackout). Flexible consumption can contribute to such ancillary services, e.g. as upward and downward regulating power.

Finally, at the low-voltage level, DSOs are responsible for the physical grid, here, avoiding congestion and controlling the voltage level of the feeders are the main issues. Congestion management and voltage control can also be accomplished by adjusting flexible loads in a smart electrical grid [11].

The new Smart Grid will entail smart infrastructure, management and protection system [12]. This will introduce new market actors to the future grid [13]. Particularly for demand side, in the Smart Grid literature, a so-called “Aggregator” has been presented as a new player in the future market, located between the grid operator and a number of flexible consumers to handle the services that can be derived from the demand these consumers represent [14], [15] (see Figure 1.2) What the aggregators responsibility is and which entities it has interaction with may be different, however. There could be various types of aggregator depending on the control strategy, type of demand, provided services etc. This thesis addresses the aggregator design for a specific class of consumers and the evaluation of the proposed setup. We focus on industrial thermal loads in this work.

## 1.2 Background and State of the Art

Utilization of consumers in power management systems by changing the time and amount of energy usage is called demand-side management (DSM). Generally, DSM programs fall into two categories, demand response (DR) and energy efficiency and conservation. DR activities aim to flatten the demand pattern by shifting load from the peak hours to off-peak hours. With a smoother demand profile, electricity can be provided at a lower cost

and initial investment. Energy efficiency and conservation programs attempt to decrease the energy consumption by either encouraging the consumers to reduce their consumption for saving money or replacing the current devices with more efficient devices with a same performance, but a lower cost [16].

### Control Policies for DSM

Different control strategies have been used to exploit the flexibility of the consumption units. However, generally we can classify these strategies into two main categories, direct control and indirect control [17], [18]. In direct control strategies, the consumers receive control commands from a grid operator based on a contract agreement. In most cases, this implies a two-way communication and data exchange between the operator and the consumers. On the contrary, indirect control is a one-way communication approach where the grid operator aims to change the consumption profile by motivating the consumers through incentive signals, e.g. electricity price. The consumers independently decide to act on the incentive or not.

With the emergence of smart grids, the both strategies can be implemented fully automatically. Thus, participants require new equipments to play. Compared to the direct control, indirect approach does not require heavy computation at the grid operator. However, the main difficulty here is to distribute appropriate incentive signal. To this end, consumers' reaction to the incentive signals should be estimated. This process deals with uncertainty which is the weakness of the indirect control. As an example, in [19], several models (FIR, non-linear FIR and ARX) has been proposed to identify the price-power consumption relationship of a price responsive unit. The model then has been used by a price generator which has the objective of following a constant power reference based on the identified parameters. On the other hand, managing the small-scale energy consumers, e.g. households, is not feasible with direct control in practice, due to the computational complexity. Moreover, some owners are not willing to permit their appliances to be controlled directly by a third party since this can disturb their privacy. In these cases, the indirect control works better. For the large-scale consumers with less privacy issues, such as industrial enterprises, it is rational and more certain to assume a central framework to control the units directly [20].

### DSM in Smart Grid

DSM programs are over 40 years old, however early programs were limited and expensive due to lack of advanced technologies. Smart Grid, with the possibility of two-way communication, real-time data exchange and using smart meters and monitoring, facilitates the DSM programs in recent years [21]. Moreover, new requirements that arise from growing use of renewable resources and DERs, can be included in the smart DSM programs.

There are many works in the literature which have investigated the DSM problems in the future Smart Grid. Some of the works have studied the contribution of household appliances in the Smart Grid and highlighted the role of smart meters in DSM. These works usually deal with smart pricing and incentive mechanisms. Smart pricing is one of the DSM methods to encourage the consumers to change their consumption behaviour. Mainly, smart pricing can be categorised into three groups, time-of-use (TOU) pricing,

critical peak pricing and real time pricing [22]. In TOU pricing, different prices are assigned to different blocks (usually off-peak, shoulder and peak periods) in a day, however, the price setting changes twice or three times a year. In critical peak pricing, changes can happen more frequently compared to TOU pricing and they are announced in advance to the consumers.

The usage of smart meters and communication enable real time changes in electricity price based on the information of the electricity market. For example, the work in [23] has suggested an energy management algorithm to optimize energy consumption within a home and in a neighborhood level based on price signals. Another examples is [24], where a scheduler has been developed to shift the energy consumption of white good appliances to the low cost periods with using hourly prices, while it respects the user's preferences.

Game theory has been adopted in several researches to solve the DSM problems involving smart pricing at the household level. For instance, in [25] an incentive-based consumption scheduling algorithm has been presented where several residential units are connected to a common energy source. Each user is equipped with an automatic energy consumption scheduler which minimizes the energy cost in a game theoretic approach based on the price signals. [26] has made a survey of game theoretic approaches in Smart Grid.

DSM at the household levels are not restricted to the home appliances. The work [27] has described an environment where the households possess electrical power storage. Load managing has accomplished with incorporating home appliances with electrical batteries. Electrical storage can be charged when the electricity price is low. During the peak hours, when the price is high, batteries can provide the electricity instead of supplying power from the grid. Other than installing separate batteries, EVs can also act as an electrical storage. EVs can be employed in V2H (vehicle-to-home) and V2G (vehicle-to-grid) modes. In V2G mode, EV injects energy to the grid, while in V2H, EV is used to supply energy to the home appliances [28].

Electrical Storages are proven technologies to mitigate the impact of increasing renewable resources on power systems. However, the main drawback of the electrical storages is that they are not environmentally friendly [29] and this is in contrast to the primary purpose of increasing renewable resources. Thermal energy storage (TES) is another solution for storing energy without the aforementioned drawbacks. Excess electrical energy can be stored in form of thermal energy in a TES for later use in the future.

Particularly, in the context of smart DSM, those TESs are of interest which are already part of the existing systems. The question is how this potential can be released to achieve the Smart Grid goals. Residential and commercial buildings have received a lot of attention as TESs in the literature. Building structure can retain the thermal energy, either in the form of warmth or coldness, for a period. The long time constant of the building thermal model can be utilized for load shifting from peak-hours to off-peak hours for saving money at local places [30]. In addition, by manipulating the heating or cooling systems, loads are able to provide ancillary services without disrespecting the comfort levels of occupants [31], [32], [33]. Apart from building materials, other equipments in heating or cooling systems can act as a TES. For instance, the works [34] and [35] describe the flexibility of small water heater in providing ancillary services.

Literature review regarding flexible demands in Smart Grid reveals that most of the references have been focused on household appliances and residential buildings, whereas



the works on industrial consumers are rather limited. Likewise, the indirect control has been chosen more than the direct approach due to privacy issues, as mentioned above. As an example of the industrial DSM, the work [36] has investigated the possibility of increasing the profit in a chemical manufacturing industry through the smart DSM. The basic idea is to equip the refinery process in such a way that the plant can adapt its energy consumption according to different electricity prices. Oil refineries industry has also been studied in [37], where the authors have proposed an optimal load control to reduce the electricity cost, considering all the operational and sequential constraints of the plant. Another example is [38], which has proposed a generalized DR algorithm for the industrial plants. The industrial process, involving also energy storage and energy generation systems, is modelled based on the state task network (STN). The DR problem is formulated as a mixed integer linear programming with the aim of minimizing the energy cost. The case study in this work is the oxygen generation facilities. In all above examples of industrial DSM, such plants are considered in which the sequence of operations is important and the subsystems are interconnected with each other. This makes the industrial DSM more challenging compared to the residential demands.

Among the industrial consumers, supermarket refrigeration systems have also drawn attention in the literature. A large amount of refrigerated foods in cold rooms and display cases at the supermarket can play a role of huge TES. It seems the integration of supermarkets to the Smart Grid will be easier than the chemical industrial plants since the plant is not subject to strict sequences and there is no need to install extra storages. For instance, in [39], a supermarket refrigeration system has been assessed as a fast reserve. Durations of up to 15 minutes have been considered when the supermarket can contribute with ancillary services to provide upward and downward regulating power. During the up-regulation period, the supermarket is asked to reduce the power consumption whereas, in the down-regulation, it will consume more power with lowering the temperature of cold rooms. The work [40] has studied the direct control of supermarket refrigeration system in Smart Grid as well.

## Taxonomy of Flexible Consumers

Even though every consumer is different from the others and it has its own characteristics, a generic classification of consumers' flexibility that covers a wide range of consumers would be beneficial for further analysis in DSM. In [41], a taxonomy of consumers has been presented entitled "Buckets, Batteries and Bakeries". A Bucket is an energy integrator which is able to store electrical energy in form of thermal energy while respecting the energy and power constraints. Supermarket refrigeration system is an example of a Bucket. A Battery is similar to Bucket except that it should store a certain amount of energy within a specified time. An electric vehicle would be an example of a Battery; when it is placed in its charge station in the evening, the customer would want to have it charged up to a certain level by the following morning. However, the battery can be charged intermittently during the charging process. A Bakery only offers flexibility in terms of the time we decide to use it. When it starts to operate, it has a fixed power consumption profile and a specified run time. A washing machine could be considered as a Bakery model since when it starts, we could neither interrupt it nor change the power.

## Aggregator

As seen in above examples, smart DSM is not only a means of optimizing local energy consumption, but it also facilitates active participation of consumers in the electricity market. It is obvious that the consumers cannot offer in the market individually; since each consumption alone, is not large enough to bid in the market and it is practically impossible to manage from the grid operator point of view. The term “Aggregator” has been recently used for a new entity which is in charge of handling the consumer services or their integration to the smart grids. This is a general definition though, and the exact function of the aggregator might be different from case to case.

For example, In [42], the VPP (virtual power plant) aggregator has been categorized according to the control strategies. The direct controlled VPP aggregator is responsible for optimally operating a portfolio of units based on the available information whereas the indirect controlled aggregator acts as a broadcast agent to distribute price signals. In [43], the aggregator has been designed to operate between the residential units and the utility operator. In the proposed setup, the aggregator will negotiate with the home owner when the operator announces its rewards for power services. After they reach an agreement, the aggregator will offer the services on behalf of the units to the operator. This setup is different from the direct aggregator since there is no direct command from the aggregator to the units. It is also different from the indirect aggregator because of the negotiation.

The other example is [44] in which the DR aggregators has been introduced as financial entities and they aim to maximize their revenue in day-ahead wholesale energy markets. The objective function at the aggregator comprises the revenue of four services, load curtailment (reducing the consumption without shifting the load to any other time period, such as turning off unused lights), load shifting (shifting the consumption to other hours such as delaying the operation of appliances), utilizing onsite generation (turning on backup generator) and utilizing energy storage. The aggregator takes into account the constraints for each services as well. In [45] however, the aggregator is more an information center than a controller which collects and stores the data it receives from home energy management systems.

Many of the publications for the aggregator design are dedicated to small energy consumers, namely EVs and home appliances. For instance, in [46], an aggregator design has been proposed which utilizes the flexibility in electric vehicles to provide frequency regulation to the grid. A vehicle can provide services as long as it is connected to the grid, except the times it is being charged by its owner’s decision. The role of the aggregator is then to control the charging process such that it maximizes its revenue. More examples are in [47]-[50].

## Smart Grid in Denmark and iPower Project

Denmark has a great potential to generate electricity from wind and in the coming years, electricity will be increasingly generated from wind and renewable resources. On the other hand, electricity consumption is also faced with major changes since oil-fired burners are replaced with electric heat pumps and the use of electric vehicles and plug-in hybrid vehicles instead of petrol-powered vehicles is becoming more common [51]. Thus, Smart Grid is a hot research area in Denmark as an effective solution to tackle the new changes.



### DK1 ancillary services:

- Primary reserves
- Secondary reserves (Load frequency control)
- Manual reserves
- Short-circuit power, reactive reserves and voltage control

### DK2 ancillary services:

- Frequency-controlled disturbance reserve
- Frequency-controlled normal operation reserve
- Manual reserves
- Short-circuit power, reactive reserves and voltage control

Figure 1.3: Ancillary services to be delivered in Denmark from Energinet.dk technical report, 2011

Balance between production and consumption of electricity should be kept all the time in any power grid. However, both the consumption and production power profiles have fluctuating natures. Thus, grid operators require to procure ancillary services to maintain the balance instantaneously and continuously which ensures reliable and safe operation of the power systems. The Danish power system is divided into two areas, the western and eastern parts, called DK1 and DK2 respectively. Ancillary services to be delivered in each region are shown in Figure 1.3, according to Danish TSO (Energinet.dk) report [52]. The Danish government has set-up goals to have 100% renewable energy for electricity and heat in 2035 and 100% renewable energy in 2050. In a traditional power system, central power plants can provide ancillary services in addition to the electric power. With moving toward a distributed generation and renewable energies, ancillary services provision will then become more challenging [53]. Smart Grid and demand response have been considered as promising options by Energinet.dk for facilitating the wind turbines integration [54].

To fulfill the Danish government objectives, many research project have been planned in the field of Smart Grid in Denmark. This PhD project is part of one of the largest research project in Denmark, called iPower project. Referring to [55], “iPower is a strategic platform where universities and industrial partners consolidates innovation and research activities for the purpose of developing intelligent control of decentralized power consumption. It is an ongoing task in iPower to produce the right tools to manage millions of flexible consumption units, as well as to uncover methods of operation in search for a way to run distribution with flexible power generation. Methods for identification of user needs and acceptance of flexible consumer units is being tested in practice. The iPower Platform develops and matures Smart Grid technologies for the electrical grid, industries and residential applications. The society needs Smart Grid technology to ensure that the electrical grid can absorb all the energy generated by wind and solar renewables. The iPower platform links research, innovation and demonstration to actual product development by specifying technologies, requirements and methods for Smart Grid products. It enables the industry partners to become first movers in a new and growing world market.”

The iPower platform has been categorized into seven work packages: “demand response (WP1 and WP2), distribution grid operation (WP3), control and market operation

(WP4), socio-economic and investor evaluation (WP5), consumer behaviour (WP6) and dissemination (WP7)”. Figure 1.4 illustrates how the work packages are connected to each other. From [55], iPower goals are:

**“Goal 1: Flexible consumption potential**

Target: Describe the flexibility potential, in terms of both kW and kWh, for relevant DERs or mid-level controllers that aggregate several mixed entities, from small to large size, in different sectors: industrial, commercial and residential. Also putting a cost estimate on flexibility from each DER or aggregator. This should be done for different levels of control, from simple and cheap to advanced.

**Goal 2: Grid demand - The demand for flexibility**

Target:

- Show that flexibility can be valuable to DSO and TSO. Fulfilling this goal also implies having described the flexibility services that are requested by the DSO and TSO
- Give in-depth description of what costs are necessary for the DSO and TSO, to utilize flexibility
- This goal focuses on the technical aspects of the flexibility demand

**Goal 3: Aggregation**

Target: Design and demonstrate an aggregator component/module, to control iPower DERs

**Goal 4: Book keeper for seamless trade of flexibility**

Target: Demonstrate seamless interaction (clearing house function) between the market players, in delivering, buying and selling flexibility services. Develop and demonstrate a flexibility market, which offers the best suitable market setup for trading flexibility products, between TSO+DSO and Aggregators

**Goal 5: Society and investor valuation of flexibility**

Target: Provide in-depth evaluation of the societal value, as well as the value for each market player in mobilizing flexibility:

- Value of a distributed flexibility market
- Non-economical value to consumers and society
- Other, relevant evaluation of the value of iPower artifacts”

This work is a part of WP2 . The focus of WP2 is on the consumer side, specifically industrial consumers. The main objectives in WP2 are:

1. “Analyze control related challenges in industrial power consuming units in a flexible power grid set-up
2. Identify and develop control schemes suitable for supporting power grid flexibility
3. On-line forecasting of flexibility and loads
4. Demonstrate the flexible power capability of products for the industrial market”

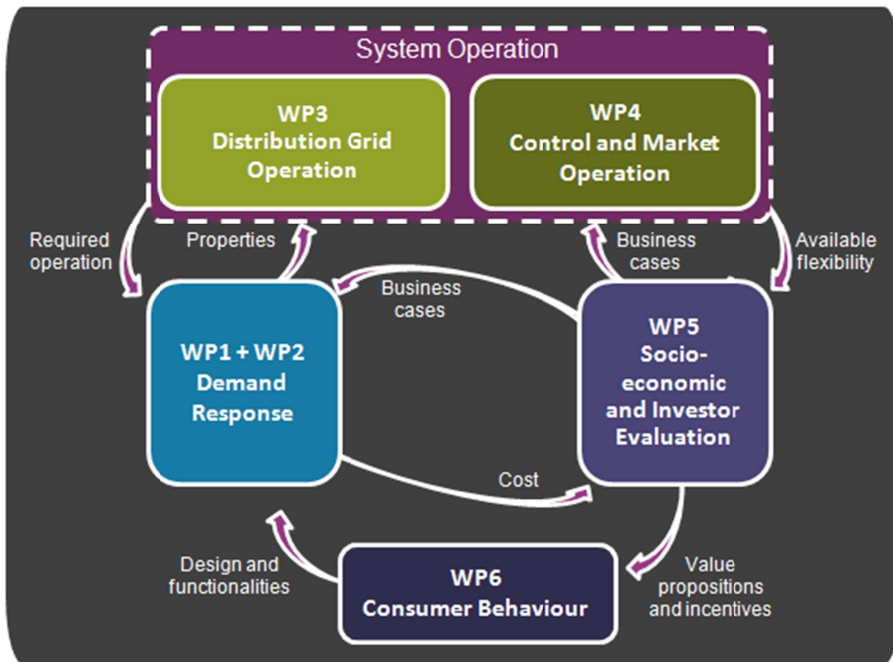


Figure 1.4: iPower work packages overview

As mentioned in [55], iPower project has emphasized on real real-life demonstrations: “A significant innovation result is an experimental verification of the proposed control schemes, where the effectiveness and potential shortcomings are highlighted in demonstrations. Two industrial consumer products are considered namely a supermarket refrigeration system and a commercial chiller with ice storage. This is expected to result in an experimental verification of the expected flexibility potential for the selected product range. A prototype implementation with the flexibility functionality integrated in the actual product and related controllers, is expected to mature the proposed methods to a level where an industrial implementation is realistic.”

## Contribution to the State of the Art

All in all, we can conclude that the Smart Grid is the most effective and promising strategy for developing a new power system with a high share of renewable resources and small-scale DERs; and among Smart Grid solutions, smart DSM is a prominent approach. Aggregator as a new market player is inevitable and central to the concept of smart DSM. We contribute to the state of the art by providing an aggregator design for a portfolio of industrial thermal loads. We have chosen industrial consumers which is consistent with the objective of WP2 and it is less addressed in the literature. We not only propose an optimal design for the aggregator, but also investigate different types of aggregation. To this end, we assume two aggregation types, namely heterogeneous and homogeneous aggregation. In the heterogeneous aggregation, the aggregator utilizes the flexibility of

TESs with different flexibility characteristics, while in the homogeneous one, all TESs have the same flexibility characteristics. Nevertheless, theoretical results might not hold in practice. We consider simplifying assumptions in theory which might not capture all features of the real system. Moreover, many practical issues will not be noticed until the practical implementation. Hence, real-life demonstrations are necessary for acceptance of the theoretical findings. As the main contribution of this work, we verify the proposed setup through a real-life industrial scale experimental setup.

### 1.3 Objectives

The main focus of this PhD project is to develop a design for the aggregator in the Smart Grid and to verify the proposed setup through the real-life demonstration. Then, this objective is in line with Goal 1, Goal 2 and mainly Goal 3 of iPower project and the items 1, 2 and 4 of WP2 objectives. In addition, the emphasis of iPower project on experimental verification is fulfilled with the demonstration setup. In this regard, this PhD project is in collaboration with two Danish companies, Danfos and Grundfos. They provide their test facilities namely, a supermarket refrigeration system and an ice storage system which are located at the refrigeration lab at the Danfoss headquarters in Nordborg and the Grundfos headquarters in Bjerringbro respectively. In summary, we aim to address the following research questions:

1. What kind of services would be of interest to the grid operators?
2. What is achieved by aggregating the flexibility of heterogeneous consumers?
3. To what extent is the proposed scenario implementable in practice?

To address the above question, we can summarize the objectives as follows:

1. **Aggregator design for the industrial thermal loads:**  
This step involves determining the appropriate control scenario, establishing the appropriate model for the consumers and specifying the required information exchange.
2. **Comparison of heterogeneous and homogeneous aggregation:**  
This step involves comparing the two aggregator setup, in one setup, the aggregator has a heterogeneous portfolio of the consumers under the control whereas, in the other setup, the aggregator controls a homogeneous portfolio of the consumers.
3. **Evaluation of the proposed setup:**  
This step involves evaluating the proposed setup through the simulation and real experiment.

### 1.4 Contributions

The objectives outlined in Section 1.3 have been fulfilled through the following papers:

- 1) **Model Predictive Control for Integration of Industrial Consumers to the Smart Grid under a Direct Control Policy**

In this paper, we study a three-level hierarchical structure for integration of industrial thermal loads to the Smart Grid. We assume a power reference following scenario in which, the aggregator is asked to follow a power reference during a specific time to provide downward regulating power. We choose the direct approach. Appropriate models are considered to model the flexibility of our case studies, including supermarket refrigeration system and chiller in conjunction with an ice storage. The optimization is formulated at the aggregator. We show better utilization of flexibility can be achieved by aggregating heterogeneous consumers.

**2) Integration of Heterogeneous Industrial Consumers to Provide Regulating Power to the Smart Grid**

In this paper, we develop an indirect setup for the power reference following scenario that is introduced in paper 1. We make a comparison between the direct and indirect setup. We show that the above mentioned power reference scenario requires the direct control.

**3) Evaluation of Aggregators for Integration of Large-scale Consumers in Smart Grid**

In this paper, we first improve the optimization formulation for the downward regulating power provided in paper 1 and 2. We also investigate the cost of employing simplified model of the consumers at the aggregator. We show the utilization of simplified models can lead to reasonable results.

**4) Power Balancing Aggregator Design for Industrial Consumers Using Direct Control**

In this paper, we complete the aggregator design by formulating the objective function for both the upward and downward regulating power scenarios. Moreover, we consider the discrepancy inherent in the aggregator/consumer interface, according to which the aggregator utilizes deliberately simplified models of the consumers, although the physical systems are known to be more complicated. To compensate for the error arising from model mismatch, we propose a feedback mechanism which propagates the error of one unit to the rest of units in our portfolio. We investigate how large uncertainties the setup can handle over a given horizon via a brute-force approach.

**5) Aggregation of Industrial Thermal Loads in Smart Grids**

In this paper, we generalize the hierarchical setup by considering a number of aggregators and explain the interplay between the aggregators and the top-level controller. We provide a comparison between the heterogeneous and homogeneous aggregation. We show the heterogeneous aggregation outperforms the homogeneous one since, it has a lower cost/greater profit from energy consumption point of view and also it can handle the unpredictable situations better compared to the homogeneous aggregation. Furthermore, instead of the feedback mechanism provided in paper 4, we include the uncertainties inside the MPC controller at the aggregator. This approach leads to a robust MPC framework in which the model structure is known. However, the model parameters are allowed to vary within a predefined convex set. Simulations indicate that the robust setup can handle the mismatch between the actual and assumed model of consumers fairly well.

6) **Industrial Demand Management Providing Ancillary Services to the Distribution Grid: Experimental Verification**

In this paper, we verify the direct aggregator design with an experimental setup involving a supermarket refrigeration system located at the refrigeration lab at the Danfoss headquarters in Nordborg, Denmark and an ice storage system located at the Grundfos headquarters in Bjerringbro, Denmark which are virtually connected to the aggregator. We aim to demonstrate a DSO type service. We show that the proposed setup can also provide acceptable results in practice.

## 1.5 Outline of the Thesis

This thesis is divided into seven chapters. After the introduction chapter, in Chapter 2, the aggregator setup is introduced. We choose the direct control policy to manage the flexibility of industrial thermal loads. We describe the scenario and the objective functions at the aggregator to provide the upward and downward regulating power services. To control the units directly, the aggregator requires a model of the consumers. The model employed at the aggregator, as well as the required information flow between the components are explained. In addition to the direct control formulation, we also formulate an indirect approach for the chosen scenario in this chapter. Chapter 3 describes the ideas to make the proposed setup more robust. In Chapter 2, the aggregator deliberately uses simplified models of the real complicated systems. In this chapter, we propose two solutions to compensate the error which arises from the model mismatch. Chapter 4 introduces our case studies in this work, involving a supermarket refrigeration system and a chiller system in conjunction with an ice storage. Simulation results are provided in Chapter 5. Simulation are mainly divided into two parts. The first part is dedicated to the comparison between the homogeneous and heterogeneous aggregation of a portfolio of consumers. In the second part, we investigate the performance of the proposed robust setup in Chapter 3. We also provide some simulation results for the indirect approach we describe in Chapter 2. Chapter 6 explains the experimental setup. This project is in collaboration with Danfoss and Grundfos companies. They provide their test facilities and real equipments to demonstrate the aggregator design. The experimental setup consists of a supermarket refrigeration lab at Danfoss and a real ice storage at Grundfos which are virtually connected to the aggregator. The results from several experiment are shown in Chapter 6. Eventually, we conclude the thesis in Chapter 7.





## 2 | Aggregator Design

This chapter describes the aggregator design for a portfolio of industrial thermal loads. We first introduce the chosen scenario we consider to utilize the flexibility of the consumers. The proposed aggregator design is based on the direct control policy and the aggregator operates in the middle of a three-level hierarchical structure. We formulate the objective function at the aggregator to optimally utilize the flexibility. The aggregator requires a model of the consumption units in this direct setup. We describe the approximate models that will be used in the aggregator, as well as the information required to be exchanged between the aggregator and the consumers. Other than the interaction between the aggregator and the consumers, we explain the interplay between the aggregator and the top-level controller at the grid operator.

### 2.1 Hierarchical Setup

As mentioned in Chapter 1, integration of the consumers to the smart grid can be implemented with two main control policies, entitled direct control and indirect control. The direct control is a two-way communication approach with information exchange between the components. In this approach, the grid operator can command the consumers directly based on a contract agreement. The indirect control refers to those strategies in which the grid operator tries to change the consumption behaviour indirectly with distributing incentive signals. However, consumers are not obligated to change their consumption. In this work, we choose the direct control policy, since we aim to design an aggregator for the industrial consumers. A few of industrial enterprises are large enough to bid in the electricity market. Thus, we can implement a central aggregator which has the consumers under its direct jurisdiction in practice. Such aggregators operate in a three-level hierarchical structure shown in Figure 2.1. The hierarchical market setup consists of three levels, a top-level controller that can be located at the TSO, DSO or BRP, a set of competitive aggregator in the middle and a number of consumers (known as DERs in the smart grid context) under the control of each aggregator at the bottom. We consider a power reference following scenario as follows:

*“The aggregator and the grid operator sign a contract which allows the grid operator to activate the aggregator for a certain period of time, called the activation time. The aggregator is asked to follow a specified power reference within the activation time.”*

In this setup, the grid operator is able to stabilize the whole power consumption of a set of aggregators at a certain power,  $P_{\text{reference}}$ , within the activation time. In Figure 2.1, we assume  $n$  aggregators, each named “Aggregator  $i$ ” ( $i = 1, 2, \dots, n$ ) and each aggregator

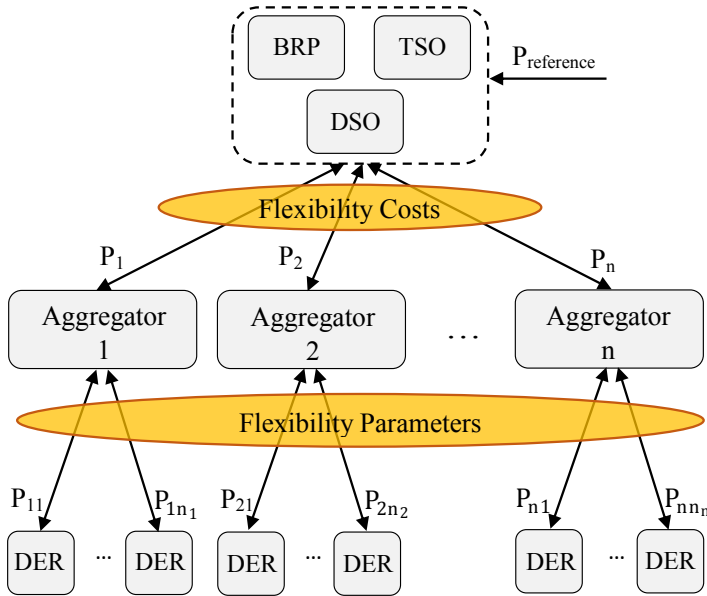


Figure 2.1: Hierarchical direct control setup

controls  $n_i$  consumers. As shown in the figure, there are other information flows than the electrical power in the hierarchical setup. The DERs should communicate the parameters which characterize their flexibility to the associated aggregators and the aggregators should transfer the cost of delivering flexibility for the whole portfolio to the grid operator.

The power reference following service can be of interest to any grid operator in the electricity market, such as BRPs, TSO or DSO. For instance, the current Nordic electricity market, a common electricity market between Denmark, Norway, Sweden and Finland, consists of several markets based on the bidding timeline shown in Figure 2.2 [56]. In summary, the financial market is a commercial market without physical delivery and it is essential for risk management. The heart of the Nordic market, called the Nord Pool market, consists of the Spot market and the Elbas market. The Market participants buy/sell the power a day before the actual consumption/production in the Spot market. Bids are given for a 24-hour period and are closed at 12:00 a day before. Trading is possible until one hour before the operation through the intra day Elbas market. To maintain the balance continuously, TSO should provide regulating powers as upward and downward regulation, meaning increase and decrease in production respectively. The proposed aggregator can bid in the regulating power market by providing upward and downward regulating power with decreasing and increasing the consumption instead. The aggregator can offer regulating powers, comprising primary, secondary or manual reserves, directly to TSO or via BRPs. The balancing power market is an after-day settlement for calculating the actual consumption and production when actual measurements are available from the meters. Needless to say, the current electricity market is subject to changes in order to accommodate new requirements. We believe that the power reference following service is even more valuable in the future electricity market.

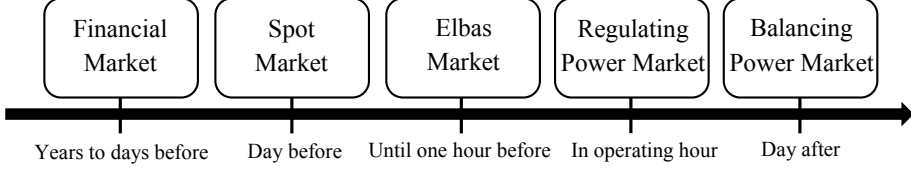


Figure 2.2: Nordic electricity markets and the timeline for bidding

The aggregator will be a for-profit entity and its main goal is to make money in the future market. In order to be economically profitable, the objective function at the aggregator should reflect not only the grid operator requirements, but also the profit obtained from attending the electricity market trading. Accordingly, we encounter the following optimization problem at the aggregator  $i$ :

$$\begin{aligned}
 & \text{Maximize } \{\text{profit of "Aggregator } i" \text{ for offering flexibility}\} & (2.1) \\
 & \text{Subject to :} \\
 & \text{Consumers' dynamic} \\
 & \text{Consumers' constraints} \\
 & P_{i1} + P_{i2} + \dots + P_{in_i} = P_i
 \end{aligned}$$

Thus, the role of the aggregator in above hierarchical direct setup is to optimally split up the power reference between the consumers while respecting their dynamics and constraints. In general, to establish an aggregator design based on the direct setup, we need to specify three items:

- (1) Model of the consumption units
- (2) Optimization problem at the aggregator
- (3) Information flow between the aggregator and the consumers

In the following, each item is explained.

## 2.2 Model of Consumers and Constraints

The aggregator requires a model of the consumption unit which characterises its flexibility. In this work, we target to utilize the flexibility of TESSs. Excess electrical energy can be stored in form of thermal energy in TESSs for later use in the future. In modeling a TES, the aim is to represent the thermal energy changes that result from input excess/shortage of electrical power. Thus, the system input,  $u \in \mathbb{R}$ , and the system state,  $x \in \mathbb{R}$  are defined:

$u(t) \triangleq$  electrical power deviation from the baseline power

$x(t) \triangleq$  thermal energy changes

where, the baseline power is the power consumption in normal operation, as long as there is no activation. Real Physical systems are composed of several components and subsystems with complicated dynamics. The main issue in the modeling is how complex the model should be to represent the consumers' flexibility. The aggregator employs deliberately simplified models of the consumers, although the physical systems are known to be more complicated. This is due to several reasons:

- Computational complexity: Using complex models will lead to unacceptable computational time in practice, where the aim is to find the optimal solution for a large number of consumers in a limited period.
- Information encapsulation: In general, the more complex models, the more information exchange required. This makes the information encapsulation becomes difficult.
- Separation of responsibility: The aggregator is not responsible for controlling the consumers in detail, such as every single pump or valve. Thus, it is not necessary to have complex models at the aggregator.

We look at the whole consumption unit as a lump TES. Hence, the model should be complex enough to describe the salient features of a TES. Various types of TESs can be distinguished by the following key features:

1. Leakiness, i.e. loss during storage
2. Efficiency in conversion
3. Power capacity
4. Energy capacity
5. Run/stop constraints
6. Operational modes

Figure 2.3 depicts such a simplified thermal storage. The storage has a limited capacity and filling rate, which represent the thermal energy ( $E_{\min} \leq E_{th} \leq E_{\max}$ ) and electrical power ( $P_{\min} \leq P_e \leq P_{\max}$ ) constraints. The storage may have a leakage, which denotes the heat loss to the surrounding. The inlet valve cannot be opened and closed as fast as we want, which describes the run/stop constraints. It means, when the system is switched on, we are not able to switch it off immediately and vice versa. The COP (Coefficient Of Performance) of a thermal unit describes the efficiency in conversion from the electrical power to the thermal energy. Different units have different COPs. For the equivalent representation of the model shown in Figure 2.3, this can be modelled with the inlet valve, as different valves have different dynamic specification. Finally, this system can be run in different operating modes.

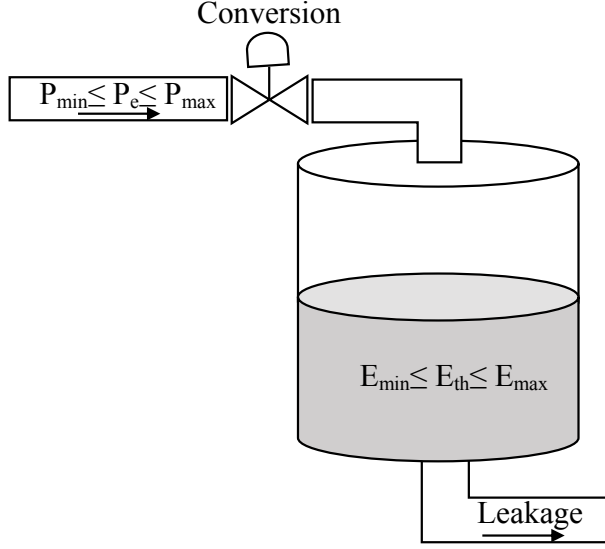


Figure 2.3: Salient features of a thermal energy storage (TES)

### 2.2.1 Model

Assume  $\begin{bmatrix} x_{ij} \\ u_{ij} \end{bmatrix} \in \mathcal{L}_{ij}$ , where  $\mathcal{L}_{ij} \subset \mathbb{R} \times \mathbb{R}$  is a polytopic set. Then, the general model of the  $j$ th TES belonging to “Aggregator  $i$ ” is expressed by (2.2)-(2.5). We consider a piece-wise linear dynamic system including two separate linear models. In this way, we can explain those systems which are operated in two different modes with significant difference between the system parameters. For instance, the system dynamics might vary significantly from day-time to night-time because of COP effects. Another example could be the two separate modes (ice-making and direct cooling) in cooling and air conditioning systems. Instead of increasing the number of models, small changes in system parameters are modeled by considering uncertain parameters in each mode. Note that we consider multiplicative uncertainties.

$$\dot{x}_{ij}(t) = \begin{cases} (A_{ij,c1} + \alpha_{ij,c1})x_{ij}(t) + (B_{ij,c1} + \beta_{ij,c1})u_{ij}(t) & \text{if } \begin{bmatrix} x_{ij} \\ u_{ij} \end{bmatrix} \in \mathcal{L}_{ij,1} \\ (A_{ij,c2} + \alpha_{ij,c2})x_{ij}(t) + (B_{ij,c2} + \beta_{ij,c2})u_{ij}(t) & \text{if } \begin{bmatrix} x_{ij} \\ u_{ij} \end{bmatrix} \in \mathcal{L}_{ij,2} \end{cases} \quad (2.2)$$

$$\mathcal{L}_{ij,1} \cap \mathcal{L}_{ij,2} = \emptyset, \mathcal{L}_{ij,1} \cup \mathcal{L}_{ij,2} = \mathcal{L}_{ij} \quad (2.3)$$

$$\mathcal{L}_{ij,1} = \left\{ \begin{bmatrix} x_{ij} \\ u_{ij} \end{bmatrix} : S_{ij,1}x_{ij} + R_{ij,1}u_{ij} \leq L_{ij,1} \right\} \quad (2.4)$$

$$\mathcal{L}_{ij,2} = \left\{ \begin{bmatrix} x_{ij} \\ u_{ij} \end{bmatrix} : S_{ij,2}x_{ij} + R_{ij,2}u_{ij} \leq L_{ij,2} \right\} \quad (2.5)$$

where  $A_{ij,c1}, A_{ij,c2}, B_{ij,c1}, B_{ij,c2} \in \mathbb{R}$  are known parameters of the continuous model and the sets  $\mathcal{L}_{ij,1}$  and  $\mathcal{L}_{ij,2}$  are polytopes defined by  $S_{ij,1}, R_{ij,1}, L_{ij,1}, S_{ij,2}, R_{ij,2}, L_{ij,2} \in$

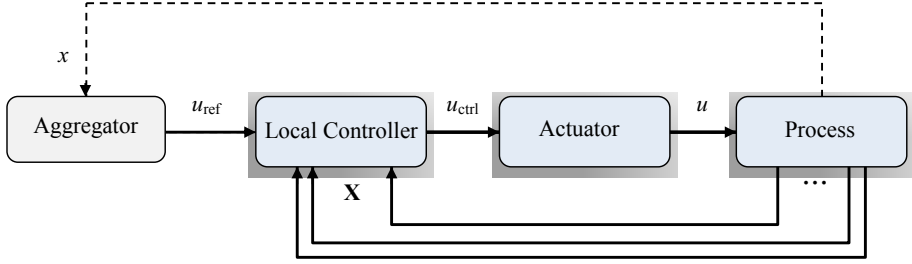


Figure 2.4: Simple sketch of a local DER setup for the power reference following scenario

$\mathbb{R}$ . The corresponding discrete-time system is given in (2.6). A polytopic uncertainty set is assumed as shown in (2.7)-(2.8), where  $\text{Co}$  denotes the convex hull and  $[\alpha_{ij,1}^k, \beta_{ij,1}^k]$ ,  $[\alpha_{ij,2}^k, \beta_{ij,2}^k]$ , are vertices of the uncertainty set.

$$x_{ij}(t+1) = \begin{cases} (A_{ij,1} + \alpha_{ij,1})x_{ij}(t) + (B_{ij,1} + \beta_{ij,1})u_{ij}(t) & \text{if } \begin{bmatrix} x_{ij} \\ u_{ij} \end{bmatrix} \in \mathcal{L}_{ij,1} \\ (A_{ij,2} + \alpha_{ij,2})x_{ij}(t) + (B_{ij,2} + \beta_{ij,2})u_{ij}(t) & \text{if } \begin{bmatrix} x_{ij} \\ u_{ij} \end{bmatrix} \in \mathcal{L}_{ij,2} \end{cases} \quad (2.6)$$

$$[\alpha_{ij,1}, \beta_{ij,1}] \in \text{Co}\{[\alpha_{ij,1}^1, \beta_{ij,1}^1], \dots, [\alpha_{ij,1}^{l_{ij,1}}, \beta_{ij,1}^{l_{ij,1}}]\} \quad (2.7)$$

$$[\alpha_{ij,2}, \beta_{ij,2}] \in \text{Co}\{[\alpha_{ij,2}^1, \beta_{ij,2}^1], \dots, [\alpha_{ij,2}^{l_{ij,2}}, \beta_{ij,2}^{l_{ij,2}}]\} \quad (2.8)$$

Figure 2.4 shows a simple sketch of a local setup at the consumer site. The local controller has the full knowledge of the process denoted by  $X$ , to control the system in detail and the aggregator aims to send an external command,  $u_{\text{ref}}$ , to follow. However, as we emphasize above, the aggregator is not required to have the full knowledge, since the aggregator would not intend and it is out of the scope of its responsibilities to control all individual parameters in the separate subsystems. We assume, the system behaves roughly like a first-order system, characterized by  $x$ . The uncertainties are included in the model to permit deviations from this simplistic model.

The above model is a mixed logical dynamical system. To model the logical part of the system, we define an auxiliary binary variable,  $\sigma_{ij}(t) \in \{0, 1\}$  such that (2.9) holds.

$$\begin{bmatrix} x_{ij} \\ u_{ij} \end{bmatrix} \in \mathcal{L}_{ij,1} \iff \sigma_{ij}(t) = 1 \quad (2.9)$$

Moreover, two auxiliary real variables,  $z_{ij}(t)$  and  $y_{ij}(t)$ , are needed as (2.10) and (2.11). Thereafter, the system dynamics can be represented by (2.12).

$$z_{ij}(t) \triangleq x_{ij}(t)\sigma_{ij}(t) \quad (2.10)$$

$$y_{ij}(t) \triangleq u_{ij}(t)\sigma_{ij}(t) \quad (2.11)$$

$$\begin{aligned} x_{ij}(t+1) = & (A_{ij,2} + \alpha_{ij,2})x_{ij}(t) + (B_{ij,2} + \beta_{ij,2})u_{ij}(t) \\ & + (A_{ij,1} + \alpha_{ij,1} - A_{ij,2} - \alpha_{ij,2})z_{ij}(t) + (B_{ij,1} + \beta_{ij,1} - B_{ij,2} - \beta_{ij,2})y_{ij}(t) \end{aligned} \quad (2.12)$$

The equation (2.9) cannot be directly used in the optimization problem and the equations (2.10) and (2.11) are also products between the two decision variables. We use the techniques proposed in [57] to convert these equations to mixed-integer linear inequalities. The equation (2.9) can be replaced by inequalities (2.13)-(2.14) and the equations (2.10)-(2.11) can be replaced by (2.15)-(2.22).

$$S_{ij,1}x_{ij}(t) + R_{ij,1}u_{ij}(t) - L_{ij,1} \leq M_{ij}(1 - \sigma_{ij}(t)) \quad (2.13)$$

$$S_{ij,1}x_{ij}(t) + R_{ij,1}u_{ij}(t) - L_{ij,1} \geq \epsilon + (m_{ij} - \epsilon)\sigma_{ij}(t) \quad (2.14)$$

$$z_{ij}(t) \leq M_{ij,x}\sigma_{ij}(t) \quad (2.15)$$

$$z_{ij}(t) \geq m_{ij,x}\sigma_{ij}(t) \quad (2.16)$$

$$y_{ij}(t) \leq M_{ij,u}\sigma_{ij}(t) \quad (2.17)$$

$$y_{ij}(t) \geq m_{ij,u}\sigma_{ij}(t) \quad (2.18)$$

$$z_{ij}(t) \leq x_{ij}(t) - m_{ij,x}(1 - \sigma_{ij}(t)) \quad (2.19)$$

$$z_{ij}(t) \geq x_{ij}(t) - M_{ij,x}(1 - \sigma_{ij}(t)) \quad (2.20)$$

$$y_{ij}(t) \leq u_{ij}(t) - m_{ij,u}(1 - \sigma_{ij}(t)) \quad (2.21)$$

$$y_{ij}(t) \geq u_{ij}(t) - M_{ij,u}(1 - \sigma_{ij}(t)) \quad (2.22)$$

where,

$$M_{ij} \triangleq \max_{[x_{ij}, u_{ij}] \in \mathcal{L}_{ij}} \{S_{ij,1}x_{ij}(t) + R_{ij,1}u_{ij}(t) - L_{ij,1}\} \quad (2.23)$$

$$m_{ij} \triangleq \min_{[x_{ij}, u_{ij}] \in \mathcal{L}_{ij}} \{S_{ij,1}x_{ij}(t) + R_{ij,1}u_{ij}(t) - L_{ij,1}\} \quad (2.24)$$

$$M_{ij,x} \triangleq \max_{x_{ij} \in \mathcal{L}_{ij}} \{x_{ij}\} \quad (2.25)$$

$$m_{ij,x} \triangleq \min_{x_{ij} \in \mathcal{L}_{ij}} \{x_{ij}\} \quad (2.26)$$

$$M_{ij,u} \triangleq \max_{u_{ij} \in \mathcal{L}_{ij}} \{u_{ij}\} \quad (2.27)$$

$$m_{ij,u} \triangleq \min_{u_{ij} \in \mathcal{L}_{ij}} \{u_{ij}\} \quad (2.28)$$

and  $\epsilon$  is a small positive number in the above equations.

### 2.2.2 Constraints

Each dynamical system is subject to physical constraints. In the power reference following scenario, we can change the power within a specified limit that is forced by the nominal consumption of each unit. This imposes the input constraint to the system, since the input is defined as power consumption deviation from the baseline power,  $u_{ij}(t) = P_{ij}(t) - P_{ij,\text{base}}(t)$ :

$$u_{ij,\min} \leq u_{ij}(t) \leq u_{ij,\max} \quad (2.29)$$

The offered flexibility is restricted due to physical limitations or the limitations considered by the local controller to optimally operate the system. This imposes the state constraint to the system:

$$x_{ij,\min} \leq x_{ij}(t) \leq x_{ij,\max} \quad (2.30)$$



In the model presented above, we assume the system input can be changed continuously. In practice, there might be on/off devices which can only operate in discrete manner. Moreover, for any practical reasons, there might be situations, where we can only assign some specific discrete levels to the system. To model these cases, we assume a system which is composed of several on/off units. For instance, suppose a TES with  $l_{ij}$  on/off compressors and let  $c_{ij,k}$  ( $k = 1, \dots, l_{ij}$ ) denotes the status of each compressor:

$$c_{ij,k}(t) = \begin{cases} 1 & \text{compressor is on} \\ 0 & \text{compressor is off} \end{cases} \quad (2.31)$$

Then, different discrete levels can be constructed by expressing the system input as below:

$$u_{ij}(t) = [p_{ij,1} \ p_{ij,2} \ \dots \ p_{ij,l_{ij}}] \times \begin{bmatrix} c_{ij,1}(t) \\ c_{ij,2}(t) \\ \vdots \\ c_{ij,l_{ij}}(t) \end{bmatrix} - P_{ij,\text{base}}(t) \quad (2.32)$$

where  $p_{ij,k}$  ( $k = 1, \dots, l_{ij}$ ) are constant values which indicate the power consumption of each compressor when it is turned on and  $P_{ij,\text{base}}$  is the baseline consumption of the TES. To exactly generate  $p_{ij,1}, p_{ij,2}, \dots, p_{ij,l_{ij}}$  levels, we need to add the following constraint:

$$\sum_{k=1}^{l_{ij}} c_{ij,k}(t) = 1 \quad (2.33)$$

For on/off devices, the system might be subject to run-time/stop-time constraints as well. When the compressor is turned on, we cannot turn it off immediately and vice versa, or the system cannot switch from one level to the other instantly. Same as [58], we apply this constraint with the following if/then conditions:

$$\text{if } c_{ij,k}(t) - c_{ij,k}(t-1) = 1 \quad \text{then} \quad \sum_{q=1}^{d_{ij}} c_{ij,k}(t-q) = 0 \quad (2.34)$$

$$\text{if } c_{ij,k}(t-1) - c_{ij,k}(t) = 1 \quad \text{then} \quad \sum_{q=1}^{d_{ij}} c_{ij,k}(t-q) = d_{ij} \quad (2.35)$$

Equation (2.34) prevents the compressor to be turned on, unless it has been off for at least  $d_{ij}$  samples. Equation (2.35) forces the compressor to stay on for at least  $d_{ij}$  samples from when it starts to work. Again, we can use the techniques in [57] to convert (2.34) and (2.35) to linear inequalities. To this end, we associate auxiliary binary variables,  $\eta_{ij,k}(t) \in \{0, 1\}$  and  $\gamma_{ij,k}(t) \in \{0, 1\}$  to the above conditions:

$$c_{ij,k}(t) - c_{ij,k}(t-1) = 1 \iff \eta_{ij,k}(t) = 1 \quad (2.36)$$

$$c_{ij,k}(t-1) - c_{ij,k}(t) = 1 \iff \gamma_{ij,k}(t) = 1 \quad (2.37)$$

Then, equations (2.36) and (2.37) can be rewritten as below:

$$f_{ij,k}(t) \leq 0 \iff \eta_{ij,k}(t) = 1 \quad (2.38)$$

$$g_{ij,k}(t) \leq 0 \iff \gamma_{ij,k}(t) = 1 \quad (2.39)$$

where,

$$f_{ij,k}(t) = 1 + c_{ij,k}(t-1) - c_{ij,k}(t) \quad (2.40)$$

$$g_{ij,k}(t) = 1 + c_{ij,k}(t) - c_{ij,k}(t-1) \quad (2.41)$$

Equations (2.38) and (2.39) can be replaced with the following inequalities:

$$f_{ij,k}(t) \geq \epsilon(1 - \eta_{ij,k}(t)) \quad (2.42)$$

$$f_{ij,k}(t) \leq 2(1 - \eta_{ij,k}(t)) \quad (2.43)$$

$$g_{ij,k}(t) \geq \epsilon(1 - \gamma_{ij,k}(t)) \quad (2.44)$$

$$g_{ij,k}(t) \leq 2(1 - \gamma_{ij,k}(t)) \quad (2.45)$$

In addition, we need to add the equality constraints:

$$\mu_{ij,k}(t) = 0 \quad (2.46)$$

$$\nu_{ij,k}(t) = d_{ij}\gamma_{ij,k}(t) \quad (2.47)$$

where,  $\mu_{ij,k}$  and  $\nu_{ij,k}$  are auxiliary integer variables defined as:

$$\mu_{ij,k}(t) = \eta_{ij,k}(t) \sum_{q=1}^{d_{ij}} c_{ij,k}(t-q) \quad (2.48)$$

$$\nu_{ij,k}(t) = \gamma_{ij,k}(t) \sum_{q=1}^{d_{ij}} c_{ij,k}(t-q) \quad (2.49)$$

Given (2.46) and (2.47), yields the right-hand side of (2.34) and (2.35) hold, when  $\eta_{ij,k}(t) = 1$  and  $\gamma_{ij,k}(t) = 1$ . Finally, (2.48) and (2.49) can be replaced with the following inequalities:

$$\mu_{ij,k}(t) \leq d_{ij}\eta_{ij,k}(t) \quad (2.50)$$

$$\mu_{ij,k}(t) \geq 0 \quad (2.51)$$

$$\nu_{ij,k}(t) \leq d_{ij}\gamma_{ij,k}(t) \quad (2.52)$$

$$\nu_{ij,k}(t) \geq 0 \quad (2.53)$$

$$\mu_{ij,k}(t) \leq \sum_{q=1}^{d_{ij}} c_{ij,k}(t-q) \quad (2.54)$$

$$\nu_{ij,k}(t) \leq \sum_{q=1}^{d_{ij}} c_{ij,k}(t-q) \quad (2.55)$$

$$\mu_{ij,k}(t) \geq -d_{ij}(1 - \eta_{ij,k}(t)) + \sum_{q=1}^{d_{ij}} c_{ij,k}(t-q) \quad (2.56)$$

$$\nu_{ij,k}(t) \geq -d_{ij}(1 - \gamma_{ij,k}(t)) + \sum_{q=1}^{d_{ij}} c_{ij,k}(t-q) \quad (2.57)$$

With having (2.46) and (2.47), we can disregard (2.51) and (2.52) though. In above equations,  $\epsilon$  is a small positive number.

The above model and constraints can describe the aforementioned features of a DER. The parameters  $(A_{ij,1} + \alpha_{ij,1})$  and  $(A_{ij,2} + \alpha_{ij,2})$  specify whether the TES is leaky or not in each operation mode. Efficiency in conversion or the COP of the system is reflected in  $(B_{ij,1} + \beta_{ij,1})$  and  $(B_{ij,2} + \beta_{ij,2})$ . Power and energy capacity are defined with input and state constraints. Run-time/stop-time constraints are also taken into account. We can list more features in addition to these. For instance, different TESs may have different operational costs or there may be other constraints than the power and energy constraints in the process of energy conversion such as pressure constraints etc. However, capturing all the features will lead to a complicated setup that is not applicable in practice.

### 2.3 Objective Function at the Aggregator

As stated in Section 2.1, we consider the following scenario: “The aggregator is paid by the grid operator to follow a power reference it receives within an activation period”. This implies the aggregator to change normal power consumption, known as baseline power. In general, the aggregator will see one of these situations at the beginning of the activation:

1. The power reference is greater than the aggregated baseline power
2. The power reference is lower than the aggregated baseline power

In other words, for the “Aggregator  $i$ ”, we have:

$$1. P_i \geq \sum_{j=1}^{n_i} P_{ij,\text{base}} \text{ (down-regulating)} \quad (2.58)$$

$$2. P_i \leq \sum_{j=1}^{n_i} P_{ij,\text{base}} \text{ (up-regulating)} \quad (2.59)$$

where,  $P_{ij,\text{base}}$  denotes the baseline power consumption of each unit. In the first case (2.58), the aggregator is able to offer downward regulating power while, in the second case (2.59), the aggregator can offer upward regulating power. In the following, we explain how we formulate the objective function at the aggregator for these two cases. First we describe our early study in this regard. Then, we explain how we improve the proposed objective function. Note that the following assumptions are considered in the rest of the thesis, unless otherwise stated:

- Consumers are naturally available to increase their power consumption. This assumption can be true in practice. For instance, at the supermarket, the temperature of cold rooms and display cases are normally kept close to the maximum level in order to reduce the power consumption.
- Consumers are continuous type, meaning that the power can be changed in a continuous manner and the units are not subject to run-time/stop-time constraints

### 2.3.1 Preliminary Formulation for Down-regulating Scenario

In this work, we deal with energy storages. Thus, a natural perspective is to formulate the objective function such that either the energy consumption is minimized or the energy saving is maximized. In the down regulating scenario, the aggregator is asked to increase its total power consumption. Thus, the aggregator needs to store some extra energy in the thermal storages at its disposal. The idea is to store as much energy as possible during the activation. After the activation, the aggregator can benefit by decreasing its normal consumption and use the stored energy, i.e. the profit of the aggregator is achieved from its energy saving at the end of activation. The objective function for “aggregator  $i$ ” is as follows:

$$\max_{u_{ij}, z_{ij}, y_{ij}, \sigma_{ij} (j=1,2,\dots,n_i)} \sum_{j=1}^{n_i} x_{ij}(N_{\text{act}}) \quad (2.60)$$

$N_{\text{act}}$  in (2.60) is the number of samples during the activation time and  $x_{ij}(N_{\text{act}})$  denotes the system state at the end of activation time. With this objective function, the aggregator maximizes the total thermal energy that will be stored in its TESs at the end of activation time.

### 2.3.2 Down-regulating and Up-regulating Formulation

The formulation provided in (2.60) can be improved in a way that exactly reflects the energy saving after the activation. In this part we present our proposed formulation for both upward and downward regulating power. To formulate the objective function, we divide the operation time into three time periods: before the activation, activation time and after the activation. Figure (2.5) shows thermal energy changes and power consumption of a typical TES during these three time periods. Under normal circumstances, when there is no activation, consumers consume the amount of power they require to run their systems in the optimal manner defined by the local controller. This power is called the baseline power,  $P_{\text{base}}$ . Baseline power can vary from time to time during a day, based on the weather conditions. However, we can reasonably assume it to be constant during an hour or so.

First let us consider the down-regulating scenario. During the down-regulation activation time, the total consumption is above the aggregated baseline power. As stated above, the aggregator has the chance to save some extra energy in its thermal storages during the activation. Right after the activation, the aggregator can benefit from this saving by using the stored energy and lowering its consumption to under baseline consumption. Thus, the optimal is to retrieve as much energy as we can after the activation. The objective function for the down-regulating scenario is formulated as bellow:

$$\max_{u_{ij}, z_{ij}, y_{ij}, \sigma_{ij} (j=1,2,\dots,n_i)} \Phi_i = \sum_{j=1}^{n_i} (P_{ij,\text{base}} - P_{ij,\text{min}}) T_{ij,\text{off}} \quad (2.61)$$

where,  $T_{ij,\text{off}}$  represents the period after the activation when the consumer decreases its consumption from the baseline,  $P_{ij,\text{base}}$ , to the minimum level,  $P_{ij,\text{min}}$ . In case of no activation, the consumer needs to consume at least the baseline consumption during this period. Thus, the consumer is able to save power corresponding to  $P_{ij,\text{base}} - P_{ij,\text{min}}$  at

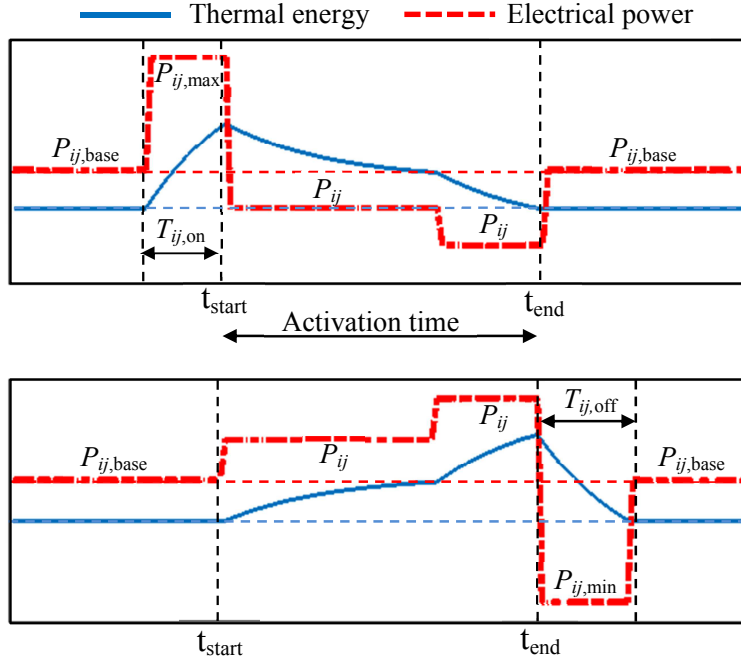


Figure 2.5: Typical power consumption profile and the stored thermal energy of the TES  $ij$  for the up-regulating (upper figure) and the down-regulating (lower figure). The interval  $[t_{\text{start}}, t_{\text{end}}]$  is called the activation time.  $T_{ij,\text{on}}$  and  $T_{ij,\text{off}}$  indicate the on-time and off-time periods respectively.

each time instant during  $T_{ij,\text{off}}$ . In fact,  $\Phi_{ij}$  is the energy saving after the activation. Reducing the power consumption to the minimum level minimizes the time needed for regaining the stored energy and consequently minimizes the heat loss to the surrounding. In other words, it is optimal to deplete the energy as fast as possible to minimize the loss. The problem in the up-regulating scenario is symmetric to the down-regulation. During the up-regulation activation time, the total consumption is below the aggregated baseline power. In this case, the aggregator needs to store some energy before the activation in order to deliver it during the activation time. The objective function for the up-regulating scenario is formulated as below:

$$\min_{u_{ij}, z_{ij}, y_{ij}, \sigma_{ij} (j=1, 2, \dots, n_i)} \Psi_i = \sum_{j=1}^{n_i} (P_{ij,\text{max}} - P_{ij,\text{base}}) T_{ij,\text{on}} \quad (2.62)$$

where,  $T_{ij,\text{on}}$  is the period before the activation when the consumer increases its consumption from the baseline to the maximum level,  $P_{ij,\text{max}}$  to store the required energy. The consumer has to consume  $P_{ij,\text{max}} - P_{ij,\text{base}}$  more than its normal operation at each time instant during  $T_{ij,\text{on}}$ .  $\Psi_{ij}$  is the cost, in terms of energy consumption, that should be paid by the aggregator. Similar to the first case, it is better to save the energy as fast as possible during the  $T_{ij,\text{on}}$  to minimize the loss. That is why the consumer consumes its

maximum power before the activation

The proposed objective functions (2.61) and (2.62) rely on  $T_{ij,\text{off}}$  and  $T_{ij,\text{on}}$ . In general,  $T_{ij,\text{off}}$  and  $T_{ij,\text{on}}$  are non-linear functions of the state of the charge at the end and at the beginning of the activation respectively. For the piece-wise linear dynamic (2.2), the function is a logarithmic function whose parameters can vary depending on the set definitions,  $\mathcal{L}_{ij,1}$  and  $\mathcal{L}_{ij,2}$ . For example, in a special case, when  $S_{ij,1} = L_{ij,1} = S_{ij,2} = L_{ij,2} = 0$ ,  $R_{ij,1} = -1$ ,  $R_{ij,2} = 1$ ,  $T_{ij,\text{off}}$  and  $T_{ij,\text{on}}$  can be obtained as below for the  $j$ th TES belonging to “Aggregator  $i$ ”:

$$T_{ij,\text{off}} = \frac{-1}{A_{ij,c1} + \alpha_{ij,c1}} \ln \left( 1 + \frac{(A_{ij,c1} + \alpha_{ij,c1})x_{ij}(N_{\text{act}})}{(B_{ij,c1} + \beta_{ij,c1})u_{ij,\text{min}}} \right) \quad (2.63)$$

$$T_{ij,\text{on}} = \frac{1}{A_{ij,c2} + \alpha_{ij,c2}} \ln \left( 1 + \frac{(A_{ij,c2} + \alpha_{ij,c2})x_{ij}(1)}{(B_{ij,c2} + \beta_{ij,c2})u_{ij,\text{max}}} \right) \quad (2.64)$$

where  $x_{ij}(N_{\text{act}})$  and  $x_{ij}(1)$  are the state of the charge of the system at the end and at the beginning of the activation time. As can be seen from equations (2.63) and (2.64),  $T_{ij,\text{off}}$  and  $T_{ij,\text{on}}$  also depend on the system parameters. Thus, with assuming uncertain parameters, that can vary within some intervals,  $T_{ij,\text{off}}$  and  $T_{ij,\text{on}}$  can vary as well. Although, it is not easy to analytically assess how  $T_{ij,\text{off}}$  and  $T_{ij,\text{on}}$  vary with change in system parameters, we can provide a rule by knowing the real physical meaning of the system parameters. A higher  $A_{ij} + \alpha_{ij}$  and  $B_{ij} + \beta_{ij}$  in each operating mode, imply a lower heat loss and a higher COP or generally a better TES. This implicitly means, the maximum of  $T_{ij,\text{off}}$  and the minimum of  $T_{ij,\text{on}}$  are achieved for the maximum of  $A_{ij} + \alpha_{ij}$  and  $B_{ij} + \beta_{ij}$  in each mode; since a better TES should have a longer  $T_{ij,\text{off}}$  and a shorter  $T_{ij,\text{on}}$ . Later, in Chapter 3, we will explain which parameters we should choose, within the uncertainty set, to develop a robust setup.

## 2.4 Information Flow

Basically, each consumer should communicate the information which describes the flexibility model and constraints to its own aggregator. The constant parameters can be transmitted once before the activation, whereas the time-varying parameters can be transmitted at each sampling time during the activation. In Chapter 6, we will provide the detailed information exchange for our specific case studies. The standard information exchange are, however listed in Table 2.1.

Parameters	Description
$A_{ij,1}, A_{ij,2}, B_{ij,1}, B_{ij,2}$	Nominal parameters of the flexibility model
$[\alpha_{ij,1}^k, \beta_{ij,1}^k], [\alpha_{ij,2}^k, \beta_{ij,2}^k]$	Vertices of the uncertainty set
$u_{ij,\text{min}}, u_{ij,\text{max}}$	Minimum and maximum power deviation
$x_{ij,\text{min}}, x_{ij,\text{max}}$	Minimum and maximum thermal energy changes
$P_{ij,\text{base}}$	Baseline power consumption

Table 2.1: Standard information exchange between the  $j$ th consumer belongs to “Aggregator  $i$ ”

## 2.5 Interactions Between the Aggregators and the Grid Operator

In the hierarchical setup shown in Figure (2.1), we assume several aggregators and the grid operator aims to provide  $P_{\text{reference}}$  from all of them. Therefore, a question arises: How the power distribution from the grid operator to the aggregators should be, where there are different aggregators with different capacities and costs. For this level, we consider a one-time optimization. The mechanism is as follows. Based on the profit function and the cost function formulation suggested in (2.61) and (2.62), the total profit/cost associated to each aggregator is the summation of all the profits/costs of the consumers related to each one. For instance for “Aggregator  $i$ ”:

$$\Phi_i = \sum_{j=1}^{n_i} \Phi_{ij} \text{ (profit function for the down-regulation)} \quad (2.65)$$

$$\Psi_i = \sum_{j=1}^{n_i} \Psi_{ij} \text{ (cost function for the up-regulation)} \quad (2.66)$$

Each aggregator communicates the cost/profit curves to the grid operator which illustrate the cost/profit, in terms of energy, per a specified power reference. Based on this information, the top-level controller performs a one-time optimization to produce  $P_1, P_2, \dots, P_n$ :

$$\min_{P_1, \dots, P_n} \sum_{i=1}^n \Psi_i \text{ (up-regulation)} \quad (2.67)$$

$$\max_{P_1, \dots, P_n} \sum_{i=1}^n \Phi_i \text{ (down-regulation)} \quad (2.68)$$

subject to:

$$P_1 + P_2 + \dots + P_n = P_{\text{reference}} \quad (2.69)$$

$$P_{i,\min} \leq P_i \leq P_{i,\max} \quad (i = 1, \dots, n) \quad (2.70)$$

where,  $P_{i,\min}$  and  $P_{i,\max}$  are the minimum and maximum power consumption of the total consumers controlled by “Aggregator  $i$ ”. These power flows ( $P_1, \dots, P_n$ ) will be fixed during the activation period.

## 2.6 Summary

In this chapter, we introduced a three-level hierarchical structure to employ the flexibility of industrial thermal loads in the future electricity market. The setup consists of a top-level controller which is located at the grid operator (BRP, TSO or DSO) and a set of aggregators, each of which controls a number of consumers. Based on a contract agreement, each aggregator is asked by the top-level controller to follow a specified power during an activation time. Likewise, the aggregator is given a permission to send power references to the consumers. We consider an optimal controller at the top-level which receives cost/profit curves per a specified power reference. Having this information, it provides the optimal power distribution. At the aggregator, we formulated the objective function for both upward and downward regulating power. The aggregator requires a

model of consumption units to run the optimization. A piecewise linear model with multiplicative uncertainties is considered for this purpose. This model is subject to several constraints. There are input and state constraints because of physical limitations at the consumer site. Moreover, to use the model in the optimization problem, the logical part of the model needs to be converted to the linear inequalities.





## 3 | Proposed Robust Design

In previous chapter, we proposed an aggregator setup with the following features:

- The aggregator aggregates the flexibilities of a few large-scale industrial thermal loads in a three-level hierarchical setup.
- The setup is based on direct control and data is exchanged between the aggregator and the consumers.
- The aggregator is asked to follow a specified power reference from a top-level controller within a certain period of time (activation time).
- The aggregator optimizes the power distribution for two cases: when the power reference is greater than the aggregated baseline consumption and when it is lower.

In the proposed setup, we deliberately used simplified models of the consumers at the aggregator, even though the physical systems are known to be more complicated. Otherwise, the setup is not applicable in practice. Rather than having to increase the model complexity on the aggregator level, in this chapter, we propose two methods to compensate for the deviation arising from the model mismatch. In the first method, we consider the model mismatch as state-dependent uncertainties and propose a simple feedback mechanism for re-distributing power discrepancies among other consumers. We analyze the potential state trajectories subject to said uncertainties, and propose a brute-force approach to determine how large uncertainties the setup can handle over a given activation horizon. In the second method, instead of the aforementioned feedback mechanism, we include the uncertainties inside the controller at the aggregator. This approach leads to a robust model predictive controller (MPC) framework in which the model structure is known. However, the model parameters are allowed to vary within a predefined convex set as explained in Chapter 2. Since, we apply model predictive controller at the aggregator level, the basic idea behind the MPC is explained briefly in the following as well.

### 3.1 Model Predictive Control

The underlying idea of MPC is to optimize the system behaviour at the current time, while the future behaviour of the system is taken into account. The main advantage of MPC, compared to other advanced methods, is its ability to deal with constraints [59]. MPC depends on the model of system to predict the future behaviour. More specifically, at time  $t$ , the current state of the system is available (either from measurement or estimation)

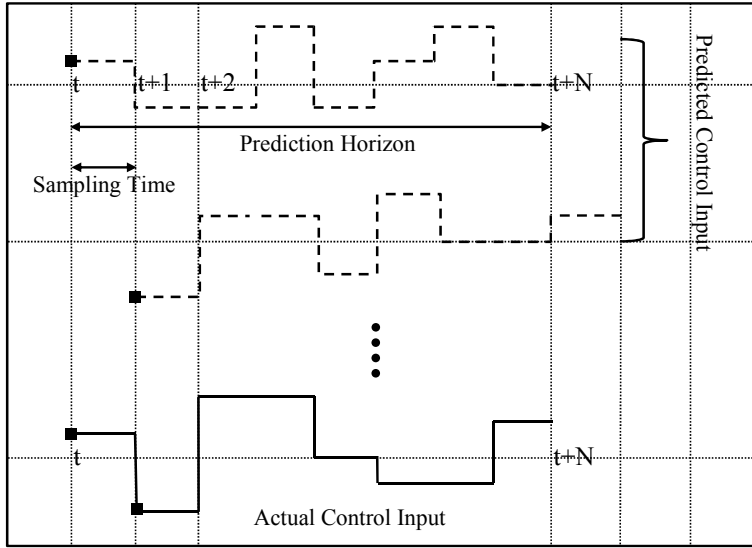


Figure 3.1: Basic idea of MPC: At each sampling time, the control input is calculated over a time horizon,  $N$ , and only the first sample is applied to the real system

and the future state is calculated from the model. Then, a cost minimizing function is computed over a finite prediction horizon to produce the control input. This provides the control input for the whole prediction horizon, however, only the first sample is applied to the real system. These steps are repeated at the next sampling time again. Thus, at each sampling time, the control input is calculated over a time horizon and the first sample is used each time [60]. The idea is depicted in Figure 3.1. Although the standard formulation for MPC is based on a linear state space model of the system and a quadratic cost function, the general formulation can be expressed as follows:

$$\min_{u(t), \dots, u(t+N-1)} \sum_{\tau=t}^{t+N} \ell(x(\tau), u(\tau)) \quad (3.1)$$

Subject to :

$$x(t+i+1) = F(x(t+i), u(t+i)) \quad (3.2)$$

$$x_{\min} \leq x(t+i+1) \leq x_{\max} \quad (3.3)$$

$$u_{\min} \leq u(t+i) \leq u_{\max} \quad (3.4)$$

$$x(t) = x_0 \quad (i = 0, \dots, N-1) \quad (3.5)$$

where,  $x(t)$ ,  $u(t)$ ,  $x_0$  and  $N$  are the controlled variable, manipulated variable, known initial state and prediction horizon respectively.  $F(\cdot)$  represents the model of the system. As mentioned above, the variables must respect the specified constraints throughout the horizon as well.

In the power reference following setup, we have an MPC-like controller at the aggregator, where we optimize objective functions (2.61) and (2.62) while respecting the equations (2.12)-(2-22), (2.29), (2.30) and also satisfying the power reference following

shown in (2.1). The controller is run at each sampling time, having the necessary information as listed in Table 2.1. This provides a vector of power consumption for each consumer by the end of activation period. The first sample indicates the desired power consumption each unit is asked to follow at current time. In the following, we will explain how to improve this setup to compensate for the deviation arising from the model mismatch, i.e. the complex model of the real system and the simplified model we use for the MPC.

### 3.2 Feedback Mechanism

In reality, the physical systems are non-linear and of high order. However, the aggregator does not know a perfect model of the consumers and utilizes simple models (first order piece-wise linear) in the optimization process. This model mismatch may lead to actual power deviation from the desired power reference. In the following, we propose a simple strategy to deal with this mismatch, and examine the potential ramifications of it. Suppose, there are  $n$  consumers under the control of an aggregator, each of which is described with the first order flexibility model as  $x_i(t+1) = A_i x_i(t) + B_i u_i(t)$ . Each consumer receives a power reference,  $P_{i,\text{ref}}$  ( $i = 1, \dots, n$ ) and equivalently, an input reference,  $u_{i,\text{ref}}$  ( $i = 1, \dots, n$ ), since  $u_{i,\text{ref}} = P_{i,\text{ref}} - P_{i,\text{base}}$ . However, due to model mismatch etc., the actual consumption,  $u_{i,\text{act}}$  ( $i = 1, \dots, n$ ), might be forced to deviate from  $u_{i,\text{ref}}$  by some amount  $\varepsilon_i$ , i.e.,  $u_{i,\text{act}} = u_{i,\text{ref}} + \varepsilon_i$ . It seems reasonable that, although  $\varepsilon_i$  is considered to be unknown by the aggregator, it should be limited to an interval proportional to the current state of the  $i$ th consumer, i.e.,  $\varepsilon \in [\delta_{i,\min} X_i(t), \delta_{i,\max} X_i(t)]$ , where  $\delta_{i,\min}$  and  $\delta_{i,\max}$  are scalars, consumer-specific constants. Taking advantage of convexity of this set, we will write the actual consumption as:

$$u_{i,\text{act}} = u_{i,\text{ref}} + \Delta_i x_i \quad (i = 1, \dots, n) \quad (3.6)$$

This assumption is reasonable since there will be larger deviation for larger energy changes. The goal remains to maintain the combined power consumption of the  $n$  units at  $P_{\text{reference}}$  for the interval  $[t_{\text{start}}, t_{\text{end}}]$ , which implies that the following constraint has to be imposed:

$$\sum_{i=1}^n u_{i,\text{act}} - \sum_{i=1}^n u_{i,\text{ref}} = \sum_{i=1}^n \Delta_i x_i = 0 \quad (3.7)$$

Instead of using complicated models or any other solutions such as having negotiation between the entities, we propose a setup consists of a series of feedback loop as illustrated in Figure 3.2

As shown in Figure 3.2, we have added  $(n-1)$  feedback gains per consumer which propagate the deviation signal to the rest of consumers in order to compensate the deviation. This implies that consumer  $j$  will be requested to consume an extra contribution:

$$u_{j,\text{add}} = \sum_{\substack{i=1 \\ i \neq j}}^n K_{ij} (u_{i,\text{act}} - u_{i,\text{ref}}) \quad (3.8)$$

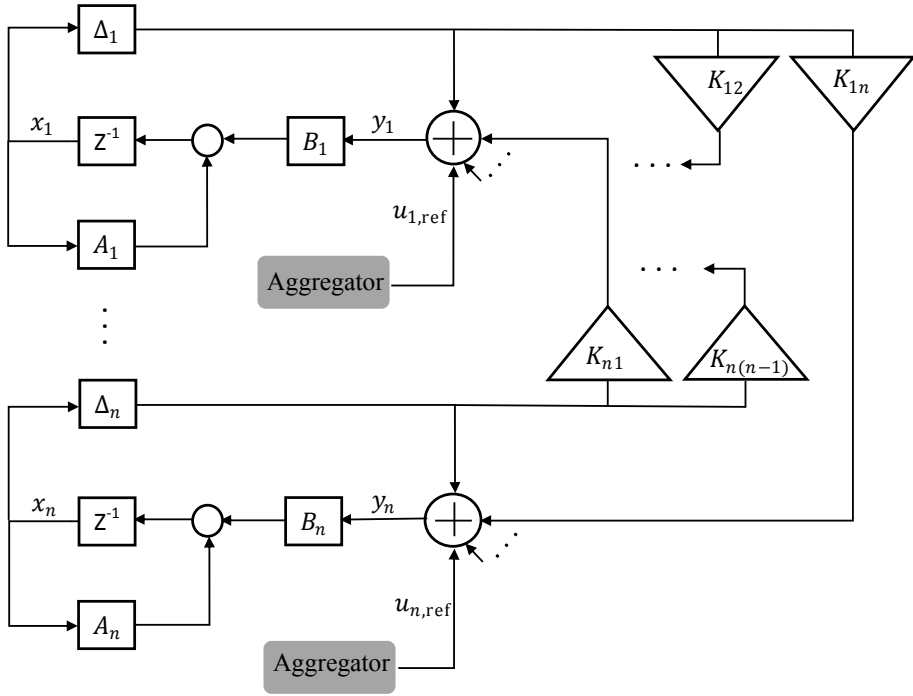


Figure 3.2: Feedback controller design to compensate for the deviation arising from the model mismatch, where we redistribute the discrepancies among the consumers

yielding the state equation:

$$x_j(t+1) = A_j x_j(t) + B_j \left( \Delta_j x_j(t) + u_{j,\text{ref}} + \sum_{\substack{i=1 \\ i \neq j}}^n K_{ij} \Delta_i x_i(t) \right) \quad (3.9)$$

Thus, we have  $n \times (n - 1)$  proportional controllers in the whole setup. The following state space model describes the whole system:

$$X(t+1) = (A + BK\Delta) X(t) + BU_{\text{ref}}(t) \quad (3.10)$$

where  $X(t) = [x_1(t) \dots x_n(t)]' \in \mathbb{R}^n$ ,  $U_{\text{ref}}(t) = [u_{1,\text{ref}}(t) \dots u_{n,\text{ref}}(t)]' \in \mathbb{R}^n$  and

$$A = \begin{bmatrix} A_1 & 0 \\ & \ddots \\ 0 & A_n \end{bmatrix}, \quad B = \begin{bmatrix} B_1 & 0 \\ & \ddots \\ 0 & B_n \end{bmatrix}, \quad \Delta = \begin{bmatrix} \Delta_1 & 0 \\ & \ddots \\ 0 & \Delta_n \end{bmatrix}$$

$$K = \begin{bmatrix} 1 & K_{21} & \dots & K_{n1} \\ K_{12} & 1 & \dots & K_{n2} \\ \vdots & \vdots & \ddots & \vdots \\ K_{1n} & K_{2n} & \dots & 1 \end{bmatrix}$$

In the above expression, we have  $\Delta \in \text{Co}\{\nabla_1, \nabla_2, \dots, \nabla_{2^n}\}$ , where each  $\nabla_i$  represents a vertex of the hypercube  $[\delta_{i,\min}, \delta_{i,\max}]^n$ . A natural choice for the feedback gains is  $K_{ij} = \frac{-1}{n-1}$ , ( $i, j = 1, \dots, n$ ) which means to propagate the error signal evenly. Generally, to compensate the error, equation (3.11) should hold:

$$\sum_{i=1}^n K(i, j) = 0 \quad (j = 1, \dots, n) \quad (3.11)$$

where,  $K(i, j)$  denotes the  $ij$ th element of the matrix,  $K$ .

### 3.2.1 Constraints vs. Uncertainties

As can be seen from the above, the system consisting of several consumers in parallel, combined with the proposed compensating feedback connections, is now a state-constrained linear system in a feedback loop with a structured uncertainty block. Unfortunately, the situation is not a standard robust control design problem, since the input has already been determined by the MPC scheme of the aggregator. We can safely assume that the *nominal* state trajectory computed by the MPC algorithm will remain within the state constraints, but there is no such guarantee for the uncertain system (3.10).  $(A + BK\Delta)$  is highly likely to have eigenvalues of magnitude greater than 1 for at least some  $\Delta \in \text{Co}\{\nabla_1, \nabla_2, \dots, \nabla_{2^n}\}$ . For instance, assume non-leaky consumers. Then the corresponding eigenvalues of  $A$  have magnitude 1. This implies that we cannot compute any norm bounds on the system in a meaningful manner. Indeed, the final state at the end of the activation,  $X(N_{\text{act}})$ , is given by the equation:

$$X(N_{\text{act}}) = (A + BK\Delta)^{N_{\text{act}}} X(0) + \Gamma \begin{bmatrix} U_{\text{ref}}(0) \\ U_{\text{ref}}(1) \\ \vdots \\ U_{\text{ref}}(N_{\text{act}} - 1) \end{bmatrix} \quad (3.12)$$

where,

$$\Gamma = [(A + BK\Delta)^{N_{\text{act}}-1} B \quad (A + BK\Delta)^{N_{\text{act}}-2} B \quad \dots \quad B] \quad (3.13)$$

from which it is seen that  $\Delta$  appears in a highly non-linear fashion, making even conservative matrix norm-based estimates difficult to compute.  $N_{\text{act}}$  is the number of samples during the activation time. On the other hand, for this specific application, the system only has to remain within the state constraints during the activation time, not indefinitely. Hence, the following question makes sense, even for unstable  $A + BK\Delta$ :

*Problem 1: Given finite  $N_{\text{act}}$  and bounded  $U_{\text{ref}}$ , how large uncertainty set  $[\delta_{i,\min}, \delta_{i,\max}]^n$  can be permitted, such that  $\{X(0), X(1), \dots, X(N_{\text{act}})\} \in \mathcal{X}$ ?*

where  $\mathcal{X}$  is a hypercube defined by the aforementioned state constraints. Since it does not appear to be possible to find analytical estimates, we choose brute-force simulation-based checking as outlined in Algorithm 1.  $0 < \varrho_i, \varsigma_i < 1$  are scalars. Algorithm 1 sequentially tries to simulate the system with ever-shrinking uncertainty sets. For each

simulation run, it breaks out of the simulation if a test trajectory corresponding to one of the vertices of the uncertainty set violates a state constraint. Algorithm 1 is terminated by the stop criterion if it does not break out of the simulation loop, in which case we may try running it again starting with a larger initial set of  $\delta_{i,\min}, \delta_{i,\max}$ , or if  $|\delta_{i,\max} - \delta_{i,\min}|$  drops below some pre-set threshold for some  $i$ .

An alternative approach to compensate the error arises from model mismatch is to incorporate the uncertainties in the aggregator's optimization problem, which then becomes a robust MPC problem. This approach will be explained in the following section.

---

**Algorithm 1** Numerical algorithm for solving *Problem 1*

---

```

1:
  Assume a subset of  $\Delta : \{\bar{\Delta}_1, \bar{\Delta}_2, \dots, \bar{\Delta}_{2^n}\}^*$ 
  for  $i = 0$  to  $i = 2^n$  do
    for  $t = 0$  to  $t = N_{\text{act}}$  do
       $X^i(t+1) = (A + BK\bar{\Delta}_i) X^i(t) + BU_{\text{ref}}(t)$ 
      if  $\exists \tau < N_{\text{act}}$  such that  $X^i(\tau) \notin \mathcal{X}$  then
        break to 2.
      end if
    end for
  end for
2:
   $\delta_{j,\min} \leftarrow \varrho_j \delta_{j,\min} \quad j = 1, \dots, n$ 
   $\delta_{j,\max} \leftarrow \varsigma_j \delta_{j,\max} \quad j = 1, \dots, n$ 
3:
  if stop criterion met then
    terminate
  else
    go to 1
  end if

```

$$* \bar{\Delta}_1 = \begin{bmatrix} \delta_{1,\min} & 0 \\ 0 & \ddots \\ & \delta_{n,\min} \end{bmatrix} \bar{\Delta}_2 = \begin{bmatrix} \delta_{1,\min} & 0 \\ 0 & \ddots \\ & \delta_{n,\max} \end{bmatrix} \dots \bar{\Delta}_{2^n} = \begin{bmatrix} \delta_{1,\max} & 0 \\ 0 & \ddots \\ & \delta_{n,\max} \end{bmatrix}$$


---

### 3.3 Two-stage Optimization

For the robust MPC setup, we assume  $n$  TESs ( $i = 1, \dots, n$ ) under the control of an aggregator. As described in Chapter 2, each consumer has the following model:

$$x_i(t+1) = \begin{cases} (A_{i,1} + \alpha_{i,1})x_i(t) + (B_{i,1} + \beta_{i,1})u_i(t) & \begin{bmatrix} x_i \\ u_i \end{bmatrix} \in \mathcal{L}_{i,1} \\ (A_{i,2} + \alpha_{i,2})x_i(t) + (B_{i,2} + \beta_{i,2})u_i(t) & \begin{bmatrix} x_i \\ u_i \end{bmatrix} \in \mathcal{L}_{i,2} \end{cases} \quad (3.14)$$

Thus, the model of the whole portfolio is as follows:

$$X(t+1) = (A + \Delta_a)X(t) + (B + \Delta_b)U(t) \quad (3.15)$$

where,

$$\begin{aligned} X(t) &\triangleq [x_1(t) \ \dots \ x_n(t)]'_{n \times 1} \\ U(t) &\triangleq [u_1(t) \ z_1(t) \ y_1(t) \ \sigma_1(t) \ \dots \ u_n(t) \ z_n(t) \ y_n(t) \ \sigma_n(t)]'_{4n \times 1} \\ A &\triangleq \begin{bmatrix} A_{1,2} & & 0 \\ & \ddots & \\ 0 & & A_{n,2} \end{bmatrix}_{n \times n} \quad \Delta_a \triangleq \begin{bmatrix} \alpha_{1,2} & & 0 \\ & \ddots & \\ 0 & & \alpha_{n,2} \end{bmatrix}_{n \times n} \\ B &\triangleq \begin{bmatrix} \mathbf{B}_{1,2} & & 0 \\ & \ddots & \\ 0 & & \mathbf{B}_{n,2} \end{bmatrix}_{n \times 4n} \quad \Delta_b \triangleq \begin{bmatrix} \boldsymbol{\beta}_{1,2} & & 0 \\ & \ddots & \\ 0 & & \boldsymbol{\beta}_{n,2} \end{bmatrix}_{n \times 4n} \\ \mathbf{B}_{i,2} &\triangleq [B_{i,2} \quad A_{i,1} - A_{i,2} \quad B_{i,1} - B_{i,2} \quad 0] \\ \boldsymbol{\beta}_{i,2} &\triangleq [\beta_{i,2} \quad \alpha_{i,1} - \alpha_{i,2} \quad \beta_{i,1} - \beta_{i,2} \quad 0] \quad (i = 1, \dots, n) \end{aligned}$$

and the model is subject to mixed constraints in which both the physical constraints (2.29)-(2.30) and the constraints related to the mixed logical models (2.13)-(2.22) are included:

$$FX(t) + GU(t) \leq H \quad (3.16)$$

where  $F \in \mathbb{R}^{14n \times n}$ ,  $G \in \mathbb{R}^{14n \times 4n}$  and  $H \in \mathbb{R}^{14n}$  are constant matrices.

### 3.3.1 Control Formulation

In Chapter 2, the objective function at the aggregator level has been formulated for the down-regulation and up-regulation scenarios as (2.61) and (2.62). They depend on the on-time and off-time periods, denoted by  $T_{i,\text{off}}$  and  $T_{i,\text{on}}$  for the consumer  $i$  respectively. To apply a robust MPC algorithm at the aggregator level in a real time situation, we propose a two-step strategy. The first step is performed long before the activation time. The aggregator solves a one-time optimization problem using the objective functions (2.61) and (2.62). In the second step, based on the information obtained from the first step, the aggregator solves an optimization problem every sampling time during the extended activation time. The extended activation time refers to the activation time, when the units are required to follow the power reference, plus the maximum off-time or on-time periods in the portfolio. In the following, we will explain each step in details:

**First stage:** For the down-regulating scenario, the aggregator performs a profit optimization as follows:

$$\max_{u_i, z_i, y_i, \sigma_i (i=1, \dots, n)} \Phi = \sum_{i=1}^n (P_{i,\text{base}} - P_{i,\text{min}}) T_{i,\text{off}} \quad (3.17)$$

In this optimization, the aggregator uses those system parameters, within the uncertainty set, which produces the maximum profit. Since the profit function is a function of  $T_{i,\text{off}}$ ,



then the aggregator should use the system parameters which produces the maximum  $T_{i,\text{off}}$  for  $k = 1, \dots, n$ . Analytically, it is not straightforward to say which parameters will generate the maximum profit. For example, as mentioned in Chapter 2, for a special case,  $T_{i,\text{off}}$  can be obtained as below:

$$T_{i,\text{off}} = \frac{-1}{A_{i,c1} + \alpha_{i,c1}} \ln \left( 1 + \frac{(A_{i,c1} + \alpha_{i,c1})x_i(N_{\text{act}})}{(B_{i,c1} + \beta_{i,c1})u_{i,\text{min}}} \right) \quad (3.18)$$

In this case,  $T_{i,\text{off}}$  decreases with the increase in  $\beta_{k,c1}$  at first glance. However,  $x_i(N_{\text{act}})$  also increases with the increase in  $\beta_{i,c1}$ , since it is dependent on  $\beta_{i,c1}$ . Moreover, the off-time period for one system is also dependent on the off-time period of the other systems and we are interested in the total profit. Nevertheless, we know the physical interpretation of the system parameters.  $A_{c1}$  and  $B_{c1}$  model the heat loss and efficiency in conversion (COP) of a TES respectively. Thus, the greater  $\alpha_{c1}$  and  $\beta_{c1}$  we have, the more profit we achieve. In other words, for  $i = 1, \dots, n$ :

$$\forall [\alpha_{i,c1}, \beta_{i,c1}] \in \text{Co}\{[\alpha_{i,c1}^1, \beta_{i,c1}^1], \dots, [\alpha_{i,c1}^{l_{i,1}}, \beta_{i,c1}^{l_{i,1}}]\}, \Phi \leq \Phi|_{\max_i\{\alpha_{i,c1}\}, \max_i\{\beta_{i,c1}\}} \quad (3.19)$$

where,  $[\alpha_{i,c1}^k, \beta_{i,c1}^k]$  are vertices of the uncertainty set.

For the up-regulating scenario, the aggregator performs a cost optimization as follows:

$$\min_{u_i, z_i, y_i, \sigma_i (i=1, \dots, n)} \Psi = \sum_{i=1}^n (P_{i,\text{max}} - P_{i,\text{base}})T_{i,\text{on}} \quad (3.20)$$

where,  $T_{i,\text{on}}$  can be obtained as below:

$$T_{i,\text{on}} = \frac{1}{A_{i,c2} + \alpha_{i,c2}} \ln \left( 1 + \frac{(A_{i,c2} + \alpha_{i,c2})x_i(1)}{(B_{i,c2} + \beta_{i,c2})u_{i,\text{max}}} \right) \quad (3.21)$$

In this scenario, the aggregator uses those system parameters, within the uncertainty set, which provide the maximum cost. With the same argument as the down-regulating scenario, we can say the maximum cost is achieved for the minimum  $\alpha_{c2}$  and  $\beta_{c2}$ . Thus, the below statement should hold for  $i = 1, \dots, n$ :

$$\forall [\alpha_{i,c2}, \beta_{i,c2}] \in \text{Co}\{[\alpha_{i,c2}^1, \beta_{i,c2}^1], \dots, [\alpha_{i,c2}^{l_{i,2}}, \beta_{i,c2}^{l_{i,2}}]\}, \Psi \leq \Psi|_{\min_i\{\alpha_{i,c2}\}, \min_i\{\beta_{i,c2}\}} \quad (3.22)$$

where,  $[\alpha_{i,c2}^k, \beta_{i,c2}^k]$  are vertices of the uncertainty set.

Let us denote the optimum state and input sequences obtained from the optimizations (3.17) and (3.20) by  $\{\mathcal{X}_{i,\text{act}}(t)\}_{t=1}^{t=N_{\text{act}}}$  and  $\{\mathcal{U}_{i,\text{act}}(t)\}_{t=1}^{t=N_{\text{act}}}$  where  $N_{\text{act}}$  is the number of samples during the activation time. The optimizations also generate the optimum values of off-time and on-time periods for each consumer:  $\mathcal{T}_{i,\text{off}}$  and  $\mathcal{T}_{i,\text{on}}$ , when the consumers consume the minimum and maximum power respectively. Thus, during the off-time and on-time periods, the system inputs are:

$$\{\mathcal{U}_{i,\text{off}}(t) = P_{i,\text{min}} - P_{i,\text{base}}\}_{t=1}^{t=N_{i,\text{off}}} \quad (3.23)$$

$$\{\mathcal{U}_{i,\text{on}}(t) = P_{i,\text{max}} - P_{i,\text{base}}\}_{t=1}^{t=N_{i,\text{on}}} \quad (3.24)$$

where  $N_{i,\text{off}}$  and  $N_{i,\text{on}}$  are the number of samples during the off-time and on-time periods corresponding to each consumer,  $i$ . Hereupon, we have  $\{\mathcal{X}_{i,\text{off}}(t)\}_{t=1}^{t=N_{i,\text{off}}}$  and  $\{\mathcal{X}_{i,\text{on}}(t)\}_{t=1}^{t=N_{i,\text{on}}}$ . Afterwards, we construct the following vectors:

up-regulating:

$$\mathcal{X}_i \triangleq [0_{1 \times (N_{\text{on}} - N_{i,\text{on}})} \quad \mathcal{X}_{i,\text{on}}(1 : N_{i,\text{on}}) \quad \mathcal{X}_{i,\text{act}}(1 : N_{\text{act}})] \quad (3.25)$$

$$\mathcal{U}_i \triangleq [0_{1 \times (N_{\text{on}} - N_{i,\text{on}})} \quad \mathcal{U}_{i,\text{on}}(1 : N_{i,\text{on}}) \quad \mathcal{U}_{i,\text{act}}(1 : N_{\text{act}})] \quad (3.26)$$

down-regulating:

$$\mathcal{X}_i \triangleq [\mathcal{X}_{i,\text{act}}(1 : N_{\text{act}}) \quad \mathcal{X}_{i,\text{off}}(1 : N_{i,\text{off}}) \quad 0_{1 \times (N_{\text{off}} - N_{i,\text{off}})}] \quad (3.27)$$

$$\mathcal{U}_i \triangleq [\mathcal{U}_{i,\text{act}}(1 : N_{\text{act}}) \quad \mathcal{U}_{i,\text{off}}(1 : N_{i,\text{off}}) \quad 0_{1 \times (N_{\text{off}} - N_{i,\text{off}})}] \quad (3.28)$$

where each vector has the length of  $N$ .  $N = N_{\text{act}} + N_{\text{on}}$  and  $N = N_{\text{act}} + N_{\text{off}}$  for the up-regulating and the down-regulating scenario respectively. Each consumer has its own on-time and off-time periods. We choose the maximum value among the whole portfolio. Hence:

$$N_{\text{on}} = \max_i \{N_{i,\text{on}}\} \quad (3.29)$$

$$N_{\text{off}} = \max_i \{N_{i,\text{off}}\} \quad (i = 1, \dots, n) \quad (3.30)$$

The rest of the vector is filled up with zeros. The extended activation time for the up-regulating and the down-regulating scenarios are shown in Figure 3.3, together with the power consumption profile and the stored thermal energy of a typical TES.

**Second stage:** During the time of service activation, the aggregator runs the MPC with the following quadratic cost function every sampling time:

$$\min_U \sum_{t=1}^N (X(t) - \mathcal{X}(t))' Q (X(t) - \mathcal{X}(t)) + (\Upsilon U(t) - \mathcal{U}(t))' R (\Upsilon U(t) - \mathcal{U}(t)) \quad (3.31)$$

subject to:

$$\sum \Upsilon U(t) = u_{\text{ref}} \quad (\text{for the interval } [t_{\text{start}}, t_{\text{end}}]) \quad (3.32)$$

$$F X(t) + G U(t) \leq H \quad (3.33)$$

$$X(t+1) = (A + \Delta_{a,\text{min}})X(t) + (B + \Delta_{b,\text{min}})U(t) \quad (\text{up-regulating}) \quad (3.34)$$

$$X(t+1) = (A + \Delta_{a,\text{max}})X(t) + (B + \Delta_{b,\text{max}})U(t) \quad (\text{down-regulating}) \quad (3.35)$$

where,  $\mathcal{X}(t) = [\mathcal{X}_1(t) \dots \mathcal{X}_n(t)]'_{n \times N}$  and  $\mathcal{U}(t) = [\mathcal{U}_1(t) \dots \mathcal{U}_n(t)]'_{n \times N}$ . In above optimization,  $X(t)$  and  $U(t)$  contain the predicted state and the predicted input over the prediction horizon,  $N$ . Thus, they have dimensions  $n \times N$  and  $4n \times N$  respectively.  $Q \in \mathbb{R}^{n \times n}$  and  $R \in \mathbb{R}^{n \times n}$  are constant weighting matrices.  $\Upsilon \in \mathbb{R}^{n \times 4n}$  is a matrix with 0 and 1 elements used for converting  $U$  to  $u$ . The above optimization starts at  $t_1$  and finishes at  $t_N$ . At each sampling time, the optimization provides the optimum input for the whole prediction horizon and only the first element is applied to the system. At the first sampling time  $t_1$ ,  $\mathcal{U}(t)$  and  $\mathcal{X}(t)$  are available for  $t = 1, \dots, N$  from the optimization in the first stage. As we proceed, we need to update them every sampling time by eliminating the first element and adding zero to the end. For instance, at  $t_1 + \tau$  ( $\tau$  is the sampling

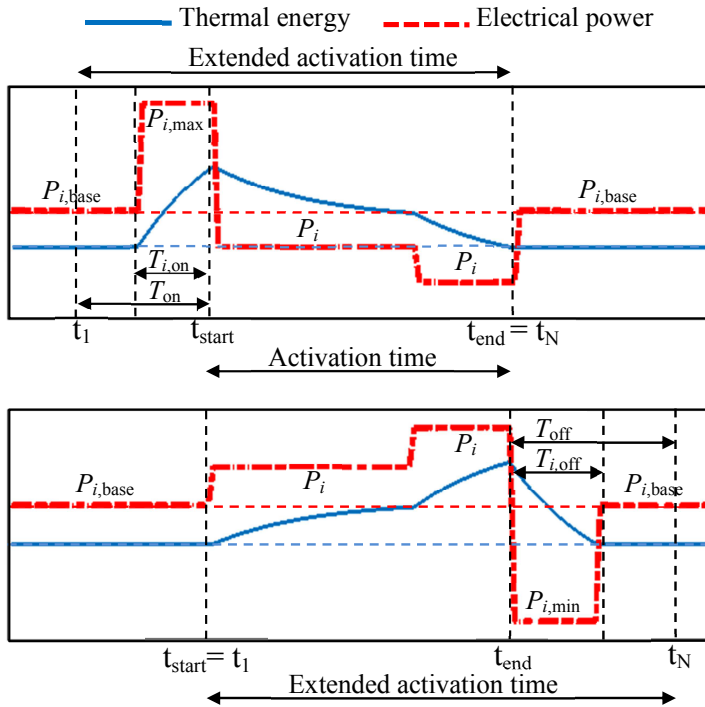


Figure 3.3: Typical power consumption profile and the stored thermal energy of the TES  $i$ , for the up-regulating (upper figure) and the down-regulating (lower figure). The interval  $[t_{\text{start}}, t_{\text{end}}]$  denotes the activation time whereas, the interval  $[t_1, t_N]$  indicates the prediction horizon in the second stage.  $T_{\text{on}}$  and  $T_{\text{off}}$  are the maximum on-time and off-time periods among the whole portfolio.

time),  $\mathcal{U}(N) = \mathcal{X}(N) = \mathbf{0}_{n \times 1}$ , at  $t_1 + 2\tau$ ,  $\mathcal{U}(N-1:N) = \mathcal{X}(N-1:N) = \mathbf{0}_{n \times 2}$  and so on. Equation (3.32) represents power reference following. For the system model, we use the minimum value of  $\Delta_a$  ( $\Delta_{a,\text{min}}$ ) and  $\Delta_b$  ( $\Delta_{b,\text{min}}$ ) for the up-regulating scenario and we use the maximum value of  $\Delta_a$  ( $\Delta_{a,\text{max}}$ ) and  $\Delta_b$  ( $\Delta_{b,\text{max}}$ ) for the down-regulating scenario in equations (3.34) and (3.35). If the real system parameters are different from these in the time of service activation, we can expect the following output: In the up-regulating scenario, the aggregator might ask some of the units to consume less than their maximum power consumption during the on-time period. In the down-regulating scenario, some of the units might consume greater than their minimum consumption during the off-time period. However, in both cases, the aggregator can follow the power reference during the activation time.

### 3.4 Summary

The direct aggregator setup proposed in Chapter 2, employs simplified models of the consumer deliberately, otherwise the setup is not implementable in practice. Rather than

increasing the model complexity, in this chapter, we proposed two methods to make the setup more robust to the model mismatch. In the first method, we considered a simple feedback mechanism in which we represented the discrepancies as state-dependent uncertainties. We then redistributed the discrepancies among the consumers. In the second method, we include the uncertainties inside the MPC controller at the aggregator, where the system parameters are allowed to vary within an uncertainty set. This approach leads to a two-step strategy. The first step is performed long before the activation time. The aggregator solves a one-time optimization problem using the objective functions (2.61) and (2.62). Based on the information obtained from the first step, the aggregator runs an optimization with a quadratic cost function during the activation time in the second step.



## 4 | Case Studies

As mentioned in Chapter 1, thermal energy storage (TES) can be an alternative to the electrical storage for storing energy with less cost and damage to the environment. Particularly, the existing thermal energy storages are of interest in the Smart Grid context. In this regard, we have chosen two specific case studies, namely a supermarket refrigeration system and an HVAC chiller in conjunction with an ice storage. Refrigerated foods in cold rooms and display cases at the supermarket can act as a huge storage for saving electrical energy in form of thermal energy. Another potential thermal storage for the Smart Grid purposes are the existing ice storages in HVAC system. In this chapter, we overview the supermarket refrigeration system and the chiller system.

In both the supermarket refrigeration system and chiller system, a vapor-compression cycle is utilized to remove heat from a cold reservoir and expel it to a hot reservoir. A basic vapor compression cycle is shown in Figure 4.1. It has four main components, including an evaporator, a compressor, a condenser and an expansion valve [61]. The cycle works based on circulating a refrigerant between two heat exchangers, i.e. an evaporator and a condenser. Starting from point 1 in Figure 4.1, The liquid refrigerant enters the evaporator where it absorbs heat from the goods in the cold rooms and display cases at the supermarket and from a so-called brine circuit at the chiller system. The refrigerant turns to vapor at point 2. The vapor then flows through the compressor to be pressurized. In the condenser, the vapor refrigerant expels the heat to the surroundings and it turns to the liquid form again. Finally, the refrigerant returns to the evaporator to close the cycle through an expansion valve, used for adjusting the pressure.

The compressor is the main power consumer in the refrigeration cycle. The work done by the compressor ( $W_c$ ) depends on the enthalpy of the refrigerant at the inlet and outlet of the compressor ( $h_{oe}$  and  $h_{ic}$  respectively) and the mass flow rate of refrigerant ( $\dot{m}_{\text{ref}}$ ) [38]. The power consumption of the compressor can be obtained as below:

$$\dot{W}_c = \frac{\dot{m}_{\text{ref}}(h_{ic} - h_{oe})}{\eta_{is}} \quad (4.1)$$

where,  $\eta_{is}$  is the isentropic efficiency. Then the cooling capacity (rate of heat removed from the cold reservoir) is provided as  $\dot{Q}_e$ :

$$\dot{Q}_e = \dot{m}_{\text{ref}}(h_{oe} - h_{oc}) \quad (4.2)$$

$h_{oc}$  is the enthalpy at the outlet of the condenser. In general, the enthalpies ( $h_{oe}$ ,  $h_{ic}$ ,  $h_{oc}$ ) are non-linear functions of the evaporating pressure ( $P_e$ ) and the condensing pressure ( $P_c$ ) and consequently the evaporating and condensing temperature. They can be

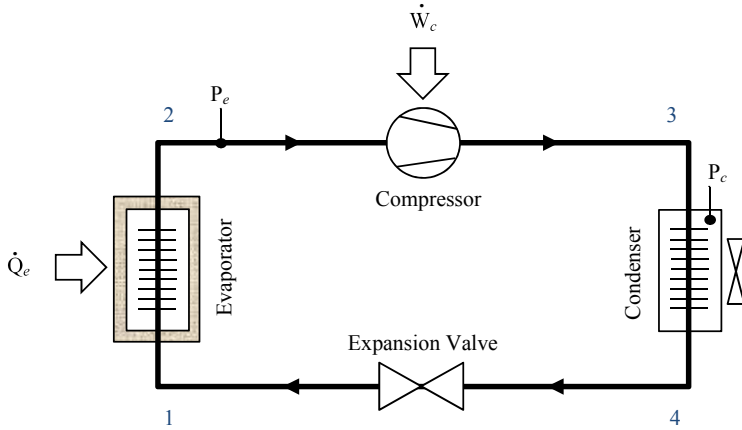


Figure 4.1: A basic vapor compression cycle

computed e.g. with the freeware software package “RefEqns” for Matlab [62] or available approximation formulas.  $\eta_{is}$  can be assumed constant for a range of operation. In the following, we explain the model of each system that is used in the aggregator setup.

## 4.1 Supermarket Refrigeration System

In supermarkets, a large amount of refrigerated foods which are preserved in cold rooms and display cases can act as a thermal storage. Temperature of the cold rooms and display cases can vary within a certain limits,  $T_{cr,min} \leq T_{cr} \leq T_{cr,max}$ , without deterioration of food quality. This opens a space for the system to be flexible to the power changes. First, let us consider a simple cold room in a supermarket. The dynamics of the cold room can simply be described by a first order equation:

$$m_{\text{food}} c_{p,\text{food}} \frac{dT_{cr}(t)}{dt} = \dot{Q}_{\text{load}}(t) - \dot{Q}_e(t) \quad (4.3)$$

where,  $m_{\text{food}}$  and  $c_{p,\text{food}}$  are the mass and specific heat capacity of the refrigerated foods.  $\dot{Q}_e$  is the rate of heat removed from the cold room by the evaporator and  $\dot{Q}_{\text{load}}$  is the rate of heat load from the surrounding. The heat load can be expressed by the overall heat transfer coefficient between the ambient and the cold room,  $UA_{\text{amb},cr}$ , as below:

$$\dot{Q}_{\text{load}}(t) = UA_{\text{amb},cr} (T_{\text{amb}} - T_{cr}(t)) \quad (4.4)$$

From the equations (4.1) and (4.2),  $\dot{Q}_e = \dot{W}_c \frac{\eta_{is}(h_{oe} - h_{oc})}{h_{ic} - h_{oe}}$ . The fraction in this equation represents the coefficient of performance (COP), which is the ratio of heating or cooling provided to the electrical energy consumed by definition. Normally, COP varies based on the temperature difference between the hot and cold side i.e. the condensing and evaporating temperature of the supermarket refrigeration system. In this work, COP is assumed to be constant. This assumption is reasonable, since the outside temperature (and so the condensing temperature) does not change significantly in a short period of

activation. Thus, the COP variations are not significant and the below equation should hold:

$$\dot{Q}_e(t) = \text{COP}_s P_s(t) \quad (4.5)$$

where,  $P_s$  and  $\text{COP}_s$  are the power consumption and COP of the supermarket system.

The following state space model describes the dynamic of a single cold room at the supermarket:

$$\dot{x}_{cr}(t) = A_{cr}x_{cr}(t) + B_{cr}u_{cr}(t) \quad (4.6)$$

$$A_{cr} = -\frac{UA_{amb,cr}}{m_{\text{food}}c_{p,\text{food}}} \quad (4.7)$$

$$B_{cr} = \text{COP}_s \quad (4.8)$$

where the state and input are defined as:

$$x_{cr}(t) \triangleq m_{\text{food}}c_{p,\text{food}}(T_{cr,\text{base}} - T_{cr}(t)) \quad (4.9)$$

$$u_{cr}(t) \triangleq P_s(t) - P_{cr,\text{base}} \quad (4.10)$$

Compressors at the supermarket need to consume  $P_{cr,\text{base}}$  to keep the cold room temperature,  $T_{cr}$  at the baseline temperature,  $T_{cr,\text{base}}$ :

$$P_{cr,\text{base}} = \frac{UA_{amb,cr}}{\text{COP}_s}(T_{amb} - T_{cr,\text{base}}) \quad (4.11)$$

The model is subject to the temperature and power consumption constraints:

$$x_{cr,\min} \leq x_{cr}(t) \leq x_{cr,\max} \quad (4.12)$$

$$P_{s,\min} - P_{cr,\text{base}} \leq u_{cr}(t) \leq P_{s,\max} - P_{cr,\text{base}} \quad (4.13)$$

where,  $x_{cr,\min} = m_{\text{food}}c_{p,\text{food}}(T_{cr,\text{base}} - T_{cr,\max})$  and  $x_{cr,\max} = m_{\text{food}}c_{p,\text{food}}(T_{cr,\text{base}} - T_{cr,\min})$ . In a real supermarket, there are several cold rooms and display cases to store the refrigerated goods. Still, we would like to describe the dynamic of the whole system with a single 1st order model. Several cold rooms in a supermarket can be lumped together using standard model reduction techniques, yielding an approximate 1st order model:

$$\dot{x}_s(t) = A_s x_s(t) + B_s u_s(t) \quad (4.14)$$

with the following constraints:

$$x_{s,\min} \leq x_s(t) \leq x_{s,\max} \quad (4.15)$$

$$P_{s,\min} - P_{s,\text{base}} \leq u_s(t) \leq P_{s,\max} - P_{s,\text{base}} \quad (4.16)$$

where,

$$P_{s,\text{base}} = \sum_{i=1}^{n_{cr}} P_{cr_i,\text{base}} \quad (4.17)$$

$$x_{s,\min} = n_{cr} \times \max_i \{x_{cr_i,\min}\} \quad (4.18)$$

$$x_{s,\max} = n_{cr} \times \min_i \{x_{cr_i,\max}\} \quad (4.19)$$



$n_{cr}$  is the the number of cold rooms in a supermarket. As can be seen in equation (4.17), the baseline power consumption of the whole supermarket,  $P_{s,base}$ , is the summation of all baseline power related to each cold room,  $P_{cr_i,base}$ . Since different cold rooms at the supermarket have different time constants, we consider conservative limits for minimum and maximum thermal energy as shown in equations (4.18) and (4.19). This ensures that we will not violate the temperature constraints in all cold rooms.

## 4.2 HVAC Chiller with an Ice Storage

In an air conditioning system, a chiller is used to remove heat from a liquid, typically brine, via a vapor-compression cycle. The chilled brine circulates through air handling units where it absorbs heat from the surrounding air. The cooled air is then distributed to the buildings to provide satisfactory comfort level. Depending on the system structure, there can also be other heat exchangers like a water loop between the brine and the air. Air conditioning systems in commercial buildings usually consume a significant amount of power, which often coincides with the high-peak hours of electricity consumption in the power grid. Adding an ice storage to this system can help the power grid and at the same time reduce the cost of energy for the buildings. The basic idea is to shift the consumption from the on-peak hours, when the electricity price is high, to the off-peak hours. The chiller can run during the night to produce ice. During the day, the chiller can either be turned off or work with a lower capacity to serve the cooling load together with the ice tank. Although the ice tank is primarily designed for load shifting, it can also be utilized for smart grid purposes such as providing regulating power.

A chiller in conjunction with an ice storage can operate in different modes. There are three basic operating modes, direct cooling, charging and passive cooling (see Figure 4.2). In the direct cooling mode, the ice storage is not utilized and the chiller operates to satisfy the cooling load from the building. In the passive cooling, the chiller is turned off and the chilled brine is provided by melting ice in the ice tank. To charge the ice tank and produce ice, the chiller operates in charging mode. In principle, the system is able to switch between the three modes or a combination of them by adjusting the three-way valves shown in Figure 4.2.

The dynamics of the ice storage is difficult to describe because of phase changes (from water to ice or vice versa) occurring during the freezing or melting process. At different times, there can be water, ice or both in the tank. Many publications have been devoted to the study of phase change behavior and modelling the ice storage, for examples [63] and [64]. To develop a simple model for the ice storage, we assume that the storage is always in two-phase. The assumption is reasonable, as the thermal energy exchange during the two-phase situation is much greater than when there is just water or ice in the tank due to the large latent heat of water. Phase change is a constant temperature process. The ice storage temperature is  $0^\circ C$  during the water freezing or the ice melting, but the mass of water changes. Thus, the following equation governs the dynamic of the ice storage:

$$L_{water} \frac{dm_w(t)}{dt} = -\dot{Q}_{ice}(t) \quad (4.20)$$

where,  $L_{water}$  is the latent heat of water and  $m_w$  is the mass of water inside the ice storage.  $\dot{Q}_{ice}$  denotes the rate of heat removed from the water inside the tank. The ice storage can

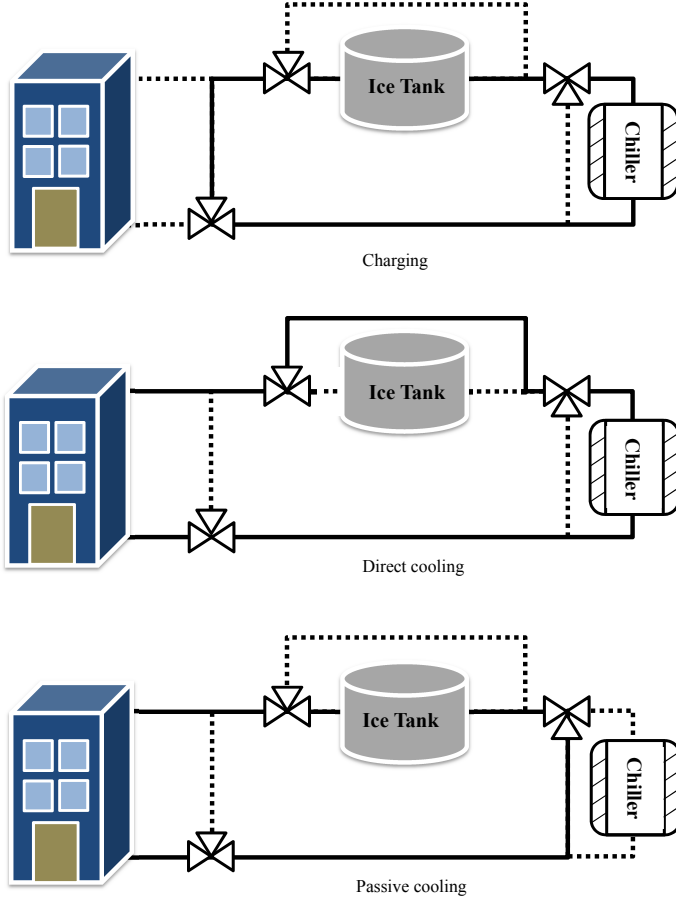


Figure 4.2: Three basic operating modes for chiller in conjunction with an ice storage.

be isolated in a way that the wasted thermal energy is almost zero. To create a state space model, we can define the system state as below:

$$x_c(t) \triangleq L_{\text{water}}(m_{w,\text{base}} - m_w(t)) \quad (4.21)$$

$m_{w,\text{base}}$  is the mass of water when the activation time starts. From here, we can follow two approaches to continue. First, suppose that only one chiller is used to produce ice and satisfy the cooling load from the building. Heat exchange between the brine loop and the water inside the tank can be expressed as:

$$\dot{Q}_{\text{ice}}(t) = UA_{b,it}(0 - T_b(t)) \quad (4.22)$$

$T_b$  and  $UA_{b,it}$  represent the brine temperature and the overall heat transfer coefficient between the brine and the ice tank respectively.  $0^\circ\text{C}$  in the above equation indicates the ice tank temperature in the two phase situation. For a constant brine temperature, as the amount of ice increases or decreases during the freezing or melting process,  $\dot{Q}_{\text{ice}}$

decreases or increases. This is because, the heat transfer coefficient between the brine and ice is lower than the heat transfer coefficient between the brine and water. In fact,  $UA_{b,it}$  is not fixed in equation (4.22). In this work, we ignore this effect, since it is not significant for a short period of activation time. However, one simple way to model this behavior is to assume that  $R_{b,it}$ , i.e. the thermal resistance, follows the relation:

$$R_{b,it} = R_0 + R_1 \frac{m_{ice}}{m_{w,max}} \quad (4.23)$$

where,  $R_{b,it} = \frac{1}{UA_{b,it}}$ ,  $m_{ice}$  and  $m_{w,max}$  are the mass of ice and the maximum mass of water in the tank, and  $R_0$  and  $R_1$  are constant parameters.

Assume there is a linear relationship between the brine temperature and the chiller power consumption,  $P_c$ :

$$T_b(t) = aP_c(t) + b \quad (4.24)$$

$a$  and  $b$  are constant parameters. The ice storage is only utilized when the brine temperature is below  $0^\circ C$ , otherwise heat transfer can not occur between the brine and the water. Considering this fact, the dynamic of the ice storage can be expressed as below:

$$\dot{x}_c(t) = \begin{cases} B_c u_c(t) & u_c(t) > 0 \\ 0 & u_c(t) \leq 0 \end{cases} \quad (4.25)$$

The system input is defined as,  $u_c(t) \triangleq P_c(t) - P_{threshold}$ , where,  $P_{threshold}$  is the amount of power which provides the brine temperature equals to  $0^\circ C$ . The ice starts to build when the chiller power consumption is above the threshold power. According to equations (4.20)-(4.22) and (4.24), the system parameters are:

$$B_c = -aUA_{b,it} \quad (4.26)$$

$$P_{threshold} = \frac{-b}{a} \quad (4.27)$$

The model is subject to the mass (capacity of the ice tank) and power consumption constraints:

$$x_{c,min} \leq x_c(t) \leq x_{c,max} \quad (4.28)$$

$$P_{c,min} - P_{threshold} \leq u_c(t) \leq P_{c,max} - P_{threshold} \quad (4.29)$$

Moreover, to satisfy the cooling load from the building, the brine temperature should not violate a maximum limit,  $T_b(t) \leq T_{b,max}$ . However, this constraint is included in power consumption constraint due to equation (4.24).

The second approach for modelling the chiller system is to consider two separate chillers, one for providing the cooling load and one for charging the ice storage. using the same chiller for both charging and direct cooling is not optimal from an efficiency point of view. The reason is that the evaporator temperature and consequently the COP of the system, is much lower in charging mode than the direct cooling. This means the chiller needs to switch between two very different operating modes. In general, a chiller that is designed for one operating point is not optimal in any other point [65]. Figure 4.3

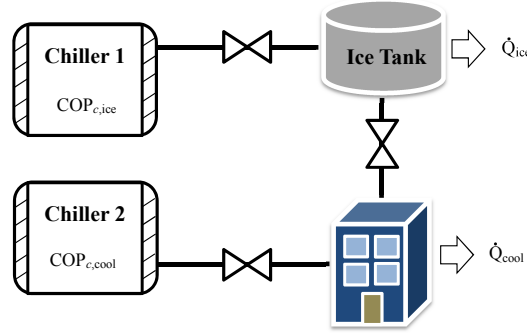


Figure 4.3: Cooling system with two separate chillers, where the total power consumption is  $P_c(t) = P_{\text{Chiller 1}}(t) + P_{\text{Chiller 2}}(t)$

shows a simple sketch of a cooling system with two chillers. In this scheme, Chiller 1 is utilized for charging the ice tank. Chiller 2 in conjunction with the ice tank is used to cool down the building. Assume, the building requires a cooling load equals to  $\dot{Q}_{\text{cool}}$ , then the baseline power consumption of this system is defined as:

$$P_{c,\text{base}} = \frac{\dot{Q}_{\text{cool}}}{\text{COP}_{c,\text{cool}}} \quad (4.30)$$

When the input power to the system is greater than the baseline power, i.e.  $P_c(t) > P_{c,\text{base}}$ , Chiller 1 consumes the rest of power to charge the ice tank:

$$\dot{Q}_{\text{ice}} = \text{COP}_{c,\text{ice}}(P_c(t) - P_{c,\text{base}}) \quad (4.31)$$

When the input power to the system is lower than the baseline power, part of the cooling load from the building should be provided by melting ice:

$$\dot{Q}_{\text{ice}} = \text{COP}_{c,\text{cool}}P_c(t) - \dot{Q}_{\text{cool}} = \text{COP}_{c,\text{cool}}(P_c(t) - P_{c,\text{base}}) \quad (4.32)$$

Thus, with assuming two chillers, the following model is provided for the whole system:

$$\dot{x}_c(t) = \begin{cases} B_{c,1}u_c(t) & u_c(t) > 0 \\ B_{c,2}u_c(t) & u_c(t) \leq 0 \end{cases} \quad (4.33)$$

where,

$$B_{c,1} = \text{COP}_{c,\text{ice}} \quad (4.34)$$

$$B_{c,2} = \text{COP}_{c,\text{cool}} \quad (4.35)$$

and  $u_c(t) = P_c(t) - P_{c,\text{base}}$ . The model is subject to the constraint defined in (4.28) and also the power constraint:

$$P_{c,\text{min}} - P_{\text{base}} \leq u_c(t) \leq P_{c,\text{max}} - P_{\text{base}} \quad (4.36)$$

Although, this model is developed for a system with two chillers, it can also be valid for a system with one chiller, when the chiller works in two different operating points. As explained in Chapter 2, the logical part of the model should be converted to linear inequalities in order to use it in the optimization problem.

### 4.3 Summary

In this chapter, we introduced our case studies and we explained how we model them for the Smart Grid purposes. One of our case studies is the supermarket refrigeration system, where a large amount of refrigerated foods, which are preserved in cold rooms and display cases, can act as a TES. This storage is leaky storage because of heat loss to the surrounding at the supermarket and we assumed a constant COP for the system. Thus, the flexibility of supermarket refrigeration system can be expressed with a 1st order model. The other case study is the chiller in conjunction with an ice storage. Here, the ice storage is a TES, without heat loss, since it is well isolated. We assumed two different COPs for the chiller system, one to model the ice making process and one to model the direct cooling mode. As explained in Chapter 3, variations of the obtained parameters can be considered at the aggregator through a robust MPC setup.

## 5 | Simulation Results

Simulation results for our case studies, namely the supermarket refrigeration system and the chiller system in conjunction with an ice storage, are provided in this chapter. We divide the simulations into five parts:

1. **Power distribution:** First of all, we examine how the aggregator distributes the power reference between the supermarkets and chillers. To this end, we simulate the setup for different power references and different objective functions and consumers' model we introduced in Chapter 2 and Chapter 4.
2. **Heterogeneous vs. homogeneous aggregation:** In this part, we assume a heterogeneous and a homogeneous setup. The heterogeneous setup consists of two aggregators, each of which controls one supermarket and one chiller. In the homogeneous setup, one aggregator controls the supermarkets, while the other one controls the chillers. In this way, we can compare the heterogeneous and homogeneous aggregation.
3. **Evaluation of aggregator:** In this part, we evaluate the aggregator setup through the simulations, to understand to what extent the utilization of simplified models at the aggregator can lead to reasonable results. For this purpose, we connect the aggregator to a complex and verified model of an actual supermarket refrigeration system.
4. **Robust setup:** In this part, we simulate our proposed methods in Chapter 3, i.e. the feedback mechanism and the two-stage optimization, which can handle the mismatch between the real consumers and the simplified model of consumers we utilized at the aggregator.
5. **Indirect control:** Although the main focus of this work is on the direct control policy, we also formulate an objective function based on the indirect control policy and simulate the setup for our specific case studies.

Except item 4, in all parts, we assume the system parameters are fixed.

### 5.1 Power Distribution

In the first step, we consider a single cold room, containing frozen meat, at the supermarket and an ice storage under the control of the aggregator. For the supermarket system,

Table 5.1: Numerical values for simulation

Supermarket		Chiller	
$m_{\text{food}}$	200kg	$L_{\text{water}}$	334kJ/kg
$c_{p,\text{food}}$	2.01 kJ/kg $^{\circ}\text{C}$	$UA_{b,it}$	1kW/ $^{\circ}\text{C}$
$UA_{amb,cr}$	0.3kW/ $^{\circ}\text{C}$	a	-3 $^{\circ}\text{C}$ /kW
$\text{COP}_s$	3	b	15 $^{\circ}\text{C}$
$T_{cr,\text{min}}$	-20 $^{\circ}\text{C}$	$m_{w,\text{min}}$	0kg
$T_{cr,\text{max}}$	-10 $^{\circ}\text{C}$	$m_{w,\text{max}}$	500 kg
$T_{cr,\text{base}}$	-10 $^{\circ}\text{C}$	$m_{w,\text{base}}$	0kg
$P_{s,\text{min}}$	0kW	$P_{c,\text{min}}$	0kW
$P_{s,\text{max}}$	10kW	$P_{c,\text{max}}$	10kW
$T_{amb}$	15 $^{\circ}\text{C}$	$T_{b,\text{max}}$	8 $^{\circ}\text{C}$

we use the model described by equations (4.6)-(4.13) and for the chiller system, we use the model described by equations (4.25)-(4.29). Numerical values of the system parameters are listed in Table 5.1. We consider a down-regulating scenario and the objective function introduced by equation (2.60) is used for the simulation. The activation time is one hour. As can be seen from Table 5.1, there is no ice inside the tank and the cold room temperature is kept at the maximum level at the beginning of activation time. Thus, the aggregator has two empty TES under its control when the activation time starts. The baseline power of the supermarket is  $P_{cr,\text{base}} = 2.5\text{kW}$  and the baseline power of the chiller is  $P_{c,\text{base}} = 2.33\text{kW}$ . In other words, the supermarket requires to consume 2.5kW to keep the cold room temperature just below the maximum limit; and the chiller requires to consume 2.3kW to satisfy the cooling load from the building. Figure 5.1 shows the simulation results.

Simulations are done for different values of power reference,  $P_{\text{reference}} = 5.2\text{kW}$ ,  $P_{\text{reference}} = 6.5\text{kW}$ ,  $P_{\text{reference}} = 12\text{kW}$  and  $P_{\text{reference}} = 13.5\text{kW}$ . The four upper plots in Figure 5.1 indicate the power distribution from the aggregator to the supermarket and chiller, i.e. the system input. The lower plots indicate the thermal energy changes in each storage, i.e. the system state. Depending on the power reference, the aggregator may assign the extra power to the supermarket, to the chiller or both of them. In general, for low deviation from the baseline, the aggregator prefers to use the flexibility in the supermarket than the chiller. As the power reference increases, the utilization of the chiller increases. This is due to two reasons. First, the heat loss of the cold room at the supermarket is rather low for low deviation from the baseline. The cold room temperature decreases as the power reference increases. Consequently, the heat load increase according to equation (4.4). Second, with utilizing the chiller for low deviation from the baseline, most of the power is just used to provide  $P_{\text{threshold}}$  rather than freezing the water inside the tank and making ice. Since the objective is to maximize the energy saving, the aggregator use the supermarket more than the chiller for lower power references.

As shown in Figure 5.1, for  $P_{\text{reference}} = 5.2\text{kW}$ , the supermarket is just utilized. The chiller system consumes 2.33kW, which is required to provide the brine temperature at 8 $^{\circ}\text{C}$  and hence the satisfactory cooling output. For  $P_{\text{reference}} = 6.5\text{kW}$ , it is still preferred to use the supermarket. The supermarket requires to consume at least 2.5kW to not violate the maximum cold room temperature. The rest of power ( $6.5 - 2.5\text{kW}$ ) is

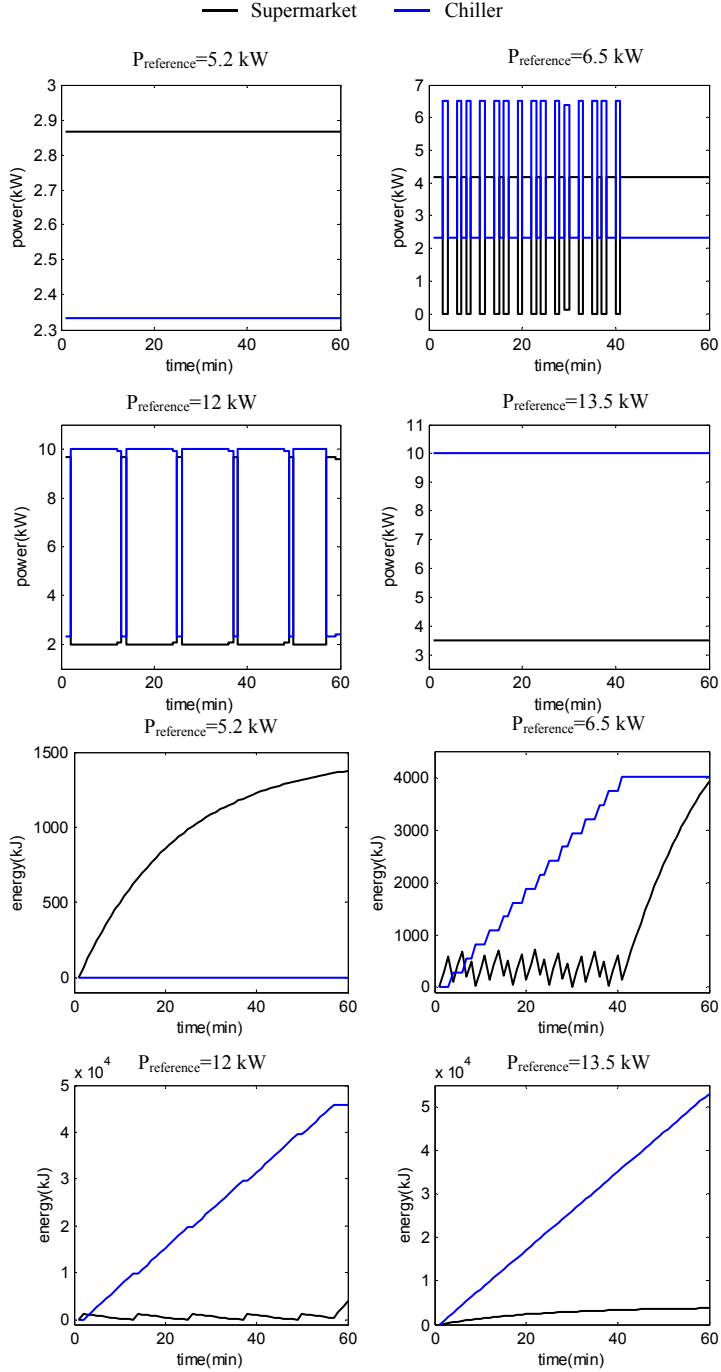


Figure 5.1: Power distribution (the four upper plots) and thermal energy changes (the four lower plots) over a one-hour activation time for the down-regulating scenario. The aggregator has one supermarket and one chiller under its direct control.



Table 5.2: Numerical values for simulation

	Baseline power	Maximum power	Maximum energy
Supermarket 1	4.3kW	15kW	22800kJ
Supermarket 2	6.2kW	15kW	22800kJ
Chiller 1	9.3kW	15kW	267200kJ
Chiller 2	8.3kW	15kW	200400kJ

not enough to provide the  $P_{\text{threshold}} = 5\text{kW}$ . However, consuming  $6.5 - 2.33\text{kW}$  for one hour by the supermarket will lead to minimum cold room temperature violation. Thus, the chiller should be utilized as well. In this situation, the aggregator first assigns the extra power ( $6.5 - 2.33\text{kW}$ ) to the supermarket. This reduces the cold room temperature. After that, the aggregator is able to assign  $6.5\text{kW}$  to the chiller, i.e. the threshold power. The supermarket consumes no power during this time and uses the energy that is stored in the previous sample. The next switching occurs as soon as the cold room temperature reaches the maximum level,  $T_{cr,\text{max}}$ , when the aggregator returns back to the supermarket again. Switching between the supermarket and the chiller continues as long as the required energy is stored in the ice storage. At the end of the horizon, the supermarket is just utilized.

For high power references like  $12\text{kW}$  and  $13.5\text{kW}$ , the more power assigned to the chiller, the more energy can be saved. Because, for high power references, the heat loss is considerable at the supermarket. On the other hand, the threshold power can be obtained which allows to store energy in the ice tank without loss. For  $P_{\text{reference}} = 12\text{kW}$ , the aggregator tends to utilize the chiller at the maximum power, equal to  $10\text{kW}$ . However, the rest of power ( $12 - 10\text{kW}$ ) is not enough for the supermarket to maintain the temperature at the maximum level. In this situation, switching occurs between the two units in order to keep the cold room temperature at  $T_{cr,\text{max}}$ . The ice storage is mainly used to store the extra energy. Finally, for  $P_{\text{reference}} = 13.5\text{kW}$ , the aggregator uses both the supermarket and the chiller from the beginning of activation time simultaneously. The chiller is asked to follow the maximum power,  $10\text{kW}$ , while the supermarket consumes the rest of power.

In the second step of simulation, we consider two supermarkets and two chillers under the control of the aggregator. Each supermarket utilizes four of its cold rooms for power reference following program. Supermarket 1 uses three medium temperature cold rooms ( $1^\circ\text{C} \leq T_{cr} \leq 6^\circ\text{C}$ ) and one low temperature cold room ( $-20^\circ\text{C} \leq T_{cr} \leq -10^\circ\text{C}$ ), while Supermarket 2 uses one medium temperature and three low temperature cold rooms. The Baseline power, the maximum power and the maximum capacity of the TESs for each unit are given in Table 5.2. For the supermarket system, we use the model described by equations (4.14)-(4.19) and for the chiller system, we use the model described by equations (4.33)-(4.36) and (4.28). We consider both the down-regulating and up-regulating scenario for simulation with the objective functions introduced by equations (2.61) and (2.62).

First, we run a simulation with two identical supermarkets and two identical chillers. For instance, we choose Supermarket 2 and Chiller 1 from our portfolio. The reason is to investigate the power distribution between the two different types of TES. The results are shown in Figure 5.2, where the upper plots indicate the power distribution to the supermarkets and chillers and the lower plots are the associated thermal energy changes.

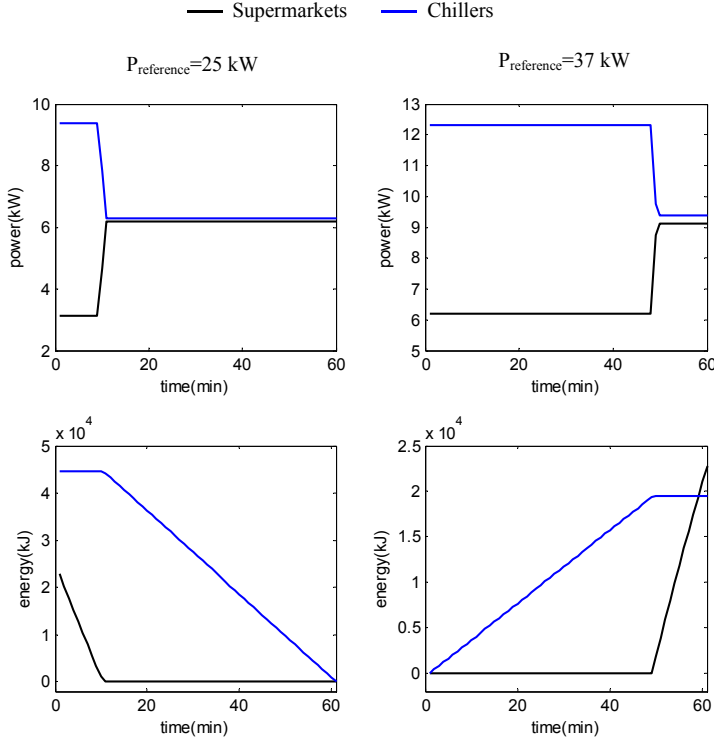


Figure 5.2: Power distribution (upper plots) and thermal energy changes (lower plots) over a one-hour activation time for the down-regulating scenario (plots on the right) and the up-regulating scenario (plots on the left). The aggregator has two identical supermarkets and two identical chillers under its direct control.

Simulations are done for two power references,  $P_{\text{reference}} = 25 \text{ kW}$  and  $P_{\text{reference}} = 37 \text{ kW}$ . The total baseline power consumption is 31 kW. As shown in Figure 5.2, in the down-regulating scenario, the chiller is mainly utilized in the beginning. The aggregator then switches to the supermarket refrigeration at the end of activation. For the up-regulating scenario, the situation is reversed. The aggregator first depletes the energy in the supermarket refrigeration system and the chiller is utilized at the end. These results are expected and reasonable. The leaky unit, i.e. the supermarket refrigeration system, should be discharged and charged in the beginning and at the end respectively. Otherwise, the charging and discharging processes are accompanied with more heat losses.

Figure 5.3 shows the power distribution and the energy changes for the aggregator with two different supermarkets and two different chillers. The total baseline consumption is equal to 28.1 kW. Six different power references are considered,  $P_{\text{reference}} = 12 \text{ kW}$ ,  $P_{\text{reference}} = 25 \text{ kW}$  and  $P_{\text{reference}} = 27 \text{ kW}$  for the up-regulating scenario,  $P_{\text{reference}} = 30 \text{ kW}$ ,  $P_{\text{reference}} = 37 \text{ kW}$  and  $P_{\text{reference}} = 42 \text{ kW}$  for the down-regulating scenario. As shown, switching from one unit to the other can occur several times when we have various consumers in our portfolio. For instance, for  $P_{\text{reference}} = 37 \text{ kW}$ , first, there is a switching from Chiller 2 to Supermarket 2. Then, the aggregator switches from Chiller 1 to Super-

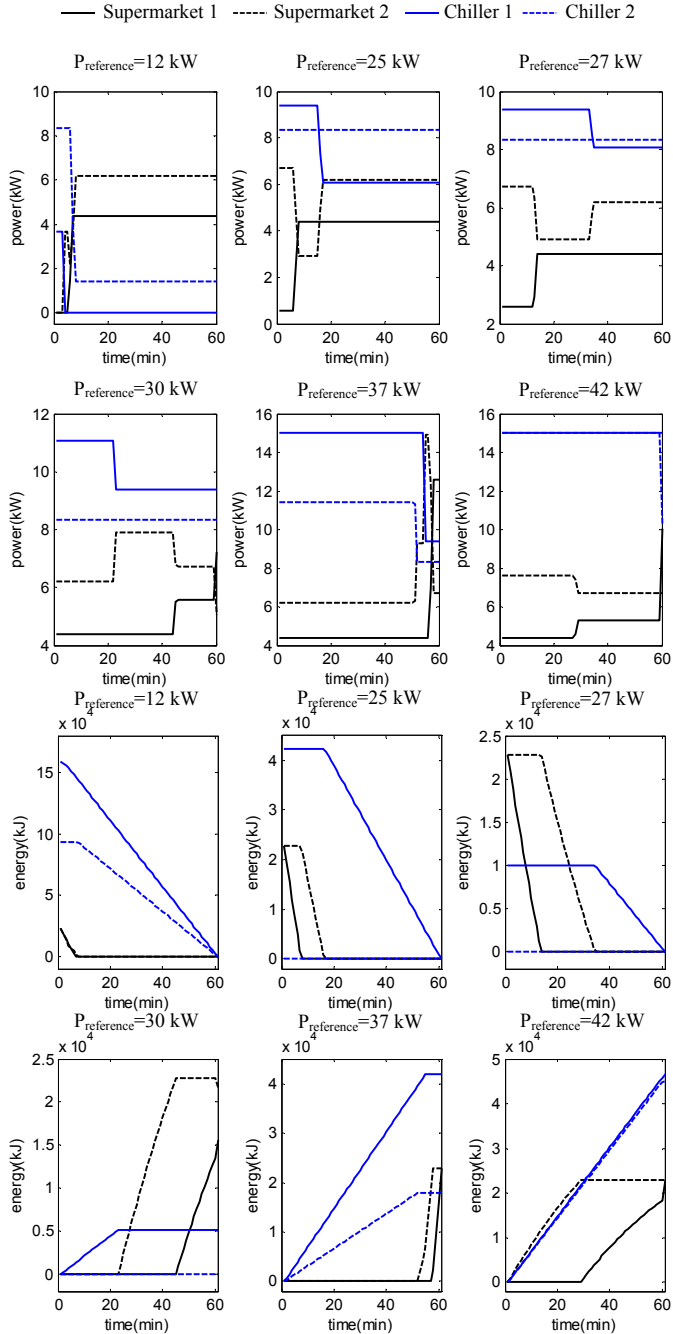


Figure 5.3: Power distribution (the six upper plots) and thermal energy changes (the six lower plots) over a one-hour activation time for the down-regulating and the up-regulating scenarios. The aggregator has two supermarkets and two chillers under its direct control.

Table 5.3: Numerical values for simulation

	Baseline power	Maximum power	Maximum energy
Supermarket 1	4.3kW	15kW	42800kJ
Supermarket 2	6.2kW	15kW	42800kJ
Chiller 1	9.3kW	15kW	267200kJ
Chiller 2	8.3kW	15kW	200400kJ

market 2. At the end, there is also another switching from Supermarket 2 to Supermarket 1. Essentially, the form of power distribution is dependent on the power reference values and the consumer characteristics. However, as a general rule, the leaky units are utilized in the beginning and at the end for the up-regulating and down-regulating scenarios, albeit other parameters are also determinant. For example, for  $P_{\text{reference}} = 42\text{kW}$ , one of the supermarkets (Supermarket 2) is utilized from the beginning since there is maximum power constraint for chiller systems. Moreover, we can conclude that the more deviation from the baseline power, the more exploitation of chiller systems occurs. This is due to state-dependent leakage of the supermarket refrigeration systems. For large deviation, the heat loss to the surrounding increases at the supermarkets. Hence, it is better to exploit the chillers.

## 5.2 Heterogeneous vs. Homogeneous Aggregation

To compare the homogeneous and the heterogeneous aggregation, a setup consists of a grid operator and two aggregators are considered as depicted in Figure 5.4. In the homogeneous setup, Aggregator 1 controls the supermarkets and Aggregator 2 controls the chillers. In the heterogeneous setup, Supermarket 1 and Chiller 1 are under the control of Aggregator 1, Supermarket 2 and Chiller 2 are under the control of Aggregator 2. Numerical values for simulation in this part are given in Table 5.3.

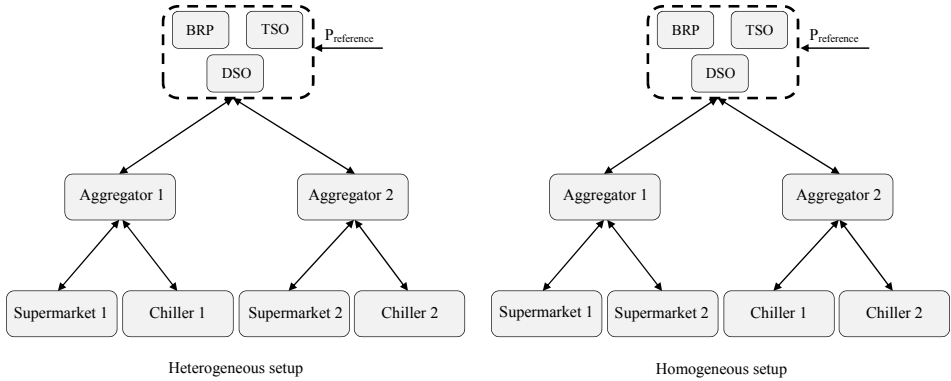


Figure 5.4: Homogeneous and heterogeneous aggregation setup

As explained in Chapter 2, we have two optimization problems. One of the optimization provides the optimal power distribution from the grid operator to Aggregator 1 and

Aggregator 2, while the other provides the optimal power distribution from each aggregator to the connected consumers. For the first optimization, each aggregator needs to communicate the cost/profit in terms of extra energy consumption/saving, per a specified power reference, for up/down-regulating scenarios. Figure 5.5 shows the cost/profit curves associated to each aggregator for both the homogeneous (the four upper plots) and the heterogeneous (the four lower plots) setup during the up/down-regulating scenarios. In order to use these curves in the optimization introduced by the equations (2.60)-(2.70), we fit the curves with second order polynomials, shown with the blue solid lines in Figure 5.5. Depending on the consumer type, each aggregator can offer different power ranges to follow in the homogeneous and the heterogeneous setup. For instance, the supermarkets have less capacity compared to the ice storages in our simulation examples. That is why the aggregator with just the supermarkets offers a smaller range of power to follow.

The top-level controller at the grid operator then provides the optimal input power to Aggregator 1 and Aggregator 2 denoted by  $P_1$  and  $P_2$  for the whole range of  $P_{\text{reference}}$ . Figure 5.6 shows the results of the optimization at the top-level controller, where  $\alpha$  indicates the ratio of the power of the first aggregator to the power reference that the top-level controller is asked to follow. Therefore, we have:

$$P_1 = \alpha P_{\text{reference}} \quad (5.1)$$

$$P_2 = (1 - \alpha) P_{\text{reference}} \quad (5.2)$$

The homogeneous setup can follow a greater range of power, [10.1kW-50.3kW], compared to the heterogeneous setup, [10.2kW-50.1kW]. However, the difference is not significant. The baseline power of the whole portfolio is  $P_{\text{base}} = 28.1\text{kW}$ , which is shown with the dashed line in Figure 5.6 to distinguish the up-regulating and the down-regulating scenarios. Again, the value of  $\alpha$  for each setup and for each scenario depends on the consumer characteristics. For instance, assume the heterogeneous setup and the up-regulating scenario. In the beginning,  $\alpha$  decreases as the deviation from baseline power increases. This means the use of Aggregator 1 increases since  $P_1$  decreases and Aggregator 1 needs to reduce its consumption more than before. However, for  $P_{\text{reference}} = 18.7\text{kW}$ ,  $\alpha = 0.2246$  and then  $P_1 = 4.2\text{kW}$ . This is the minimum power that can be followed by Aggregator 1 in the heterogeneous, up-regulating scenario. Thus,  $\alpha$  should increase as the deviation increases from this point in order to keep  $P_1$  at 4.2kW.

During the time of activation, an optimization is run at each aggregator every sampling time to define the optimum power distribution from the aggregators to the relevant consumers. Figure 5.7 and Figure show the results of the optimization at the aggregators for the homogeneous and the heterogeneous setup. For each up-regulating and down-regulating scenario, we consider two power references to show the results of large and small deviation from the baseline power (28.1kW). In addition to power distributions, the thermal energy changes are also shown. For the heterogeneous setup, for small deviations from the baseline ( $P_{\text{reference}} = 26\text{kW}$  and  $P_{\text{reference}} = 31\text{kW}$ ), only Aggregator 1 is utilized in both the up-regulating and the down-regulating scenarios. However, for large deviations from the baseline ( $P_{\text{reference}} = 15\text{kW}$  and  $P_{\text{reference}} = 42\text{kW}$ ), both aggregators are required to change their consumption. In our simulation examples, Supermarket 1 has a higher COP than Supermarket 2. Although Supermarket 1 has a higher heat loss than Supermarket 2, the difference in COPs are more important for our examples. On the other hand, Chiller 2 is more efficient than Chiller 1 since it has a lower difference

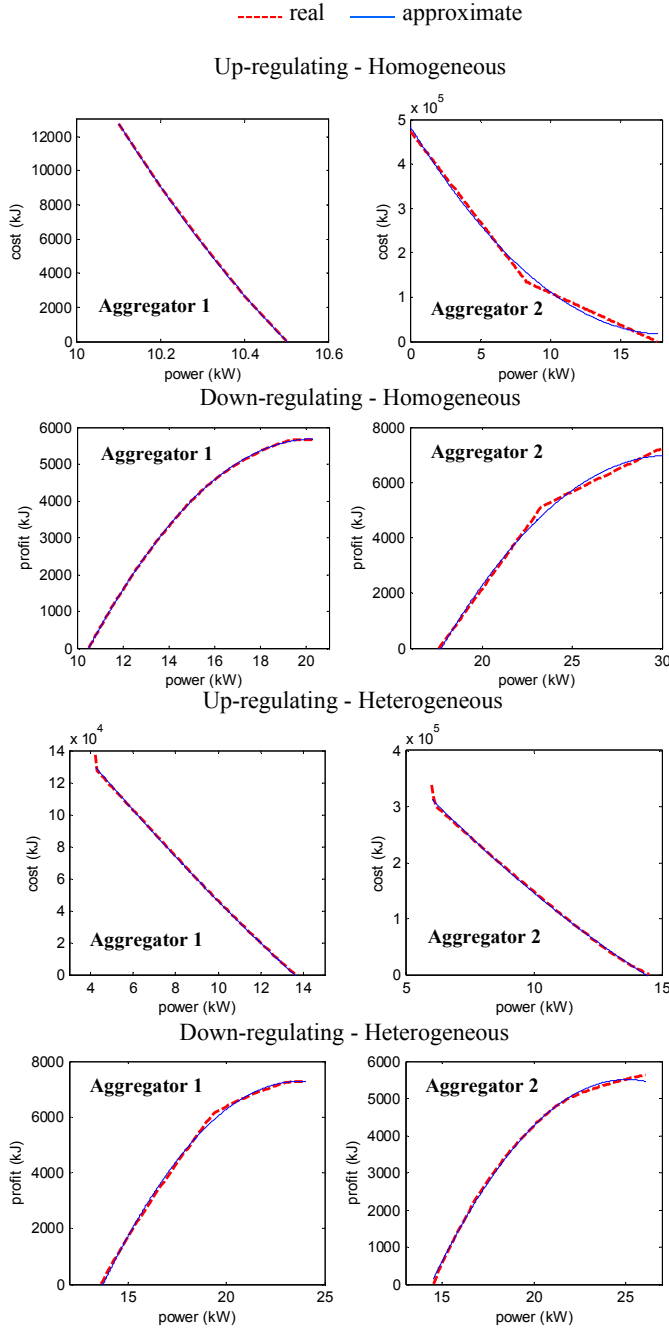


Figure 5.5: Cost/profit curves, in terms of extra energy consumption/saving, that are communicated by each aggregator to the grid operator in the up-regulating and the down-regulating scenarios. The real communicated values are shown with dashed red lines while the blue solid lines show the fitted second order polynomial

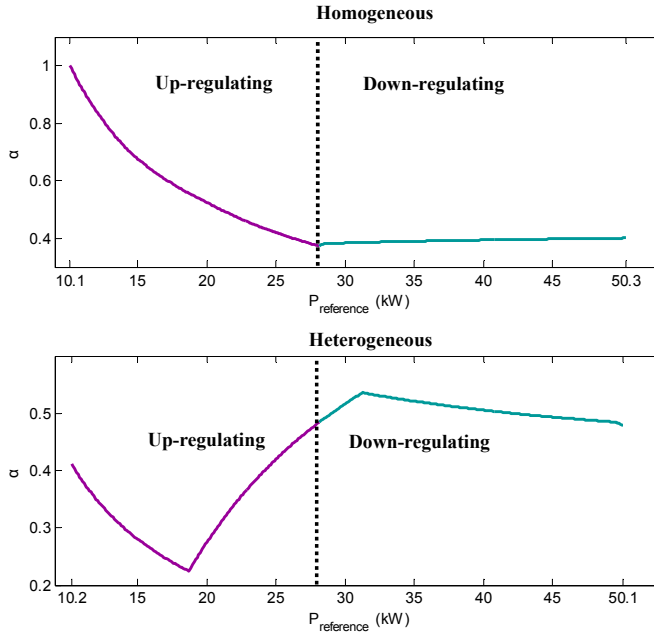


Figure 5.6: Optimization at the top-level controller:  $\alpha = \frac{P_1}{P_{\text{reference}}}$ , where  $P_1$  is the input power to the Aggregator 1 and  $P_{\text{reference}}$  is the input power to the top-level controller. Upper plot shows the optimum value of  $\alpha$  for the homogeneous setup while the lower plot is for the heterogeneous one.

between the two COPs of cooling and charging modes. Thus, the combination of Supermarket 1 and Chiller 2 is more efficient than the other two. Another thing that can be seen is that there is a switching between the supermarket and the chiller which are connected to each aggregator in such a way that the supermarket is mostly utilized in the beginning in the up-regulating and at the end in the down-regulating scenarios. This is reasonable due to the leaky nature of the supermarket as we explained earlier in this chapter.

Likewise, for the homogeneous setup, different power distributions can be seen for different power references. Between the two supermarkets of Aggregator 1, there could be several switchings depending on the system dynamics. For instance, for  $P_{\text{reference}} = 15\text{kW}$ , Supermarket 1 is utilized first due to the higher heat loss than Supermarket 2, while for  $P_{\text{reference}} = 42\text{kW}$ , Supermarket 2 is utilized first for the same reason. Between the two chillers of Aggregator 2, the one (Chiller 1 in our example) with the higher ratio of  $\frac{\text{COP}_{\text{ice}}}{\text{COP}_{\text{cool}}}$  is utilized first as long as there is ice in the tank and the maximum power is not reached. After that, the second chiller becomes active.

Total profit and total cost of the whole setup (consisting of Aggregator 1 and Aggregator 2) for the whole range of power reference are shown in Figure 5.9. The heterogeneous setup has a lower cost and a higher profit than the homogeneous setup. The difference is greater for the larger deviations from the baseline.

In above simulations, we assumed that the consumers are naturally available to increase their power consumption. We assumed the temperature of cold rooms and display

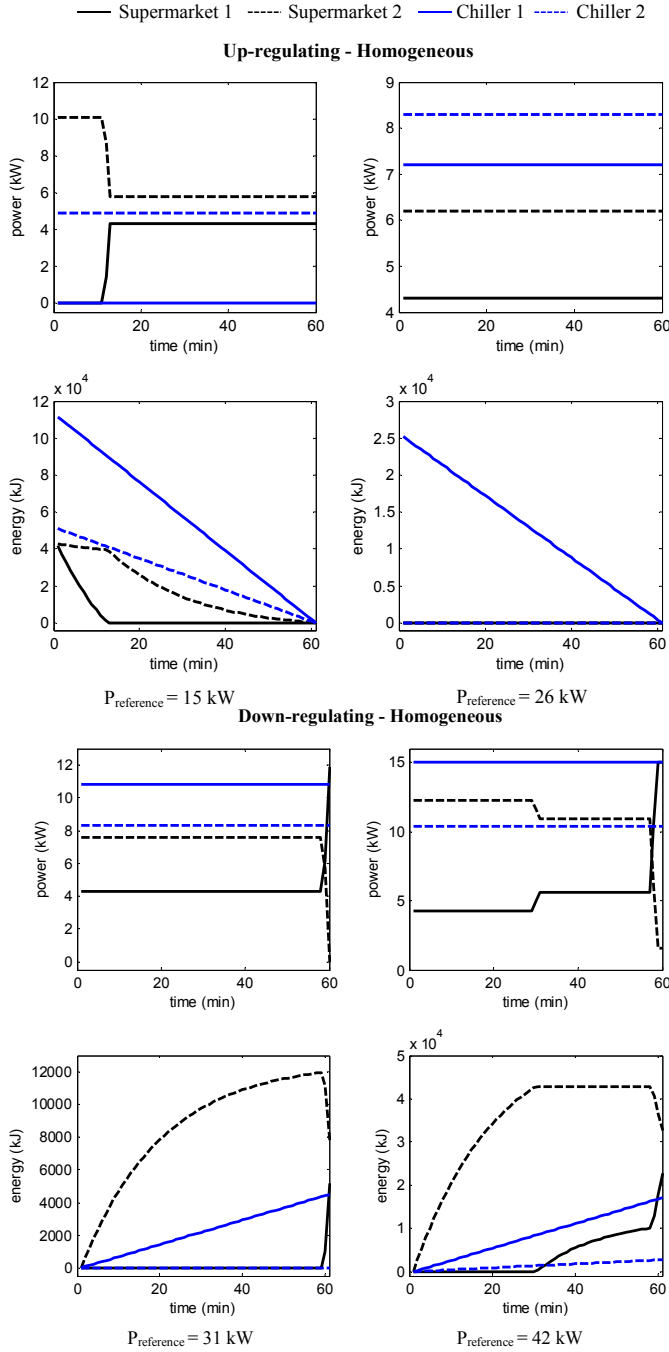


Figure 5.7: Power distributions from Aggregator 1 and Aggregator 2 to the consumers in the homogeneous setup and the associated thermal energy changes in each consumer



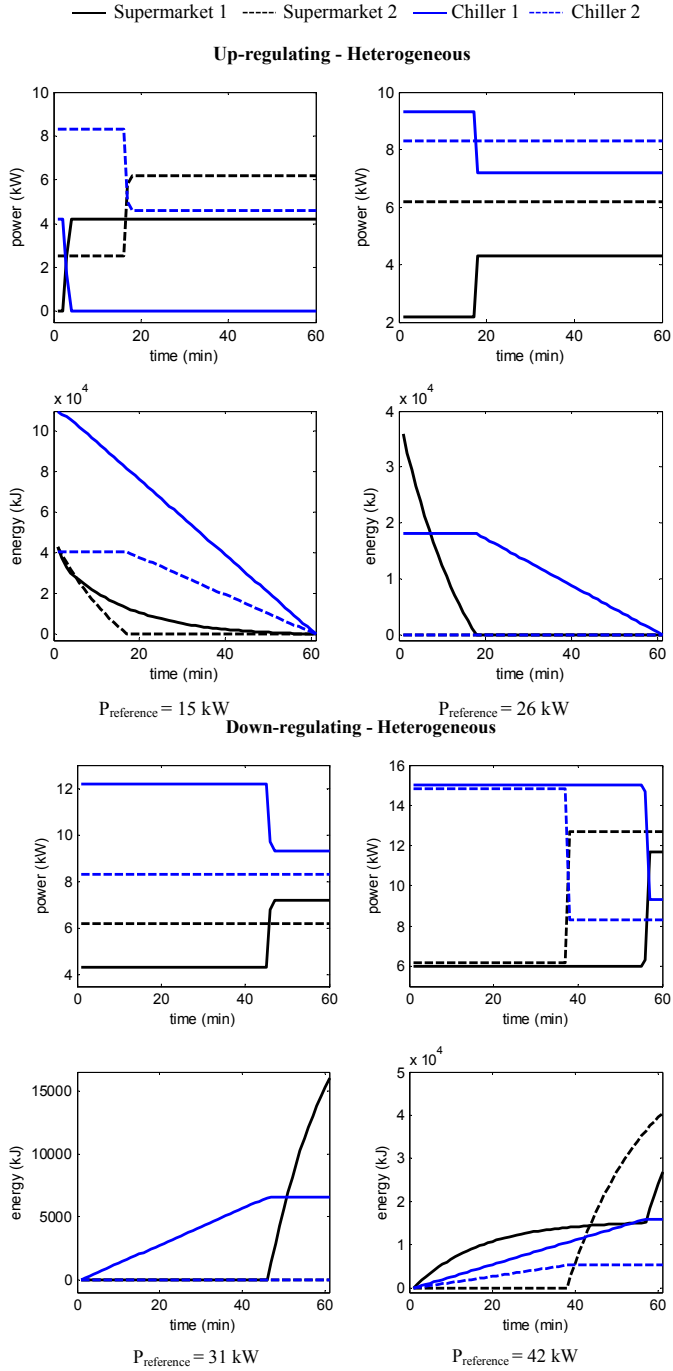


Figure 5.8: Power distributions from Aggregator 1 and Aggregator 2 to the consumers in the heterogeneous setup and the associated thermal energy changes in each consumer

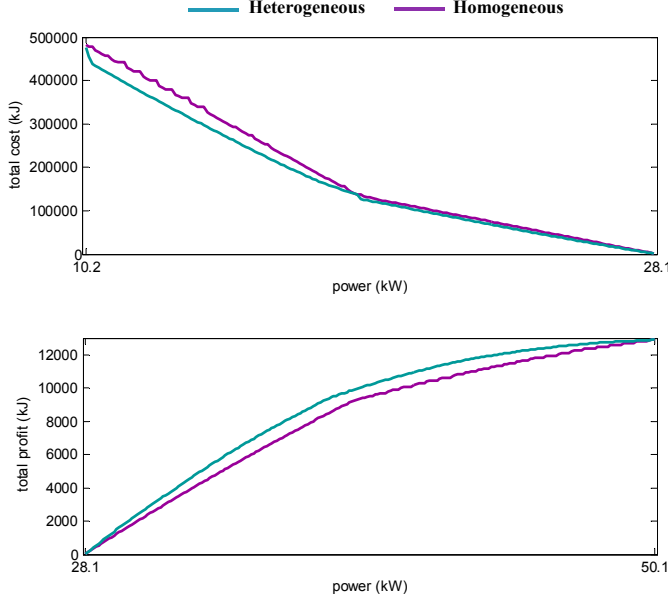


Figure 5.9: Total cost (extra energy consumption) and total profit (extra energy saving) for the homogeneous and heterogeneous setup.

cases at the supermarket are normally kept at the maximum level in order to reduce power consumption. Moreover, there is also enough space at the ice tank in normal situation. Let us consider a situation in which the both ice tanks are fully charged at the beginning of activation time. Figure 5.10 shows the result of simulating this situation for the heterogeneous setup, where we assume two identical supermarkets and chillers (Supermarket 2 and Chiller 2 in our examples) in order to eliminate the power distribution problem from the top-level controller to the aggregators. Hence, each aggregator receives  $\frac{P_{\text{reference}}}{2}$  to follow.

The top-level controller should follow  $P_{\text{reference}} = 40\text{kW}$  during a one-hour activation time while the  $P_{\text{base}} = 29\text{kW}$ . Thus, the service is down-regulating. The chiller is not able to consume more than its baseline,  $8.3\text{kW}$ , since the ice tank is fully charged and the supermarket cannot consume the rest of power,  $11.7\text{kW}$ , for one hour since the minimum temperature of the cold rooms will be violated. The heterogeneous aggregator can handle this situation in this way: In the beginning of activation time, the chiller consumes a little bit below its baseline power. So, it needs to melt some ice to provide the cooling load from the building. Melting ice in this period provides some space in the ice tank. Then the chiller is able to consume above its baseline and the supermarket can decrease its consumption to decrease the rate of energy saving. As we can see, several switchings occur between the supermarket and chiller during the ice building period. At the end of the activation time, we again have a fully charged ice tank. This flexibility is not available in the homogeneous setup.

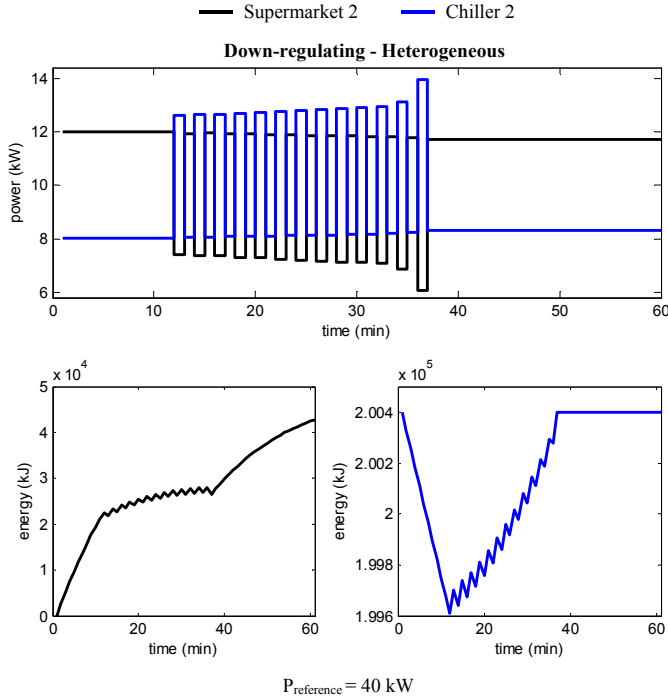


Figure 5.10: Power distributions and thermal energy changes for the heterogeneous setup with two identical supermarkets and chillers and for the down-regulating scenario. The both ice storages are fully charged at the beginning of activation time.

### 5.3 Evaluation of Aggregator

As explained in previous chapters, the aggregator in the direct setup requires a model of each consumer. To develop a realistic aggregator, the models should be extremely simple; however, this may lead to inaccurate results. In this part, we connect the aggregator with the simplified models to a complex and verified model of a supermarket that is available at the time of doing this project [66]. Then, by comparing the estimated results obtained from the aggregator with the actual results, we are able to evaluate our proposed aggregator setup. In the following, the supermarket refrigeration benchmark with a CO<sub>2</sub> booster configuration is explained.

The basic layout of a typical refrigeration system including several cooling units with two racks of compressors in a booster configuration is shown in 5.11. Starting from the receiver (REC), two-phase refrigerant (mix of liquid and vapor) at point ‘8’ is split out into saturated liquid (‘1’) and saturated gas (‘1b’). The latter is bypassed by a bypass valve (BPV), and the former flows into expansion valves where the refrigerant pressure drops to medium (‘2’) and low (‘2’’) pressures. The electronic expansion valves EV\_MT and EV\_LT are responsible for regulating the air temperature inside the medium temperature (MT) and the low temperature (LT) cooling units, respectively, by controlling the entering mass flows into the evaporators. Flowing through medium and low tempera-

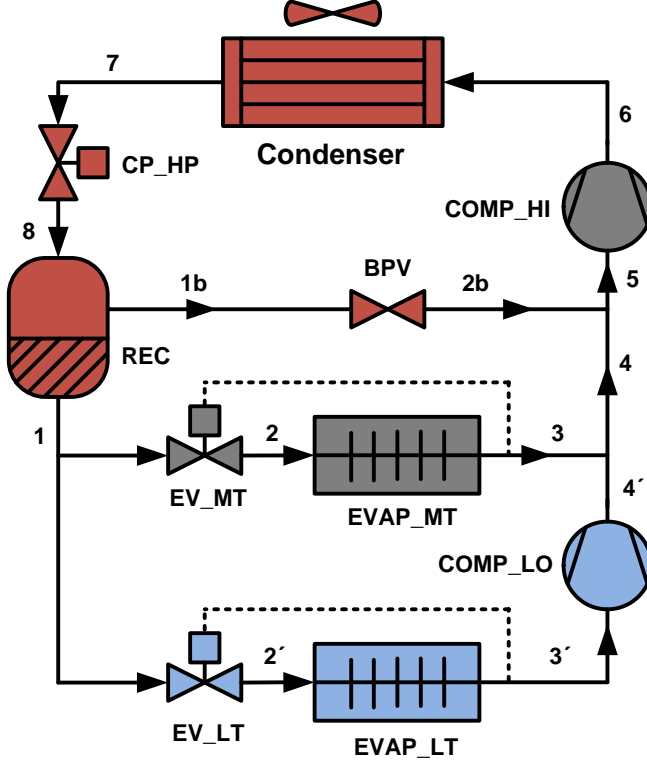


Figure 5.11: Basic layout of a typical supermarket refrigeration system with booster configuration [66]

ture evaporators (EVAP\_MT and EVAP\_LT), the refrigerant absorbs heat from the cold reservoir. The pressure of low temperature units (LT) is increased by the low stage compressor rack (COMP\_LO). All mass flows from COMP\_LO, EVAP\_MT and BPV outlets are collected by a suction manifold at point '5' where the pressure is increased again by high stage compressors (COMP\_HI). Afterward, the gas phase refrigerant enters the condenser to deliver the absorbed heat from cold reservoirs to the surrounding. The detailed dynamical model of the system is found in [66].

The supermarket benchmark is equipped with a local MPC that can regulate the power consumption of the compressor racks to the assigned set-points for smart grid services. The objective function for power following is defined as:

$$J_P = \sum_{t=1}^N \|P_c(t) - P_{\text{ref}}(t)\|_2^2 \quad (5.3)$$

where  $P_{\text{ref}}$  is the power reference and  $N$  is the prediction horizon in terms of the number of time steps (samples). Manipulated variables are the opening degrees of the expansion valves ( $OD$ ) and the evaporation temperature set-point ( $\hat{T}$ ). In the present work, for the sake of simplicity, we have considered a fixed evaporation temperature set-point. Looking

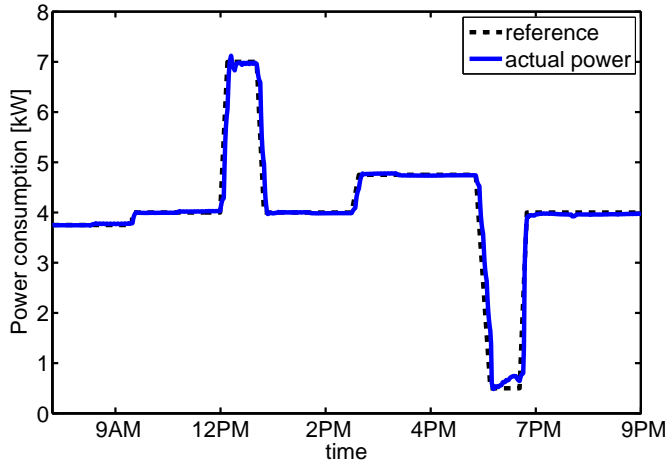


Figure 5.12: Power following performance of the supermarket refrigeration benchmark for energy imbalance management.

Table 5.4: Numerical values for simulation

	Baseline power	Maximum power	Maximum energy
Supermarket	4.1kW	11.6kW	169200kJ
Chiller	2.5kW	10kW	83520kJ

at the compressor rack as a closed loop system controlling the evaporation temperature, it turns out that the power consumption ( $P_c$ ) is the nonlinear function of the evaporation temperature ( $T_e$ ); and the cooling capacity ( $\dot{Q}_e$ ) is also a nonlinear function of both the evaporation temperature and opening degree of expansion valves ( $OD$ ). In [67], it is shown that how a convex optimization problem can be formulated by (i) introducing a fictitious manipulated variable; (ii) novel incorporation of  $T_e$  into the MPC scheme; and (iii) choosing appropriate sampling time and prediction horizon. Figure 5.12 shows how the predictive controller is able to follow a power reference even with a dramatic magnitude changes for energy balancing services.

At the aggregator, we again use the chiller model described by equations (4.33)-(4.36) and (4.28). For the supermarket system, we apply system identification methods to the supermarket refrigeration benchmark to develop a first-order model as:

$$\frac{x_s(s)}{u_s(s)} = \frac{K_p}{1 + T_p s} \quad (5.4)$$

Numerical values for simulation are listed in Table 5.4. The supermarket consists of seven medium temperature and four low temperature cold rooms with temperature limits  $[1^\circ C, 5^\circ C]$  and  $[-24^\circ C, -18^\circ C]$  respectively. We consider a down-regulating scenario in which, the energy saving after the activation time  $((P_{s,base} - P_{s,min}) \times T_{s,off} + (P_{c,base} - P_{c,min}) \times T_{c,off})$  represents the profit attained by the aggregator. Due to mismatch between the simple and the complex model, there will be discrepancy between the actual profit and

the estimated profit computed by the aggregator. To evaluate the aggregator against the verified model of the supermarket, we compare the actual profit with the estimated profit. In this way, we can understand how accurate the proposed model is in estimating the actual profit. The aggregator distributes power references at each sampling time during the one hour activation time. After the activation, the local MPC at the supermarket will receive power references in the following way:

$$\begin{cases} P_s(t) = P_{s,\min} & x_s(t) > X_s \\ P_s(t) = \rho P_{s,\text{base}} & x_s(t) \leq X_s \end{cases} \quad (5.5)$$

where  $\rho$  is a constant value close to one. The supermarket consumes its minimum power as long as the stored energy reaches a certain value close to zero ( $X_s$ ). To retrieve the remaining energy, the supermarket then keep its consumption at a level a bit below the baseline. Afterwards, the supermarket consumes its baseline consumption. This strategy minimizes the time needed for regaining the stored energy and consequently minimizes the heat loss to the surrounding. The constant values,  $\rho$  and  $X_s$ , are considered to ensure the temperature constraints are not violated at the supermarket. A simple local controller can handle the time after the activation since the aggregator does not know the actual energy level.

Actual power consumption of the supermarket during the activation for three power references to the aggregator ( $P_{\text{reference}} = 8, 15, 18\text{kW}$ ) is shown in Figure 5.13. Double-sided arrows indicate the activation time when the supermarket is asked to follow the power reference. After the activation, the supermarket does not need to follow the reference. As we stated before, minimum power (0kW here) is just distributed to deplete the storage as fast as possible. It is shown the supermarket can follow the power reference in a satisfactory manner, although there is a delay in response to power changing. This delay is due to the different sampling times of the aggregator and the supermarket. Figure 5.14 shows the temperature variation of different cold rooms at the supermarket during and after the activation for  $P_{\text{reference}} = 18\text{kW}$ . As can be seen, the medium temperature cold rooms are exploited more than the low temperature cold rooms. The reason is the lower loss because of the lower temperature difference between the ambient and the medium temperature cold rooms.

The actual and estimated profit in terms of energy saving after the activation for the power references from  $8\text{kW}$  to  $20\text{kW}$  are shown in Figure 5.15. The estimated profit is obtained from the optimization at the aggregator whereas, for the actual profit, we consider the actual energy regained after the activation at the supermarket. For all power references, the actual profit is greater than the estimated profit, however for high power references, the discrepancy between the actual and estimated profit is higher. This is not unexpected. In the simple model of supermarket, we assume the COP to be constant. This assumption is no longer valid when the power consumption increases. The average difference between the actual and estimated profit is 11.2%. It should be noted, the results shown here evaluate a distribution obtained from an optimization based on two simple models of the supermarket and the chiller against a verified model of the supermarket and a simple model of the chiller. However, if we have a verified model of the chiller as well, a comprehensive scenario for evaluation can be considered. In this case, we can investigate if there is other power distribution between the consumers which leads to higher profit in practice. We have studied the nature of profit curves for different switching strategies between the supermarket and the chiller. Those turned out to be very ‘flat’ close to the

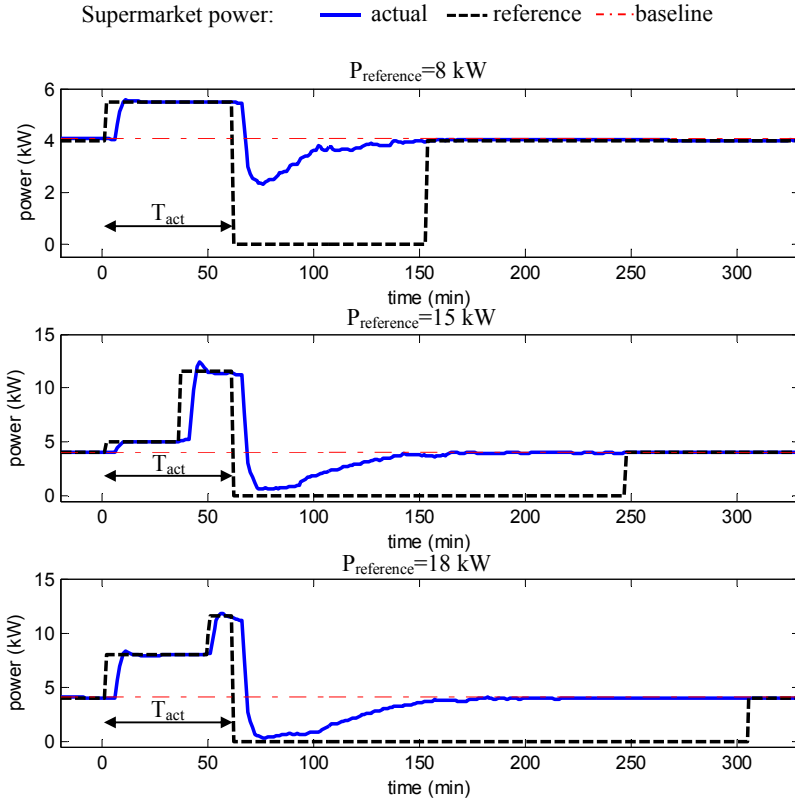


Figure 5.13: Actual power consumption of the supermarket for different power references to the aggregator, where double sided arrows indicate the activation time.

optimum. We take this to be evidence for the following conjecture: The discrepancy between the estimated and actual profit could be very small if we evaluate the aggregator against the two verified models of supermarket and the chiller.

## 5.4 Robust Setup

This part covers two types of simulations, the proposed feedback mechanism and the two-stage optimization.

### 5.4.1 Feedback Mechanism

Again we consider the aggregator with two identical supermarkets and two identical chillers same as Section 5.1. Power distributions for this setup are shown in Figure 5.2 and numerical values for simulation are listed in Table 5.2. Applying Algorithm 1 proposed

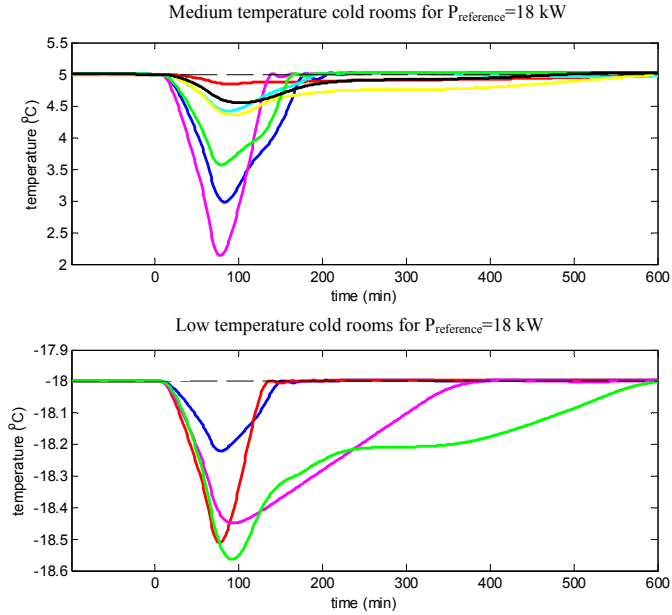


Figure 5.14: Temperature variation of the cold rooms at the supermarket during and after the activation.

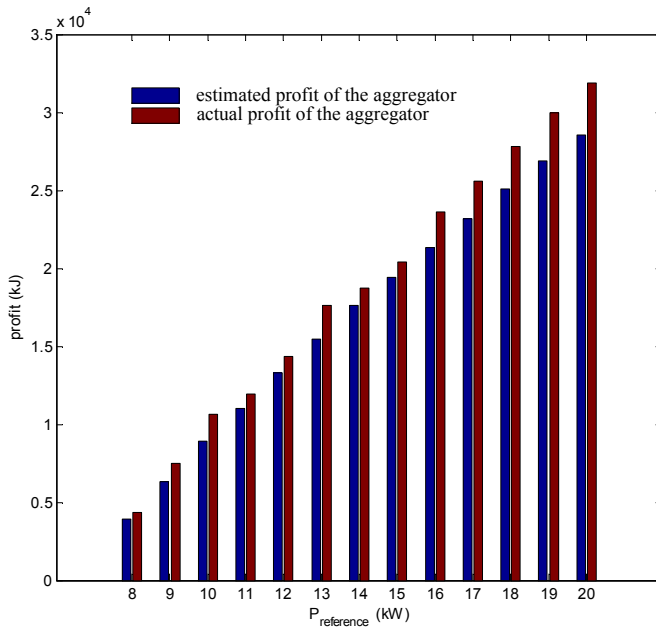


Figure 5.15: Profit of the aggregator in terms of energy saving after the activation.



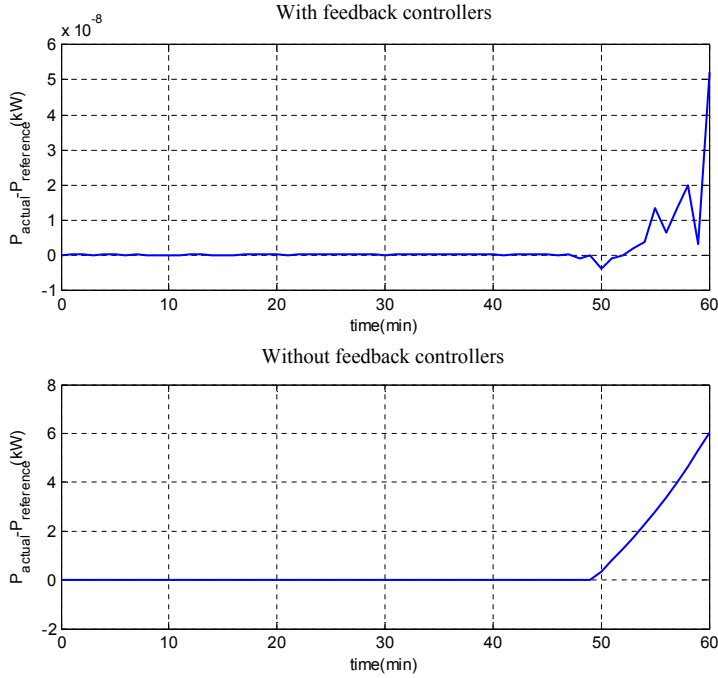


Figure 5.16: Discrepancy between the actual power consumption and the power reference for  $P_{\text{reference}} = 37\text{kW}$ ,  $\Delta_{s1} = \Delta_{s2} = 10^{-5}$ ,  $\Delta_{c1} = \Delta_{c2} = 10^{-9}$ . Note the different scale on the ordinate axis

in Chapter 3 for  $P_{\text{reference}} = 37\text{kW}$  provides:

$$\begin{aligned} \delta_{s1,\max} &= \delta_{s2,\max} = 10^{-5} && \text{for the supermarkets} \\ \delta_{c1,\max} &= \delta_{c2,\max} = 10^{-9} && \text{for the chillers} \end{aligned}$$

In the simulation, we assume  $\delta_{si,\min} = -\delta_{si,\max}$ ,  $\delta_{ci,\min} = -\delta_{ci,\max}$  (for  $i = 1, 2$ ) and

$$K = \begin{bmatrix} 1 & -\frac{1}{3} & -\frac{1}{3} & -\frac{1}{3} \\ -\frac{1}{3} & 1 & -\frac{1}{3} & -\frac{1}{3} \\ -\frac{1}{3} & -\frac{1}{3} & 1 & -\frac{1}{3} \\ -\frac{1}{3} & -\frac{1}{3} & -\frac{1}{3} & 1 \end{bmatrix}$$

Figure 5.16 shows the discrepancy between the actual power,  $P_{\text{actual}}$ , and the desired power reference. As shown in the figure, without the feedback loops, the discrepancy is significant (lower plot). However, with having the feedback loops, the difference is almost zero (upper plot). In addition, the system state constraints are not violated. Energy changes for one supermarket and chiller during the activation correspond to  $\Delta_{s1} = 10^{-5}$ ,  $\Delta_{c1} = 10^{-9}$  is depicted in Figure 5.17. As shown, the system states remain in the cube defined by the constraints during the activation.

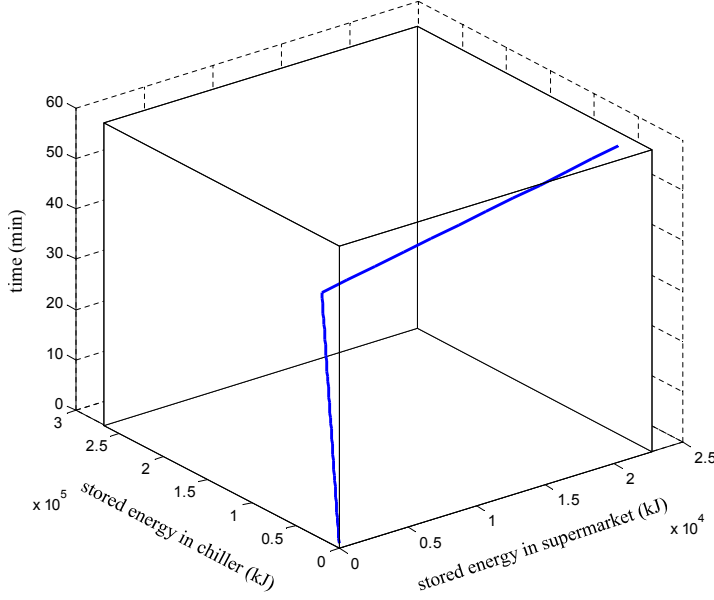


Figure 5.17: System states evolution with the feedback loops during the activation for  $P_{\text{reference}} = 37kW$ ,  $\Delta_{s_1} = 10^{-5}$ ,  $\Delta_{c_1} = 10^{-9}$ . Note that the time axis is vertical in this plot

### 5.4.2 Two-stage Optimization

For the simulation of the proposed two-stage optimization in Section 3.3, an aggregator setup is considered which controls two supermarkets and two chillers. The nominal values of the system parameters are same as Table 5.3, however the system parameters are allowed to varies within a predefined convex set. We assume the following dynamics for the four units:

Supermarket 1:

$$x_1(t+1) = (A_{1,1} + \alpha_{1,1})x_1(t) + (B_{1,1} + \beta_{1,1})u_1(t) \quad (5.6)$$

Supermarket 2:

$$x_2(t+1) = (A_{2,1} + \alpha_{2,1})x_2(t) + (B_{2,1} + \beta_{2,1})u_2(t) \quad (5.7)$$

Chiller 1:

$$x_3(t+1) = \begin{cases} x_3(t) + (B_{3,1} + \beta_{3,1})u_3(t) & u_3(t) \geq 0 \\ x_3(t) + (B_{3,2} + \beta_{3,2})u_3(t) & u_3(t) < 0 \end{cases} \quad (5.8)$$

Chiller 2:

$$x_4(t+1) = \begin{cases} x_4(t) + (B_{4,1} + \beta_{4,1})u_4(t) & u_4(t) \geq 0 \\ x_4(t) + (B_{4,2} + \beta_{4,2})u_4(t) & u_4(t) < 0 \end{cases} \quad (5.9)$$

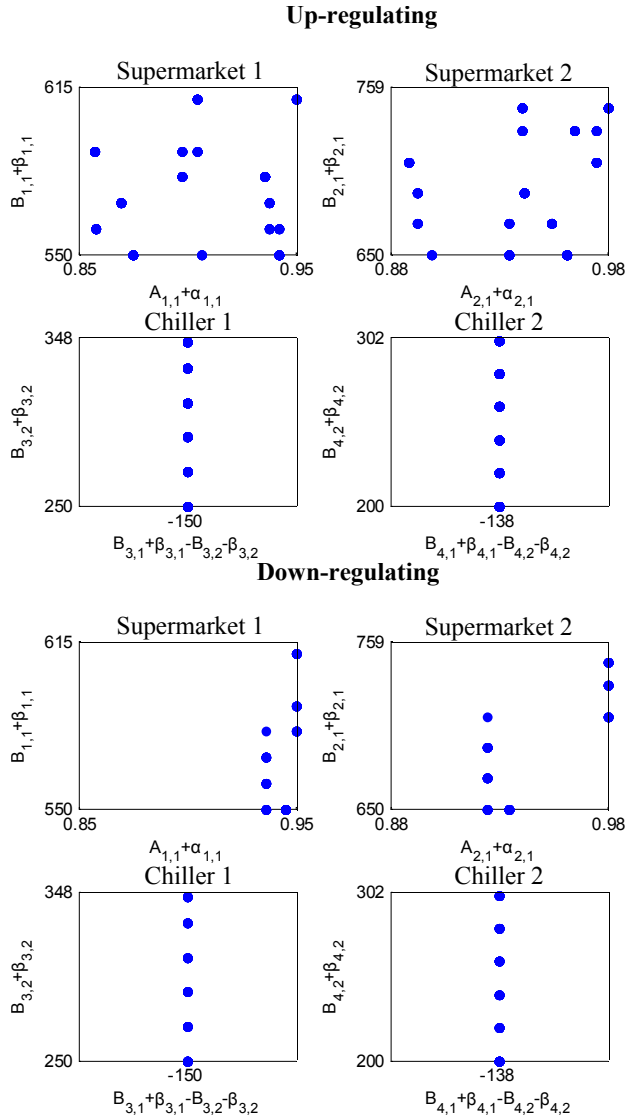


Figure 5.18: Uncertainty set of the model parameters for the up-regulating and the down-regulating scenario. Dots indicate the actual value of the parameters

Uncertainty sets of the system parameters for the up-regulating and the down-regulating scenarios are shown in Figure 5.18. For the supermarkets, we assume that the parameters  $A_{1,1}$  and  $A_{2,1}$  are changed randomly every 30 minutes, since these parameters describe the heat loss to the surrounding and are dependent on the customers' behaviour at the supermarkets.  $B_{1,1}$  and  $B_{2,1}$  reflect the COP of the compressors. We assume these parameters decrease during the activation time, since the consumers are operated outside of their optimum region. For the chillers,  $B_{3,1}$  and  $B_{4,1}$  represent the COP in charging

mode ( $\text{COP}_{\text{ice}}$ ), whereas  $B_{3,2}$  and  $B_{4,2}$  reflect the COP in cooling mode ( $\text{COP}_{\text{cool}}$ ). We also assume these parameters decrease during the activation with the same rate, such that the differences ( $B_{3,1} + \beta_{3,1} - B_{3,2} - \beta_{3,2}$  and  $B_{4,1} + \beta_{4,1} - B_{4,2} - \beta_{4,2}$ ) which appear in the final models, are fixed.

Simulation results for the up-regulating ( $P_{\text{reference}} = 12\text{kW}$ ) and the down-regulating ( $P_{\text{reference}} = 40\text{kW}$ ) scenarios are shown in Figure 5.19 and Figure 5.20. The total baseline consumption is 28.1kW. The red dashed lines are the desired values, which are obtained from the offline optimization with the fixed model parameters long before the activation time (the first stage as defined in Section 3.3), whereas the blue solid lines are the real values during the service activation, when the model parameters are time-varying (the second stage as defined in Section 3.3). As we described earlier, an online optimization is run during the service activation which aims to minimize the deviation between the desired and real values with a quadratic cost function. The On-time and the off-time periods of each consumer are also shown in the figures. The chillers have quite longer on-time periods in the up-regulating scenario than the supermarkets for our simulation examples. The difference between the desired and real power is also greater for the chillers in up-regulation.

The total electrical power and the thermal energy changes of the four consumers are shown in Figure 5.21. The values are shown during  $T_{\text{act}} + T_{\text{on}}$  for the up-regulating scenario and during  $T_{\text{act}} + T_{\text{off}}$  for the down-regulating scenario, where  $T_{\text{on}}$  is the maximum on-time period and  $T_{\text{off}}$  is the maximum off-time period of the four consumers.  $T_{\text{act}}$  denotes the activation time. The results are as we expected. In both scenarios, the aggregated power consumption is equal to  $P_{\text{reference}}$  during  $T_{\text{act}}$ . For the up-regulating scenario, the actual power consumption is lower than the value which is obtained from the offline optimization. This is reasonable since the offline optimization has been performed for the worst case in which the cost is maximum. However, the situation is better during the service activation and accordingly, lower energy consumption is needed during  $T_{\text{on}}$ . On the other hand, in the down-regulating scenario, the offline optimization has been performed for the best case in which the profit is maximum. That is why the power consumption is above the offline value during the off-time period, which means the lower profit.

## 5.5 Indirect Control

Similar to the direct setup, we consider a power reference following scenario as depicted in Figure 5.22. In the indirect setup, there is no feedback from the consumers to the grid operator. Here, we assume a good estimate of the aggregated power consumption,  $\bar{P}(t)$ , is available at the aggregator. The aggregator acts as a price generator which aims to generate the price signals,  $\mathcal{P}(t)$ , in such a way that the aggregated power consumption follows the power reference,  $P_{\text{reference}}$  during an activation time. Unlike the direct setup, we consider only one aggregator in the indirect setup, since a same price should be communicated to all the DERs. Moreover, the indirect aggregator has a less complicated design and can handle a greater number of DERs than the direct aggregator. We assume a simple PI (proportional-integral) controller at the aggregator to produce the price signals. PI controller is one of the most useful controller in practice, especially when no model of the system is available for the operator [68]. It comprises two parts, the proportional part generates an output proportional to the current input error while the integral part pro-

## Up-regulating

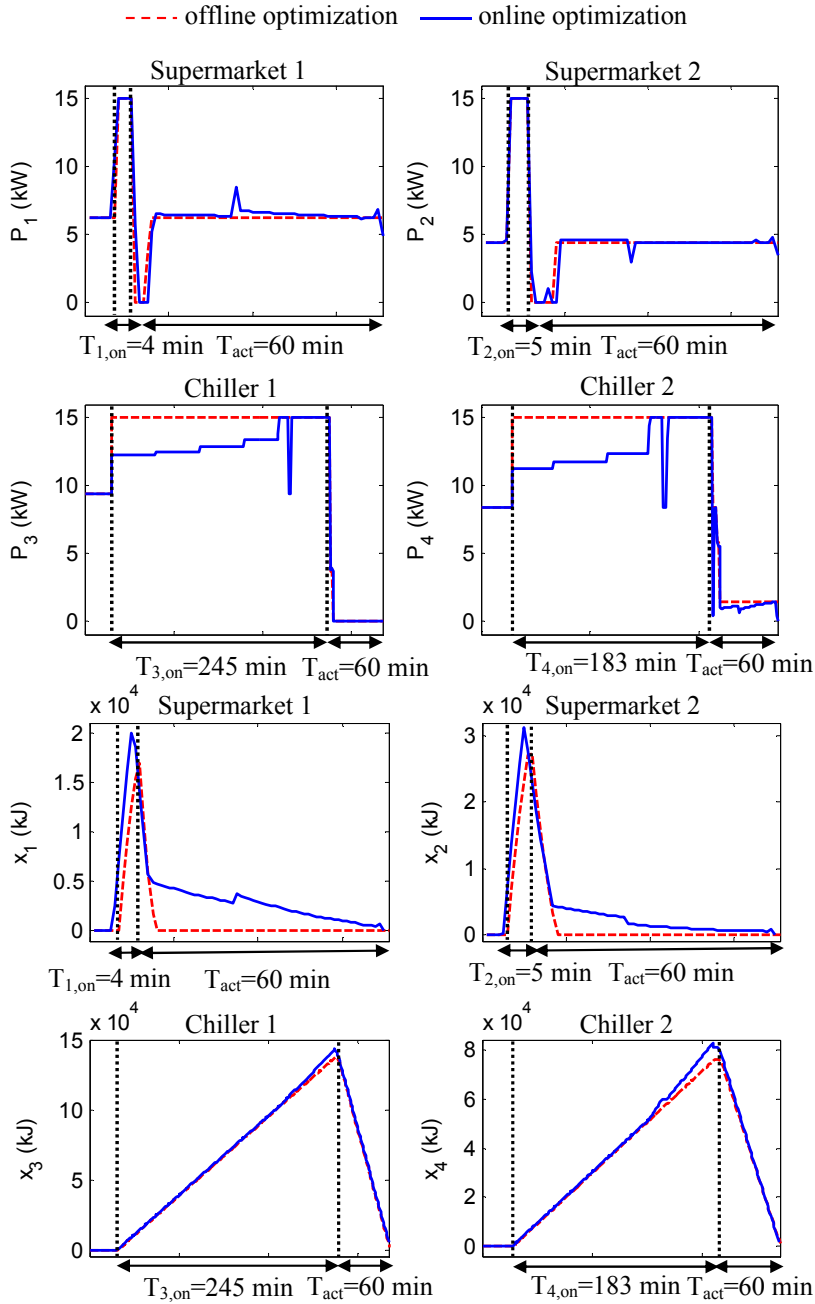


Figure 5.19: Robust MPC setup: Power distributions (the four upper plots) and the thermal energy changes (the four lower plots) during the extended activation time in the up-regulating scenario for  $P_{reference} = 12\text{kW}$

## Down-regulating

--- offline optimization    — online optimization

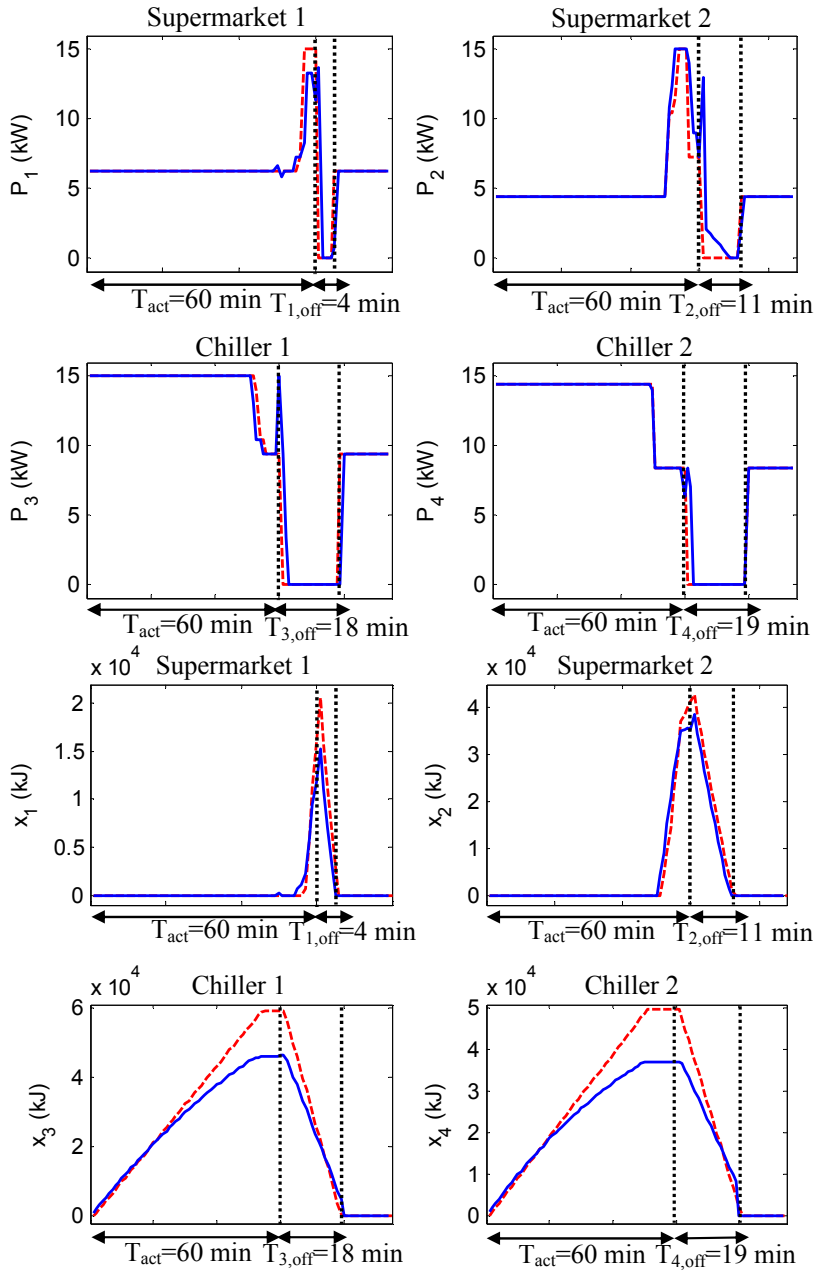


Figure 5.20: Robust MPC setup: Power distributions (the four upper plots) and the thermal energy changes (the four lower plots) during the extended activation time in the down-regulating scenario for  $P_{\text{reference}} = 40\text{kW}$

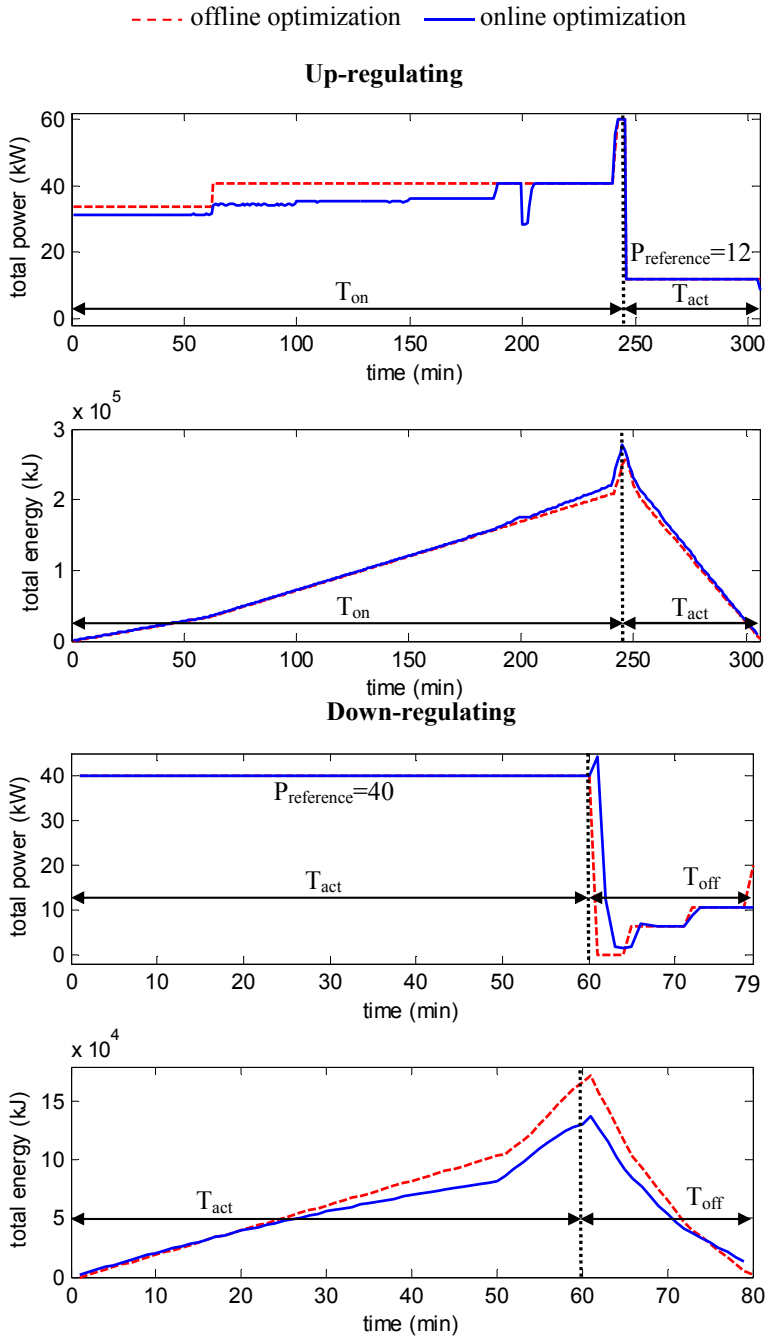


Figure 5.21: Robust MPC setup: The total power distribution and the thermal energy changes during the activation time plus the maximum on-time/off-time period of the four consumers for the up/down-regulating scenario

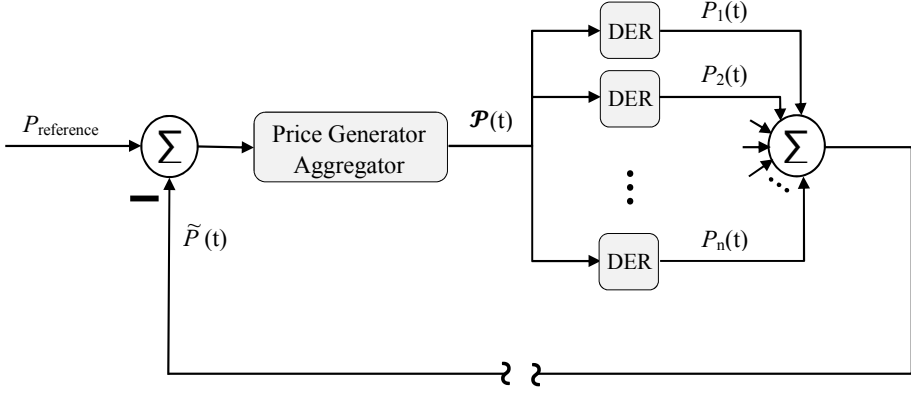


Figure 5.22: Indirect control setup, where  $\mathcal{P}(t)$ ,  $P_i(t)$  ( $i = 1, \dots, n$ ) and  $\tilde{P}(t)$  denote the price signal, power consumption of each DER and estimation of the aggregated power consumption respectively

duces an output proportional to the accumulated error from the beginning to the current time, i.e. the output of the PI controller is  $u(t) = k_P e(t) + k_i \int_{t=0}^t e(t) dt$ . Thus, in the discrete-time format, the price is calculated as below:

$$\mathcal{P}(t) = \mathcal{P}(t-1) + k_p(e(t) - e(t-1)) + k_i T_s e(t) \quad (5.10)$$

$$e(t) = P_{\text{reference}} - \tilde{P}(t) \quad (5.11)$$

where,  $k_p$  and  $k_i$  are the proportional gain and the integral gain respectively.  $T_s$  is the sampling time. On the other hand, the DERs should be equipped with price-responsive controllers locally. We assume, a simple model of each DER is available at the local places. With having a model of the system, a natural candidate for the local price - responsive controller can be the model predictive controller (MPC).

For the local MPC formulation in the indirect setup, we consider the down-regulation scenario. Suppose, the aggregator aims to motivate the consumers to increase their power consumption during an specific activation time. To this end, the grid operator needs to lower the price from its normal value at the beginning of the activation time. We indicate the normal electricity price with  $\mathcal{P}(0)$ , which is the price of electricity outside of the activation period and it is known for the local units. Then, the proposed MPC formulation for the  $k$ th DER is as follows:

$$\min_{u_k} \left[ \left( \mathcal{P}(t) \times \sum_{t=1}^N u_k(t) \right) - \left( \mathcal{P}(0) \times T_{k,\text{off}} \times (-u_{k,\text{min}}) \right) \right] \quad (5.12)$$

Subject to :

Consumer's dynamic

$$x_{k,\text{min}} \leq x_k(t) \leq x_{k,\text{max}} \quad (5.13)$$

$$u_{k,\text{min}} \leq u_k(t) \leq u_{k,\text{max}} \quad (5.14)$$

where, the system input ( $u_k$ ) and the system state ( $x_k$ ) are subject to constraints. At the beginning of activation, the aggregator distributes lower price than the normal price to



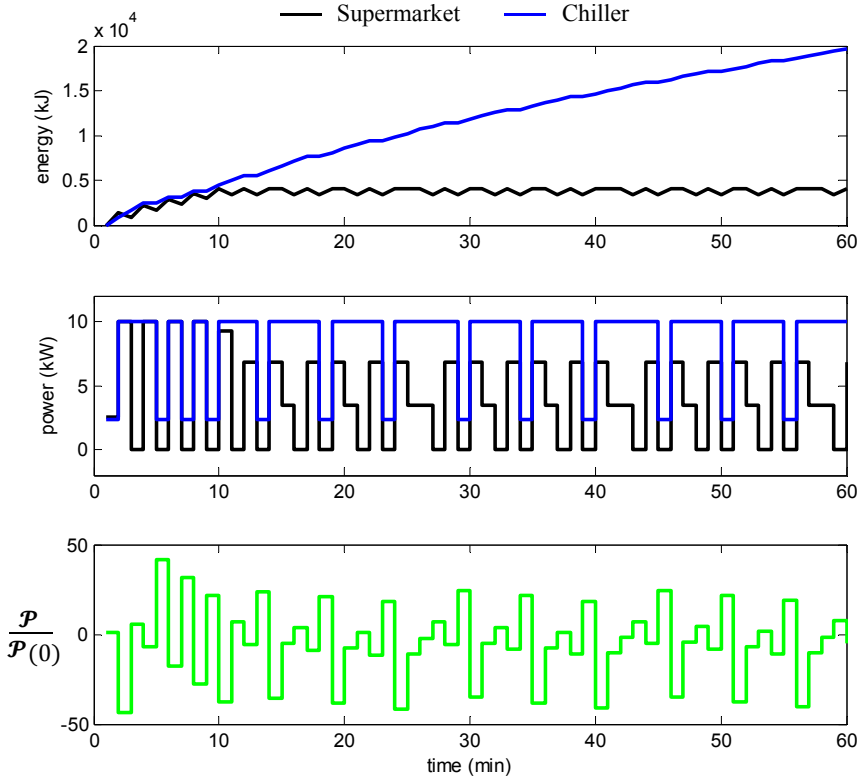


Figure 5.23: Power distribution, thermal energy changes and the price signal in the indirect setup for  $P_{\text{reference}} = 12\text{kW}$

see the increase in consumption. In this situation, the DERs may decide to store some extra energy in their thermal storages at a lower cost. Thus, they can benefit thereafter by turning off their devices when the price returns back to the original value. The objective function (5.12) consists of two parts. The first part represents the cost of energy consumption during the prediction horizon,  $N$ , at the lower price,  $\mathcal{P}(t)$ , since  $u_k$  indicates the power deviation from the baseline power. The second part represents the revenue can be achieved during the off-time period,  $T_{k,\text{off}}$ , when the power consumption is equal to the minimum power and  $u_k(t) = u_{k,\text{min}} = P_{k,\text{min}} - P_{k,\text{base}}$ . In other words, the DER is able to save  $\mathcal{P}(t) \times (P_{k,\text{base}} - P_{k,\text{min}})$  at each sampling time during the activation. The optimization is run at each sampling time during the activation. The first sample of the vector,  $[u_k(1) \ u_k(2) \ \dots \ u_k(N)]'$  is then applied to the real system.

For simulating an indirect scenario, we consider a setup consists of a supermarket and a chiller. Same as the first part of Section 5.1, for the supermarket system, we use the model described by equations (4.6)-(4.13) and for the chiller system, we use the model described by equations (4.25)-(4.29). We also use the numerical values listed in Table 5.1. The activation time and the prediction horizon of the local MPC are chosen one hour and half an hour respectively. The grid operator aims to follow  $P_{\text{reference}} = 12\text{kW}$ , while the baseline consumption is equal to  $4.83\text{kW}$ . The results are shown in Figure 5.23.

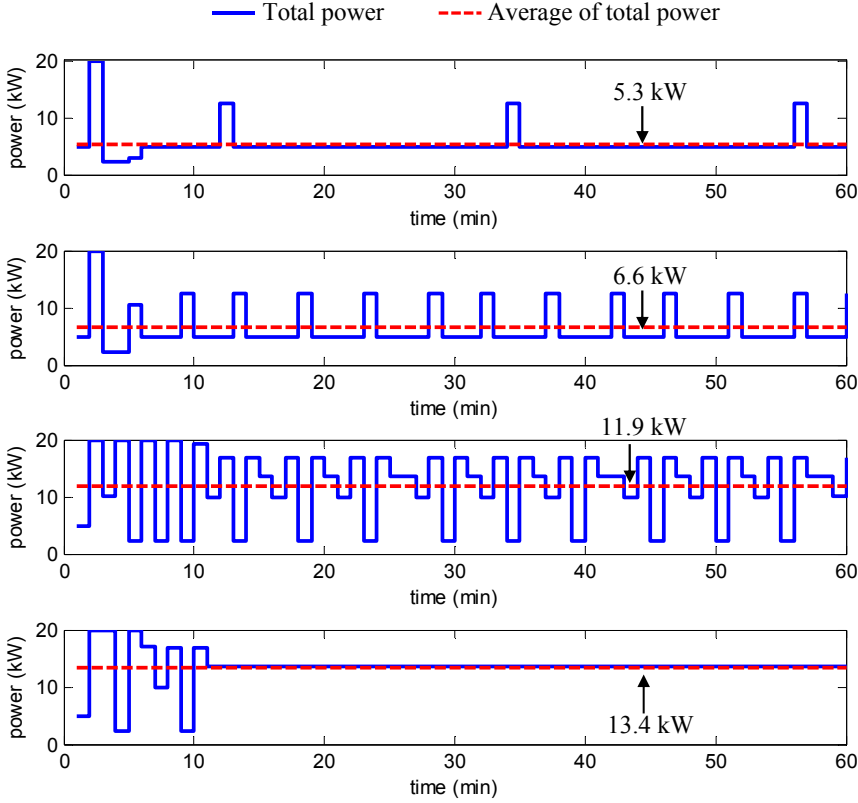


Figure 5.24: Total power and the average of total power in the indirect setup for  $P_{\text{reference}} = 5.2 \text{ kW}$ ,  $P_{\text{reference}} = 6.5 \text{ kW}$ ,  $P_{\text{reference}} = 12 \text{ kW}$  and  $P_{\text{reference}} = 13.5 \text{ kW}$

The plot on the top shows the thermal energy changes in each TES and the plot in the middle shows the power distribution among them. The plot at the bottom indicates the ratio of price signal to the normal electricity price. As can be seen, at the beginning of activation, the price generator reduces the price to motivate the consumers to consume more power. It even produces negative price. This causes the significant increase in the power consumption of the consumers such that the aggregated consumption exceeds the power reference. To compensate the deviation, the price generator increases the price consequently and this process continues during the whole horizon. As the energy plot shows, both the TESs are utilized from the beginning. The total power and the average of total power for four power references,  $P_{\text{reference}} = 5.2 \text{ kW}$ ,  $P_{\text{reference}} = 6.5 \text{ kW}$ ,  $P_{\text{reference}} = 12 \text{ kW}$  and  $P_{\text{reference}} = 13.5 \text{ kW}$  are shown in Figure 5.24. The aggregated power cannot follow the power reference at all times during the activation. However, the average of power over the horizon is almost equal to the power reference.

## 5.6 Summary

In this chapter, we presented the simulation results of applying the proposed models, control methods and algorithms in the previous chapters, to our case studies. The results were provided in five sections, while the power reference following scenario is common in all of them.

Section 5.1 showed the power distributions from one aggregator to the supermarkets and the chillers for different power references. The aggregator assigned different power profiles to each consumer to follow, depending on the consumers' model and its own objective function.

In Section 5.2, we investigated what if we aggregate different consumers or the same type of consumers, where we had a set of aggregators in our setup. To this end, we considered two types of aggregation: the homogeneous aggregation in which each aggregator controls the same consumer type and the heterogeneous aggregation in which each aggregator controls a heterogeneous portfolio of consumers. Simulation results for the two different consumers, supermarket and chiller, showed the heterogeneous aggregation outperforms the homogeneous one. Firstly, the heterogeneous aggregation has a lower cost and greater profit from energy consumption point of view. Secondly, unpredictable situations can be better handled with the heterogeneous aggregation. In other words, the heterogeneous aggregation is more flexible than the homogeneous one.

Simplified model of the consumers that are utilized at the aggregator might not capture all dynamics and features of the real systems. In Section 5.3, we evaluated the aggregator against a verified model of an actual supermarket. Simulation results showed there is a 11.2% difference between the estimated profit obtained from the optimization problem with the simple model of the consumers and the actual profit. Moreover, we saw that the actual supermarket is able to satisfy the aggregator's objective in terms of following a specified power reference.

Section 5.4 showed the simulation results of applying the two proposed methods for compensating the error arises from model mismatch. First, we simulated a setup, which consists of an MPC controller together with a series of feedback loop. The largest uncertainties can be handled in our setup was determined via a brute-force approach. As shown, the error in following the power reference is much lower with the feedback loops. Second, simulation of the proposed robust MPC for our particular case studies revealed that the robust design can handle the mismatch between the actual and assumed model of consumers pretty well.

Finally, in Section 5.5, we proposed and simulated an indirect setup, where the price generator aimed to control one supermarket and one chiller indirectly. The results showed that the aggregator cannot follow the power reference in all time during the activation, however, the average power over an activation is almost equal to the specified power reference. Thus, this setup is more suitable for an energy reference following scenario. Moreover, heterogeneity of the consumers did not matter in the indirect setup, while in the direct setup, the aggregator utilized the flexibility of the consumers in a clever way considering the type of consumers and their flexibility characteristics.

## 6 | Experimental Verification

As mentioned in Chapter 1, iPower project, which this PhD project is a part of, has emphasized on real-life demonstrations. To meet the iPower vision as well as verify the theoretical studies, we introduce an experimental setup, in which we are able to demonstrate the power reference following scenario. In this chapter, we first explain the experimental setup, involving different components of the experiment and the experimental scenarios. Then, the experimental results are provided.

### 6.1 Experimental Setup

#### 6.1.1 Components

The DERs available for the experiment are a real supermarket, a supermarket refrigeration lab and a real chiller in conjunction with an ice storage. The real supermarket is a fakta supermarket that is located in Otterup, Denmark. The supermarket refrigeration lab is located at the refrigeration lab at the Danfoss headquarters in Nordborg, Denmark. The ice storage system is located at the Grundfos headquarters in Bjerringbro, Denmark. In addition to the DERs, a flexible intelligent energy laboratory, called SYSLAB, that is located on DTU's Risø campus in Roskilde, Denmark, is also used in part of the experiment. The experimental setup consists of only one aggregator which is run on the campus of Aalborg University, Denmark. As seen, different components are situated several hundred kilometers apart (see Figure 6.1) and they are virtually connected through the internet connection. A simple whiteboard server was developed and deployed on a publicly accessible web server, where each component has full read/write access to the whiteboard.

#### 6.1.2 Service Chosen for the Experiment

As shown in Figure 1.4, there should be collaboration between the different work packages of iPower project. It is important that one work package can apply and use the findings from the other work packages. In this regard, we choose the services proposed by the work package 3 of iPower project for the experimental setup. Work package 3 of iPower project has already worked on the definition of services provided by DER portfolios that would be of interest to the distribution system operators (DSOs). The outcome of this work can be found in [69]. In summary, seven service types are described. These services can be categorized as shown in Table 6.1. From the proposed services, "PowerCut



Figure 6.1: Location of the different components of the experimental setup

planned”, “PowerCut urgent” and “Power reserve” are less interesting for the experiment, since in these services, the aggregator will send static pre-defined setpoints to the DERs and there there is no closed aggregator loop. The last two services in Table 6.1, i.e. “VoltageSupport” and “VArSupport”, include both active and reactive power resources, with the reactive resources being preferred. Thus, these services cannot be the candidates, since the DERs available for the experiment are controllable only with respect to their active power consumption. The most interesting candidates for the experiment are therefore the “PowerMax” and “PowerCap” services.

Table 6.1: Distribution grid services from [69]

Service name	Closed aggregator loop	Closed DSO loop	Active power	Reactive power
PowerCut planned			X	
PowerCut urgent			X	
Power reserve			X	
PowerCap	X	X	X	
PowerMax	X		X	
VoltageSupport	X	X	(X)	X
VArSupport	X		(X)	X

The basic idea behind the “PowerMax” and “PowerCap” services is that by buying these flexibility products, the DSO can be ensured that a feeder of interest will never

be higher loaded. These services are similar but specifically differ in the involvement of the DSO. In the “PowerMax” service, the DSO only provides a static setpoint to the aggregator, whereas in the PowerCap service the DSO is part of the closed control loop, providing dynamic feedback about the state of the grid. This means, the aggregator commits to limiting the absolute active power consumption of its combined portfolio of units to stay below a maximum value while the service is activated. The maximum value in the “PowerMax” service is typically set long before service activation, as part of a load prognosis performed by the DSO. However, in the “PowerCap” service, the maximum value changes during the service activation based on the DSO feedback from the grid.

## 6.2 Sequence of Operations

In this section, the sequence of operations in both “PowerMax” and “PowerCap” experiment are described. At the time of running the “PowerMax” experiment, the only supermarket available was the supermarket refrigeration lab at the Danfoss headquarters. Thus, the DERs for the “PowerMax” experiment are the supermarket lab and the real chiller. For the “PowerCap” experiment, we had the chance to connect the setup to the real supermarket. Thus, the DERs for the “PowerCap” experiment are the real supermarket and real chiller. Moreover, the SYSLAB test facilities were not utilized in the “PowerMax” experiment. Because, in this experiment, the aggregator receives a static setpoint and the state of the grid is not updated during the service activation. For the “PowerCap” experiment, however, some parts of the SYSLAB are used as explained in the following.

### 6.2.1 PowerMax Service

Basic components of the “PowerMax” experimental setup together with the power flows and the sequence of operations are shown in Figure 6.2. An overview of sequence of operations is as follows:

1. Using the load forecast, the DSO is able to define the required daily load reduction. Thus, the DSO sends the “PowerMax” signal to the aggregator which includes the information of maximum permissible power consumption.

**At each sampling time during the service activation:**

2. The aggregator runs an optimization which provides the desired power reference for the supermarket,  $P_{s,desired}$ , and the chiller,  $P_{c,desired}$ .
3. Each consumer changes its local settings to follow the power reference in the best possible way. Afterwards, they will announce the actual measured power,  $P_{s,measured}$  and  $P_{c,measured}$ , to the aggregator.
4. The aggregator announces the actual aggregated power consumption to the DSO.

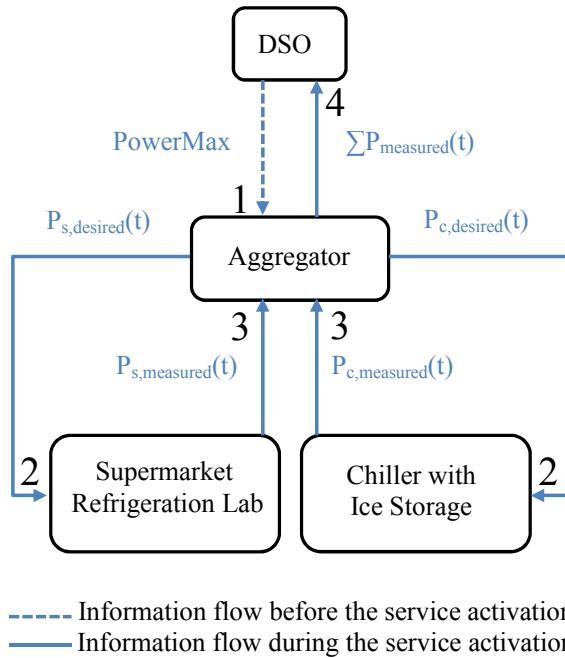


Figure 6.2: Electrical power flow at the “PowerMax” experimental setup with the sequence of operations.

### 6.2.2 PowerCap Service

For demonstrating the “PowerCap” service, we use some parts of the SYSLAB laboratory. One of the feeder at the SYSLAB is chosen for the experiment. The feeder is connected to a house, called FlexHouse, which plays the role of non-flexible load in our experimental setup, in a sense that the aggregator has no control over the FlexHouse power consumption. It is not possible to connect the feeder to the real supermarket and chiller, since they are situated several hundred kilometers apart. Instead, we use the dump loads available at the SYSLAB to emulate the consumption of the chiller and the supermarket. Dump loads are electrical resistors which are used to burn the total consumption of the supermarket and the chiller.

The feeder is fed by a diesel generator. It was planned to connect the feeder to the wind turbine available at the SYSLAB, to support the idea of using the flexible consumption to mitigate the impact of fluctuating renewable resources on the power grid. However, the generation of a single wind turbine is too fluctuating and an aggregator with just two DERs under its control will not be able to compensate that amount of fluctuations. Instead, we use the diesel generator to emulate the wind turbine generation with less fluctuations such that it is appropriate for our setup. Figure 6.3 shows the basic components of the “PowerCap” experimental setup. An overview of sequence of operations is as follows:

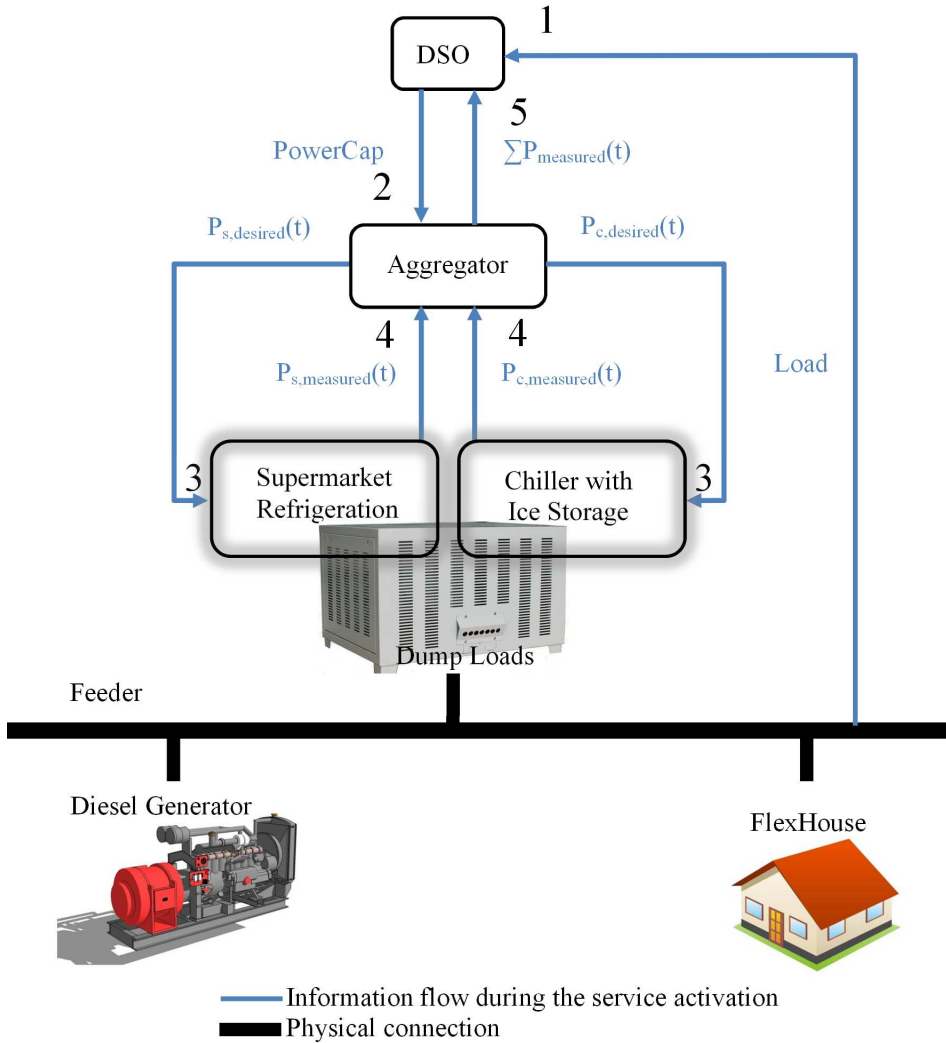


Figure 6.3: Electrical power flow at the “PowerCap” experimental setup with the sequence of operations.

**At each sampling time during the service activation:**

1. The DSO measures the load on the feeder that is specified by the consumptions and generations connected to the feeder.
2. Based on the measured load, the DSO calculates the required load reduction and sends the “PowerCap” signal to the aggregator, which is the maximum permissible power consumption.
3. The aggregator runs an optimization which provides the desired power reference for the supermarket,  $P_{s,desired}$ , and the chiller,  $P_{c,desired}$ .



4. Each consumer changes its local settings to follow the power reference in the best possible way. Afterwards, they will announce the actual measured power,  $P_{s,\text{measured}}$  and  $P_{c,\text{measured}}$ , to the aggregator.
5. The aggregator announces the actual aggregated power consumption to the DSO.

In order to have an appropriate range of powers, we use scaling factors in our setup. The supermarket refrigeration lab and also the real supermarket are scaled up by the factor of 5. The total consumption of the aggregator is scaled down by the factor of 0.2 to be emulated at the dump loads.

### 6.3 Aggregator Design for the Experimental Setup

In Chapter 2, we described that the aggregator design in the direct control framework requires the following three major items:

- Model of the consumption units
- Optimization problem at the aggregator
- Information exchange between the components

For the experimental setup, these items are same as they are defined in the previous chapters, but with slight changes, which are noticed during the several runs of the experiments. We use the models described by equations (4.14)-(4.16) for the supermarket and equations (4.28), (4.33), (4.36) for the chiller. The only difference is, due to practical reasons, the chiller in our experimental setup can only accept discrete levels of power, which are  $P_{c,\text{min}}$ ,  $P_{c,\text{base}}$  and  $P_{c,\text{max}}$  as the reference. Thus, the system input for the chiller system,  $u_c(t)$ , can be expressed as:

$$u_c(t) = [P_{c,\text{min}} \ P_{c,\text{base}} \ P_{c,\text{max}}] \begin{bmatrix} c_1(t) \\ c_2(t) \\ c_3(t) \end{bmatrix} - P_{c,\text{base}} \quad (6.1)$$

where,  $c_k(t) \in \{0, 1\}$  and  $\sum_{k=1}^3 c_k(t) = 1$ . Another constraint should be taken into account for the chiller system is the run-time/stop-time constraints. This constraint arises because the chiller cannot switch from one level to the other one immediately and it can be handled as explained in Section 2.2.2.

The control strategy at the aggregator consists of an MPC design plus a manual controller. For the MPC, the optimization problem is formulated as below:

$$\min \sum_{t=1}^N w_s \|P_s(t) - P_{s,\text{base}}\|_2^2 + w_c \|P_c(t) - P_{c,\text{base}}\|_2^2 \quad (6.2)$$

subject to

$$P_s(t) + P_c(t) \leq \text{PowerMax/PowerCap} \text{ for } t_{\text{start}} \leq t \leq t_{\text{end}} \quad (6.3)$$

$$\text{Consumers dynamic and constraints} \quad (6.4)$$

In the “PowerMax” and “PowerCap” scenarios, the aggregator is not required to follow the power reference exactly. The total consumption should be below the maximum limit as considered in (6.3). For these scenarios, the objective function is formulated such that the power deviation from the baseline power, i.e. the preferred consumption, is minimized.  $w_s$  and  $w_c$  are weight parameters and  $N$  is the prediction horizon in (6.2). The optimization might be infeasible at some sampling times because of any practical reasons at the consumers site; in this case, the manual controller is activated which simply re-send the information from one sampling time before.

The information flow between the components in the experimental setup is described comprehensively in Table 6.2, 6.3 and 6.4.

Table 6.2: Information flow between the DSO and the aggregator

Parameters [unit]	Description
<b>DSO → Aggregator</b>	
PowerMax [kW]	24-hour power schedule, vector, constant, transmitted once before the activation
PowerCap [kW]	Maximum permissible power consumption, single value, time-varying, transmitted at each sampling time during the activation
<b>Aggregator → DSO</b>	
$\sum P_{\text{measured}}$ [kW]	Total measured power, single value, time-varying, transmitted at each sampling time during the activation

Table 6.2 describes the information flow between the aggregator and the DSO. The “PowerMax” signal is a 24-hour power schedule for the next following day. In case of no activation, the references are set to the maximum value of the whole portfolio. The aggregator extracts the time and duration of activation from the “PowerMax” signal. The “PowerCap” signal, however, is communicated during the activation time. The total measured power is needed at the DSO for the aggregator’s evaluation.

Table 6.3 and Table 6.4 describe the information flow between the aggregator and the DERs. The information exchange depends on the type of DERs and their special requests. In general, the aggregator must have access to model parameters and constraints as explained in Section 2.4. In addition to this, other information exchange may be needed, depending on the type of consumers. For instance, in our experimental setup, the supermarket needs to know the time and duration of the first up-regulation in order to calculate its flexibility. The up-regulation time is the time in which the supermarket is asked to consume lower than its baseline power. These values are extracted at each sampling time from the desired power prediction vector provided by the MPC. Conversely, the chiller system receives integer values, 0, 1 and 2, from the aggregator and is subject to a switching time constraint. Thus, in this case, the minimum time required before switching,  $t_d$  should be communicated. Hence, the aggregator needs to know the status of the chiller  $n_d$  samples before the activation to check if there is any switching during this time.  $Q_{\text{up}}$  and  $Q_{\text{down}}$  basically specify the state of the charge. These values only need to be communicated at the beginning of activation. The aggregator can update these values at each sampling time in its model of the consumers.

Table 6.3: Information flow between the supermarket and the aggregator

Parameters [unit]		Description
<b>Aggregator → Supermarket</b>		
$t_{\text{start}}$		Time of the activation, single value, constant, transmitted once before the activation
$D_{\text{act}}$ [sec]		Duration of the activation, single value, constant, transmitted once before the activation
$t_{s,\text{act}}$		Time of the first up-regulation, single value, time-varying, transmitted at each sampling time during the activation
$D_{s,\text{act}}$ [sec]		Duration of the first up-regulation, single value, time-varying, transmitted at each sampling time during the activation
$\Delta P_{s,\text{desired}}$ [kW]		Desired deviation from baseline power, vector, time-varying, transmitted at each sampling time during the activation and provided from the current time to the end of activation
<b>Supermarket → Aggregator</b>		
$P_{s,\text{measured}}$ [kW]		Measured power, single value, time-varying, transmitted at each sampling time during the activation
$P_{s,\text{min}}$ [kW]		Minimum power, single value, time-varying, transmitted at each sampling time during the activation
$P_{s,\text{max}}$ [kW]		Maximum power, single value, time-varying, transmitted at each sampling time during the activation
$P_{s,\text{base}}$ [kW]		Baseline power, single value, time-varying, transmitted at each sampling time during the activation
$Q_{s,\text{up}}$ [kJ]		Thermal energy for up-regulation, single value, time-varying, transmitted once at the beginning of activation
$Q_{s,\text{down}}$ [kJ]		Thermal energy for down-regulation, single value, time-varying, transmitted once at the beginning of activation
$K_s$ [sec], $\tau_s$ [sec]		First-order model parameters, single value, constant, transmitted once at the beginning of activation

## 6.4 Danfoss Supermarket Refrigeration System

This section provides a description of the refrigeration lab located at Danfoss headquarters. The refrigeration system used in this work is a laboratory refrigeration system which replicates a refrigeration system from a small to medium sized supermarket. The refrigeration system is a very versatile system and can be configured to emulate many different refrigeration application. However, the description only covers a single configuration of the system and that is the supermarket refrigeration setup. The system used for the experiment is a standard CO<sub>2</sub> based booster system and it is comprised of four medium temperature display cases and three low temperature display cases. Each of the seven display cases are different and therefore possess different properties. Figure 6.4 shows two of the display cases, a vertical medium temperature display case and a horizontal low temperature display case.

From a flexibility point of view, the different display cases in the refrigeration system have very different properties. The vertical medium temperature display cases are not

Table 6.4: Information flow between the chiller and the aggregator

Parameters [unit]		Description
<b>Aggregator → Chiller</b>		
$t_{\text{start}}$		Time of the activation, single value, constant, transmitted once before the activation
$D_{\text{act}}$ [sec]		Duration of the activation, single value, constant, transmitted once before the activation
$P_{c,\text{desired}}$ [kW]		Desired power, single integer value: 0, 1, 2 which means to consume $P_{\text{max}}$ , $P_{\text{min}}$ , $P_{\text{base}}$ , time-varying, transmitted at each sampling time during the activation
<b>Chiller → Aggregator</b>		
$P_{c,\text{measured}}$ [kW]		Measured power, single value, time-varying, transmitted from $n_d$ samples before the activation and also at each sampling time during the activation
$P_{c,\text{min}}$ [kW]		Minimum power, single value, constant, transmitted once at the beginning of activation
$P_{c,\text{max}}$ [kW]		Maximum power, single value, constant, transmitted once at the beginning of activation
$P_{c,\text{base}}$ [kW]		Baseline power, single value, constant, transmitted once at the beginning of activation
$Q_{c,\text{up}}$ [kJ]		Thermal energy for up-regulation, single value, time-varying, transmitted once at the beginning of activation
$Q_{c,\text{down}}$ [kJ]		Thermal energy for down-regulation, single value, time-varying, transmitted once at the beginning of activation
$t_d$ [sec]		Minimum switching time, single value, constant, transmitted once before the activation
$\text{COP}_{c,\text{ice}}$		Average COP in charging mode, single value, constant, transmitted once at the beginning of activation
$\text{COP}_{c,\text{cool}}$		Average COP in cooling mode, single value, constant, transmitted once at the beginning of activation

considered to be the most optimal display cases with respect to flexibility both due to the fact that they are not covered during the opening hours of the supermarket and secondly they are usually used to refrigerate food with relative low thermal capacity such as cheese and various deli products. The temperature is therefore expected to increase relatively fast if the refrigeration is stopped in these display cases. However, for the horizontal display case, both the low temperature and the medium temperature, the physical design is more favorable with respect to flexibility, especially the display cases with glass lids. In addition, the horizontal display cases are usually used to store food with higher thermal capacity such as larger cuts of meat, soups, and frozen vegetables. That means that the horizontal display cases will be able to maintain their temperature within the allowable constraints for a longer time period if the refrigeration system is required to up-regulate, i.e., reduce the power consumption.

The flow in the refrigeration system is created by two low temperature compressors and four medium temperature compressors. The installed cooling capacity is 40 kW. The



Figure 6.4: A vertical medium temperature and a horizontal low temperature display case at the Danfoss refrigeration laboratory

main objective of the refrigeration system is to maintain the correct temperature within the different display cases of the system. Hence, the temperature control of the system has priority over the power control of the system. Figure 6.5 shows a simplified diagram of a supermarket refrigeration system of the same type as the one used for the experiment. It shows that each of the display cases have their own temperature controller and that the temperature is controlled by manipulating the inlet of refrigerant into the evaporator of the given display case. The control task of the controller for the compressors is to maintain the required suction pressure to provide the sufficient temperature difference over the evaporators in the display cases to enable refrigeration.

The task of the power controller for the supermarket refrigeration system is to get the power consumption of the system to follow a power reference. In the system, the majority of the power is consumed by the compressors and the power controller is therefore designed to control the power consumption of the compressors. The strategy behind the power controller relies on the fact that the power consumption of the compressors can be controlled by manipulating the amount of gas that the compressors have to compress at a given point of time and this can be achieved by manipulating the thermostats of the display cases. The temperature within each of the display cases are controlled using a thermostatic approach. In other words, when the temperature within a given display cases becomes too hot, the valve will switch on and refrigerant will start to flow into the evaporator and thereby bring down the temperature until the lower temperature limit is reached where the valve will switch off and stop the flow of refrigeration. Thus, when the power controller needs to reduce the power consumption of the compressors, it will look at the temperature and the state of the thermostat controller and see if the gas production from the given display case can be stopped at the moment. If that is the case, the power controller will switch the state of the thermostat controller for the given display case and thereby stop the gas production from that particular display case, which will then reduce the power consumption of the compressors.

The working principle can be seen in Figure 6.6, where the lines marked “a” and “b” indicate state changes of the thermostat control due to that the air temperature,  $T_{\text{air}}$ , inside the display case has reached an upper or a lower temperature constraint called CutIn or CutOut, respectively. At the intersection of the line marked “a”, and upper

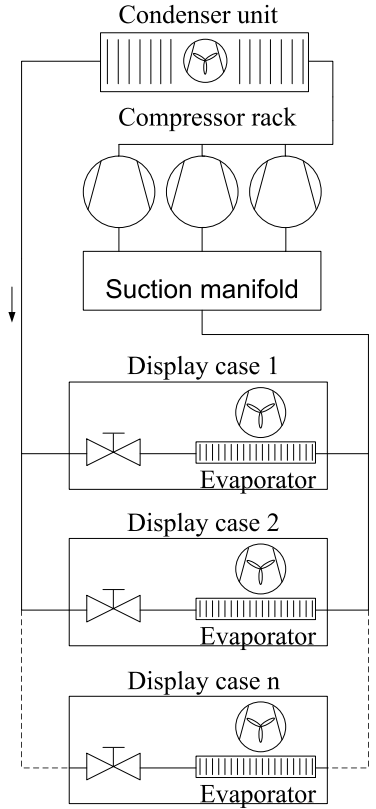


Figure 6.5: Sketch of a simplified supermarket refrigeration system with power controller and estimator

temperature constraint,  $CutIn$ , the valve will open and refrigerant will start to flow into the evaporator of the display case and after a small overshoot, the temperature will start to decrease. When  $T_{air}$  reached the intersection of the line marked “b” and the lower temperature constraint,  $CutOut$ , the valve will close and the temperature will start to increase after a small undershoot. The lines marked “c” and “d” indicates state changes that serves the purpose of power control. At the intersection of the line marked “c” and  $T_{air}$  the state of the thermostat has been switched on, with the purpose of forcing the valve to open and thereby increase the amount of gas that will reach the compressor and consequently increase the power consumption of the compressors. The opposite situation can be seen where the line marked “d” and  $T_{air}$  intersects. In that case the thermostat is switched off with the purpose of reducing the amount of gas that reaches the compressors and thereby decrease the power consumption of the compressors.

For the power controller to follow a power reference using the explained working principle, it will have to be able to map the state changes of a thermostat in a number of display case to a change in the power consumption of the compressors. To be able to do that, the controller will need to calculate the contribution to power consumption of the compressors that each of the display cases is responsible for or can be responsible

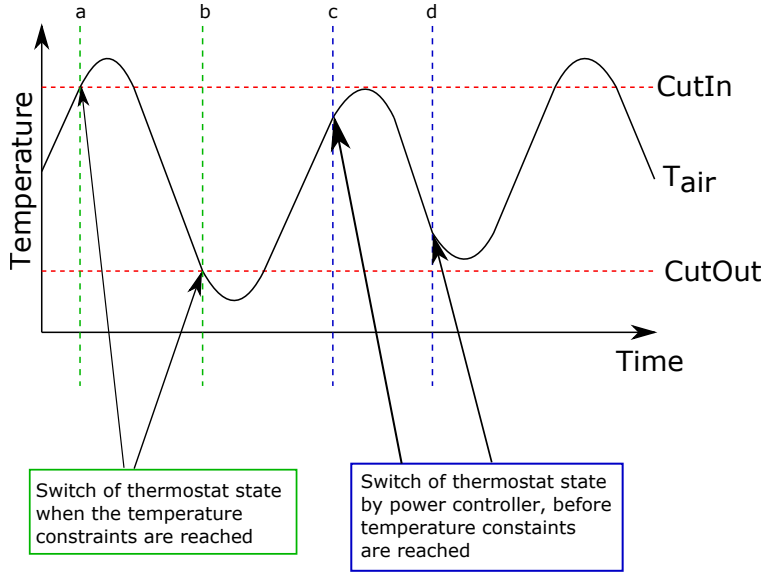


Figure 6.6: Sketch of the working principle of the thermostat control both when operating normally and when the thermostat is switched by the power controller

for. That is done by estimating the cooling provided by each of the display cases and then using the COP of the refrigeration cycle to calculate the contribution to the power consumption of the compressors from each of the display cases. This estimation is done using the following equations:

$$\dot{m}_i = OD_i \cdot \alpha \cdot \sqrt{2 \cdot \rho_{\text{suc}} \cdot (p_c - p_{\text{suc}})} \quad (6.5)$$

$$\dot{Q}_i = \dot{m}_i \cdot (h_{oe} - h_{oc}) \quad (6.6)$$

In (6.5) the mass flow rate of refrigerant through the  $i^{\text{th}}$  display case is denoted by  $\dot{m}_i$ , the opening degree of the inlet valve is denoted by  $OD_i$ ,  $\alpha$  denotes the orifice constant,  $\rho_{\text{suc}}$  is the density of the refrigerant at the suction side of the compressors. The pressure on the high and low pressure side of the inlet valve is denoted by  $p_c$  and  $p_{\text{suc}}$ , respectively. The cooling capacity of the  $i^{\text{th}}$  display cases, which is denoted by  $\dot{Q}_i$  is estimated by (6.6), where the enthalpy at the outlet and the inlet of the evaporator is denoted by  $h_{oe}$  and  $h_{oc}$ , respectively. Using

$$W_i = \frac{\dot{Q}_i}{\text{COP}} \quad (6.7)$$

the power consumption of the compressors that the  $i^{\text{th}}$  display case responsible for, denoted by  $W_i$ , can then be estimated. Based on the estimate of the amount of power consumption of the compressors that each of the display cases are responsible for, the controller dispatches the relevant display cases to match the change in power consumption requested by the aggregator  $\Delta P_{s, \text{desired}}$ .

The estimation of minimum and maximum power consumption, denoted  $P_{s,\min}$  and  $P_{s,\max}$ , of the supermarket refrigeration system are dependent on the durations that the supermarket refrigeration system is required to maintain the minimum or maximum power consumption. Hence, the estimation of  $P_{s,\min}$  and  $P_{s,\max}$  are dependent on  $D_{\text{act}}$  and  $D_{s,\text{act}}$ . The process of estimating the maximum and minimum power consumption,  $P_{s,\min}$  and  $P_{s,\max}$ , starts by checking which of the display cases that fulfills the switching criteria. To fulfill the switching criteria a given display case is required to, either be able to switch off or on and at the same time the display case is has to be able to stay in the off or on position for the remaining time period. This is done by using empirical knowledge of the warm up and cool down times of each of the display cases and the remaining time that the refrigeration system should maintain maximum or minimum power consumption. If a given display cases fulfill the switching criteria it will be counted as one of the cases that is able to reduce or increase the power consumption of the compressors and the power consumption that the particular display cases is responsible for,  $W_i$ , is then used in the estimation of either  $P_{s,\min}$  or  $P_{s,\max}$ , depending on what the particular display case is able to assist with at the given point of time. The value  $P_{s,\text{base}}$  is simply estimated by low pass filtering  $P_{s,\text{measured}}$ . The energy levels  $Q_{s,\text{up}}$  and  $Q_{s,\text{down}}$  are calculated based on the estimates of  $P_{s,\min}$  and  $P_{s,\max}$ , respectively and the current energy level of the supermarket. The time constant,  $\tau_s$ , and the gain  $K_s$  are estimated by using a step response from historical data from the system.

#### 6.4.1 Fakta Supermarket

The Fakta supermarket used for the “PowerCap” experiment consists of seven medium temperature cabinets and four low temperature cold rooms. Figure 6.7 shows one of the cold rooms and the compressor rack at the Fakta supermarket. The total cooling capacity is around 37kW and the average baseline consumption is around 7kW. All of the cold rooms and display cases at the supermarket are used for the experiment except one of them. From the local control strategy point of view, the Fakta supermarket is similar to the supermarket refrigeration lab. The only difference is related to the real-life challenges. For example, there is a defrost procedure in a real supermarket. The gas delivered to a particular display case cannot be controlled as long as it is defrosting. Thus, the flexibility of the supermarket is rather low if a significant number of the cold rooms and display cases are in a process of defrosting. Another example is that the real supermarket is subject to various disturbances compared to the refrigeration lab because of the customers and employees’ behavior.

### 6.5 Grundfos Chiller System with Ice Storage

In this section we explain the main characteristics of the chiller system with ice storage located at Grundfos headquarters. The system is used to cool two buildings, one in which the main cooling demand stems from air conditioning of office space, and one where it mainly stems from cooling of industrial processes. The peak cooling demand of the two buildings combined occurs in high summer, and is around 300 kW, while the lowest cooling demand is around 80 kW in the winter. Apart from a seasonal variance, there is also a daily variance, which is related to office hours. The chiller, which is providing the cooling, was installed without the intention of adding an ice storage system, and has



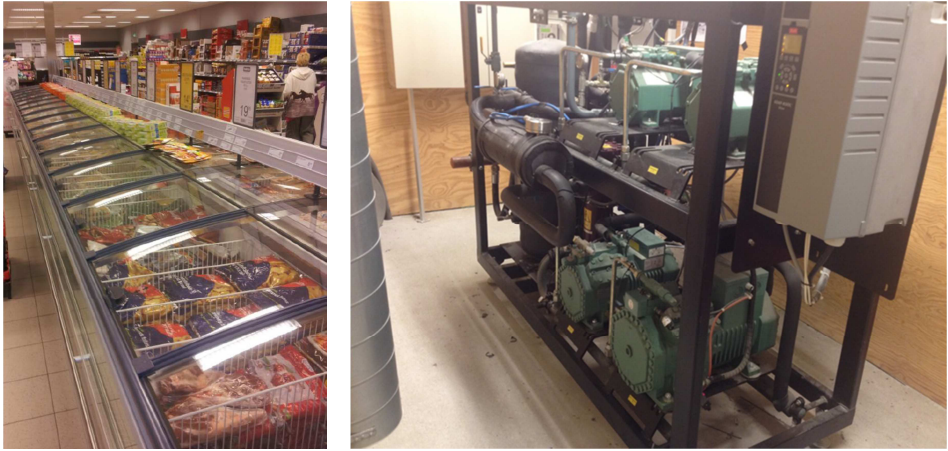


Figure 6.7: Fakta supermarket used for the “PowerCap” experiment (The cold storages and the compressor rack)



Figure 6.8: Grundfos chiller with the ice storages

a peak cooling capacity of around 290 kW, which means that it is unable to meet the cooling demand by itself in high summer. The ice storage system was retro fitted to the chiller system in order to provide a realistic laboratory for testing smart grid technologies, while also providing extra peak cooling capacity. Figure 6.8 shows the Grundfos chiller together with the ice storages.

The layout of the chiller with ice storage system is shown in Figure 6.9. The chiller accepts a temperature set point called  $T_{bs,desired}$  and uses its internal controller to maintain  $T_{bs}$  at the set point.  $T_{bs}$  is the brine supply temperature coming from the chiller. The chiller provides a measurement of its power consumption called  $P_e$ . The internal temperature controller of the chiller uses a frequency converter to control the speed of the compressor, and thus the cooling power. However, it does not do this in a continuous manner, but rather in steps. Furthermore, the compressor frequency can only be varied between 35 Hz and 65 Hz. This means that whenever  $T_{bs}$  can be realized with less than

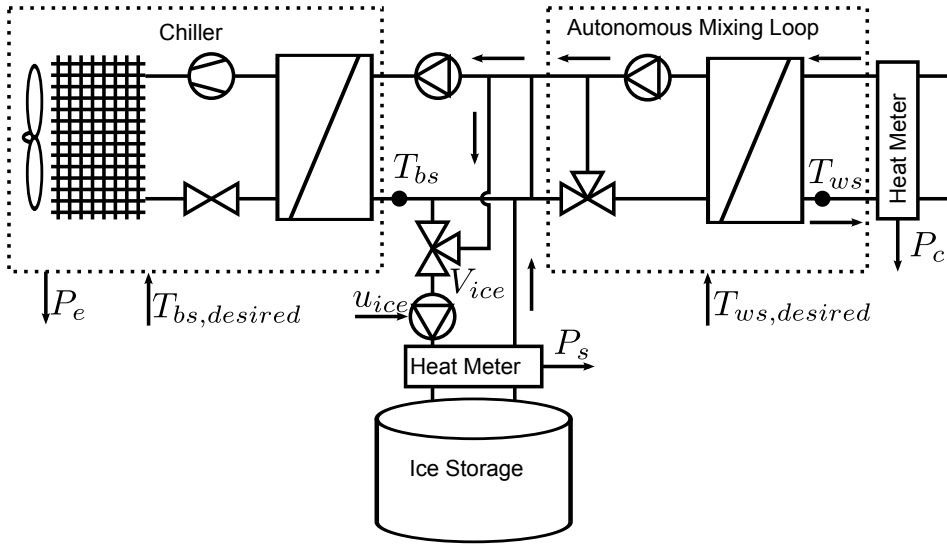


Figure 6.9: The Chiller accepts a set point for its supply temperature and provides a measurement of the consumed electrical power. A brine loop enables freezing of the ice storage, without freezing the transport medium. An autonomous mixing loop ensures a constant supply temperature to the building, regardless of the brine temperature. Heat meters measure the heat transfer to the building and the ice storage, respectively.

the minimum frequency of the compressor, the internal temperature controller resorts to on/off control, which has a duty cycle of around 10 minutes depending on the load. The duty cycle makes it hard to determine the base load at any given time, since it cannot simply be taken as the current power consumption of the compressor.

The chiller can generally operate in three modes; direct cooling mode, charging mode, and discharging mode. In direct cooling mode  $u_{ice} = 0$ , where  $0 \leq u_{ice} \leq 1$  corresponds to the speed of the pumps supplying the ice tanks with brine, 0 representing a stopped pump.  $T_{bs}$  is kept at a temperature, which causes the mixing loop to open fully, while still keeping  $T_{ws}$  at  $T_{ws,desired}$ , where  $T_{ws}$  and  $T_{ws,desired}$  are the water supply temperature to the building, and the associated setpoint, respectively.  $T_{ws}$  is the water supply temperature to the building. In charging mode  $u_{ice} = 1$  and  $T_{bs,desired} = \underline{T_{bs,desired}} = -10^{\circ}C$ . This makes the internal controller of the chiller cool as much as possible, as fast as possible, but if it was off when the mode changed, it would take a few minutes to come back on due to its internal controller. The mixing loop keeps  $T_{ws} = T_{ws,desired}$ , and the rest of the cooling power is used for freezing the ice storage. In discharging mode  $u_{ice} = 1$  and  $T_{bs,desired}$  is set to a value which would only activate the chiller if  $T_{ws}$  deviates around 1 degree from  $T_{ws,desired}$  due to an entirely open mixing loop, which in turn is caused by insufficient cooling for the brine by the ice tanks. In case the ice tanks can provide the cooling, the chiller will be off. It takes some time for the internal controller of the chiller to turn the compressor off, even though the ice tanks are covering the cooling load.  $V_{ice}$  is the three way valve that controls whether the ice tanks and chiller are connected in parallel or in series. In charging mode  $V_{ice}$  is set to let the ice tanks draw the cold brine

from the chiller (series), and in discharging mode it is set to draw warmer brine from the return line (parallel), in order to improve heat transfer in both cases.

The values  $P_{c,base}$  and  $P_{c,measured}$  are both calculated in the same way using a low pass filtered version of  $P_c$ , which is divided by  $COP_{c,cool}$ , where  $P_c$  is the current thermal load of the building. The  $Q_{c,up}$  and  $Q_{c,down}$  is calculated by mapping the water level of the ice tanks to the energy content of the ice tanks. This is done using ultrasonic sensors to measure the water level, and then by exploiting the fact that ice is less dense than water, so a higher water level in the ice tanks indicates more ice. The measured thermal power of the ice tank,  $P_s$ , was used to calibrate the mapping, which is simply an affine mapping.  $COP_{c,ice}$  and  $COP_{c,cool}$  were calculated using  $P_c$ ,  $P_s$  and  $P_e$  in charging mode, and direct cooling mode, respectively.  $P_{c,min}$  and  $P_{c,max}$  are simply the nameplate minimum and maximum power consumption of the chiller.  $t_d$  is the minimum time that should elapse after the mode of operation was changed until it may change again. It is there to protect the compressor from going on and off too often, and it also accounts for the lack of responsiveness of the internal controller of the chiller.

## 6.6 SYSLAB Test Facility at Risø

The current SYSLAB facility is spread across three sites on DTU Risø's campus. A 400V, 3-phase grid with a total of 14 busbars serves as the electrical backbone of the facility. The SYSLAB facility is a distributed energy system laboratory consists of energy sources (2 wind turbines: 10kW and 11kW, 3 PV plants: 10kW, 10kW and 7kW, diesel generator set: 48kW/60kVA), energy loads (controllable dump loads, office building load with flexible load control, EVs etc.) and energy storages (vanadium battery). For more information about SYSLAB, you can refer to [70]. Using the flexibility provided by a crossbar switchboard, the grid can be configured into a range of different topologies. Figure 6.10 shows an example topology of the overall system, with those parts of the system in use by the experiment highlighted in red.

## 6.7 Experimental Results

In this section, we first explain the idea behind the aggregation of two different DERs and what powers we expect from the aggregator to distribute. Afterwards, the experimental results are presented. As noted in Section 6.3, the aggregator has a mandate to keep the total consumption below the maximum level during the service activation. This implies power consumption reduction. However, consumers might easily refuse this request since it can lead to damage or discomfort in their system, such as deterioration of foods at the supermarket or unsatisfactory comfort level at the air conditioning system. In this experiment, we aggregate the flexibility of two different thermal storages with different characteristics to achieve our goal.

First assume the “PowerMax” service. On one side, there is a chiller equipped with an ice storage. The chiller can save some ice during the off-peak hours. Then, during the service activation, the chiller can be turned off and the cooling load can be provided from the ice tank. The ice tank is isolated in such a way that there is almost no heat loss to the surrounding environment. Although utilization of the ice tank enables the aggregator to reduce the consumption for a period of time, the chiller cannot be kept off

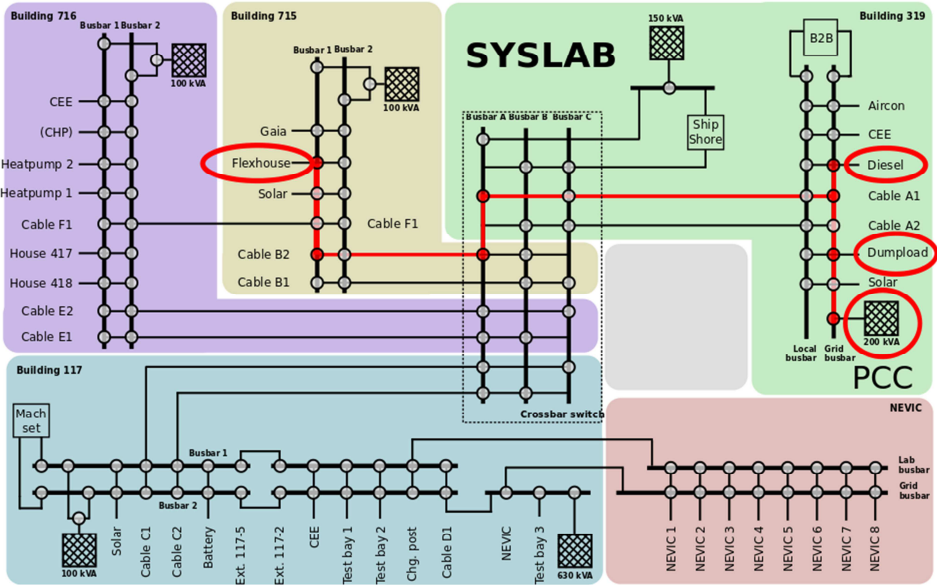


Figure 6.10: Layout of the SYSLAB test grid with active parts highlighted in red.

for a long time. This can be for several reasons such as local control strategy. Sometimes, the required cooling load is high such that both the chiller and the ice tank should be utilized simultaneously in order to satisfy the load. On the other side, saving energy in the refrigerated foods at the supermarket is accompanied with heat loss. Thus, it is almost pointless to store energy from long before the activation time. However, the supermarket can store energy during the activation time, when the chiller is turned off. All in all, we expect a power distribution similar to the one shown in Figure 6.11. At the beginning, the chiller reduces its consumption from the baseline to the minimum level. The supermarket has an opportunity to save some energy in the refrigerated foods during this time by increasing its consumption. Thereafter, the supermarket can decrease its consumption and release the stored energy, when the chiller needs to be turned on again. Switching between the supermarket and the chiller can occur several times during the activation, depending on the systems' status, constraints etc. For the "PowerCap" service, the situation is the same, except that the maximum limit changes during the activation. Accordingly, the power distribution should also change. Since the chiller system can only accept certain levels of power, the variation may mostly affect the power reference to the supermarket.

### 6.7.1 PowerMax Experimental Results

Figure 6.12 and Figure 6.13 show the experimental results of the two separate tests for "PowerMax"=55kW (Experiment 1) and "PowerMax"=67kW (Experiment 2). The activation time is one hour. To see tangible responses from the both systems, we scale the supermarket system up by a factor of 5; since the cooling capacity of the supermarket system is much lower than the chiller system in our experiment. The following points are

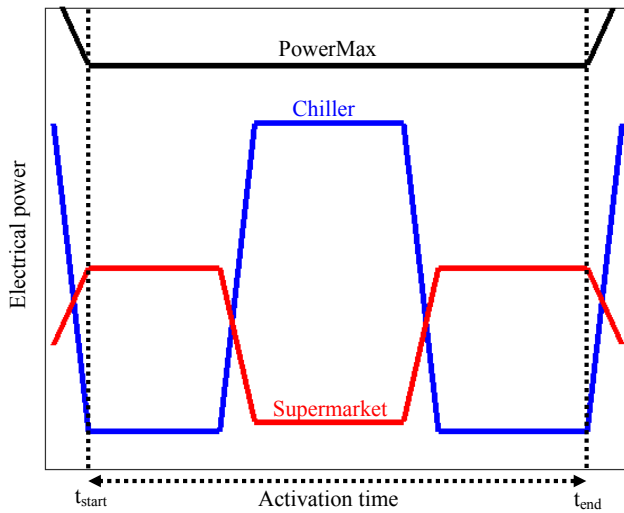


Figure 6.11: Expected power distribution from the aggregator for the “PowerMax” service

notable for the shown results:

- 1) Power distributions from the aggregator to the consumers are as we expected and showed in Figure 6.11. The only difference is that the power consumption assigned to the supermarket is a bit non-smooth in some areas. This is due to the time-varying minimum and maximum power of the supermarket ( $P_{s,min}$   $P_{s,max}$ ) which forces the aggregator to change the power reference accordingly. The aggregator distributes the power in such a way that the aggregated power stays just below the maximum level in order to minimize the cost function (6.2)
- 2) The chiller system has an almost constant delay in response to the change in power reference. It can follow the minimum level ( $P_{c,min}=0kW$ ) perfectly. However, the baseline level ( $P_{c,base}=32.4kW$  for “Experiment 1” and  $P_{c,base}=44.4kW$  for “Experiment 2”) is followed with an overshoot at the beginning, small deviations in “Experiment 1” and rather large deviations in “Experiment 2”. There is no problem as long as the measured power is less than the desired power, but the initial overshoot can lead to “PowerMax” limit violation, as seen in the both figures.
- 3) For the supermarket system, the delay is not the same in all areas. As can be seen, the delay in response to a power increase is less than the delay in response to a power decrease. In addition, the first order response to the step change in power reference is more perceptible for the supermarket than for the chiller.
- 4) The total measured power violates the “PowerMax” limit in some places, especially when there is switching from the chiller to the supermarket.

Considering all the above points, we can conclude the “PowerMax” service is provided by combining the flexibilities of two different DERs in a satisfactory manner, although the maximum limit is violated in a few short periods of time. From most DSOs’ points of view, such short term violations would be inconsequential, as they do

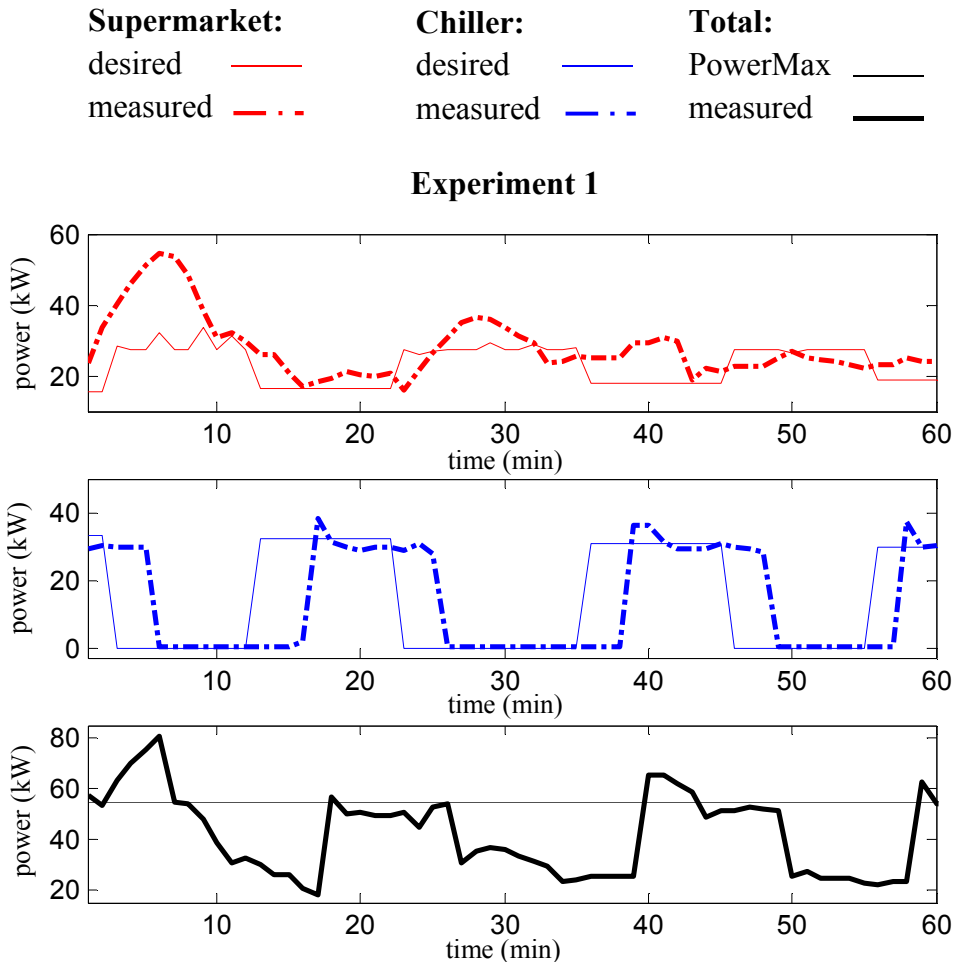


Figure 6.12: Experimental results for “PowerMax”=54.6kW during the one hour activation time. The aggregated baseline power is equal to 60.7kW just before the activation time.

not threaten to overload the grid.

Thermal energy changes for “Experiment 2” are shown in Figure 6.14. The upper plots show the offered flexibility for both up-regulation and down-regulation services during the one-hour activation time while the lower blocks illustrate the flexibility at the beginning and at the end of activation time. The blue areas show the available flexibility, in terms of the stored thermal energy, for up-regulation. In the other words, the units are able to reduce their consumption and use these amounts of stored energy to keep their systems in normal operation within the constraints. The white areas show the available flexibility, in terms of free space for saving additional thermal energy, for down-regulation. This means the units are able to increase their consumption and use these spaces to save the extra energy to keep their systems in normal operation within the constraints. Each of

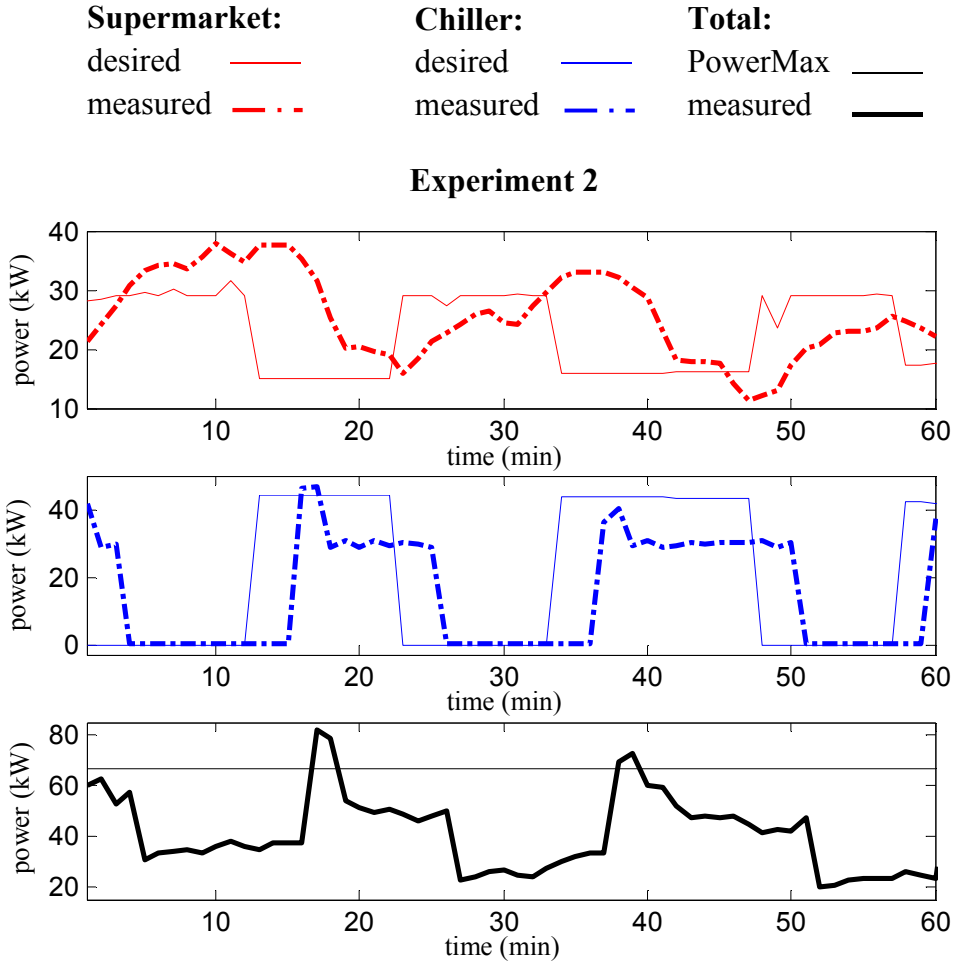


Figure 6.13: Experimental results for “PowerMax”=66.9kW during the one hour activation time. The aggregated baseline power is equal to 74.3kW just before the activation time.

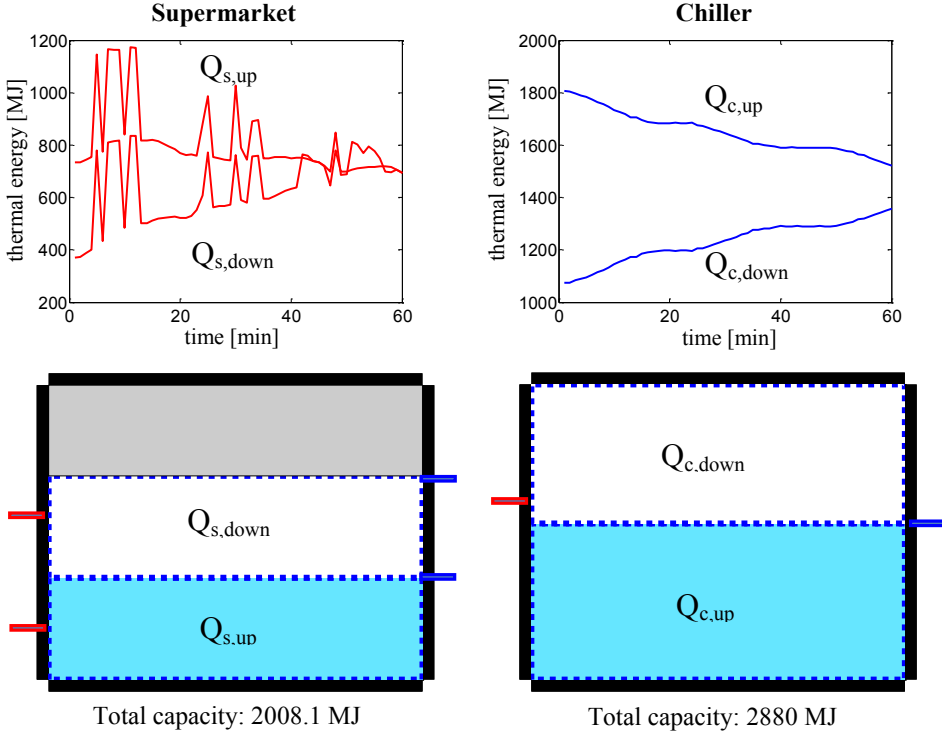


Figure 6.14: Upper plots show the flexibility changes for both up-regulation and down-regulation services during a one-hour activation. Lower graphs depicts the available flexibility for both up-regulation and down-regulation services at the beginning and at the end of activation time. The results are for “Experiment 2”

the blocks displays the maximum capacity, however, the maximum value is not reachable all the time. At some time during the service activation, the total capacity of the supermarket system (equal to 2008.1MJ) is available such that  $Q_{s,down} + Q_{s,up} = 2008.1\text{MJ}$  as shown in the top-left plot. For instance, at the beginning and at the end of activation, a portion of the total capacity is not reachable. The grey area shows the unreachable part for the supermarket system in the bottom-left plot. Red and blue dashes on the left and right side of the graph indicate the levels of each area at the beginning and at the end of activation respectively. This behaviour is due to the suction pressure saturation in the vapour compression cycle at the supermarket. The total capacity of the ice storage (equal to 2880 MJ) is available all the time and  $Q_{c,down} + Q_{c,up} = 2880\text{MJ}$  always holds.

### 6.7.2 PowerCap Experimental Results

As explained earlier in Section 6.1 and Section 6.2, in the “PowerCap” service, the aim is to avoid the feeder of interest to be higher loaded. The FlexHouse connected to the feeder has a baseline consumption around 15kW and the baseline consumption of the aggregator is around 16.4kW (considering the scaling factors). However, the diesel generator



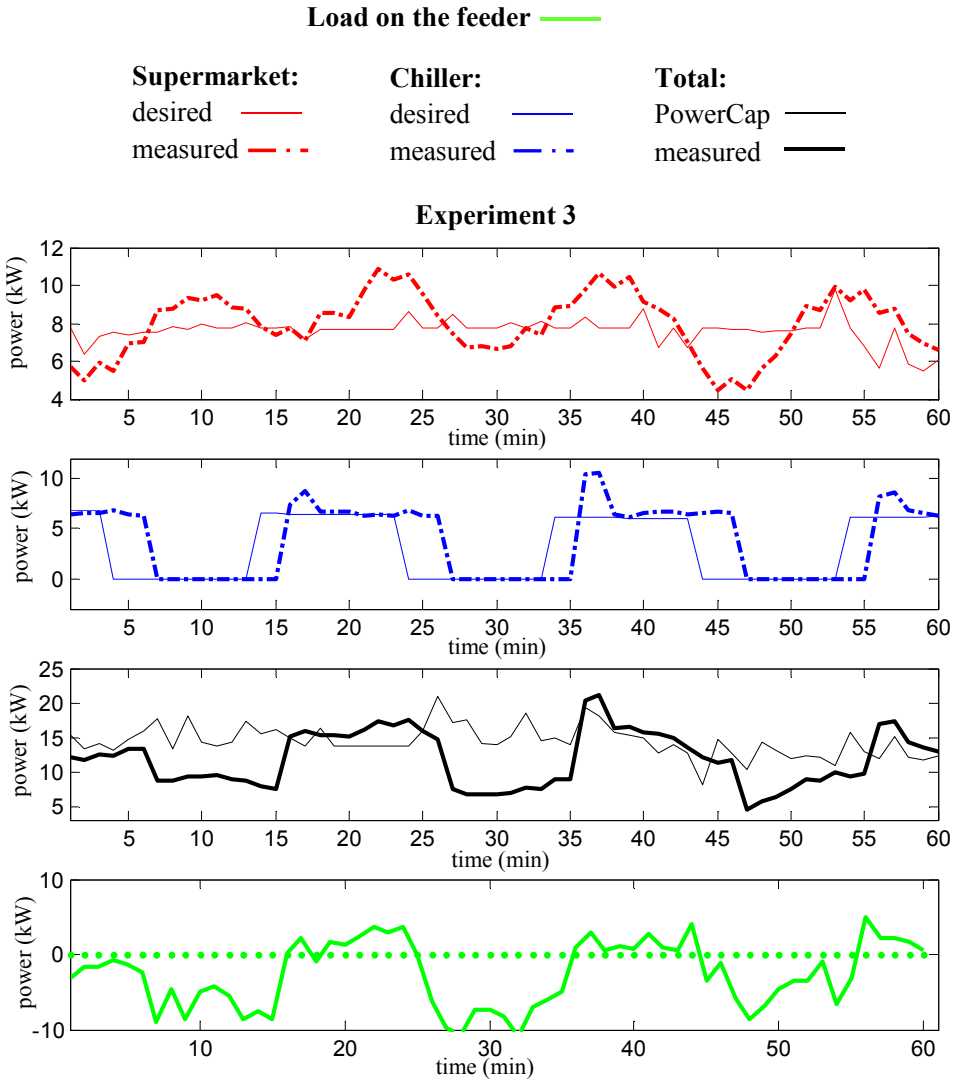


Figure 6.15: Experimental results for “PowerCap” service during the one hour activation time.

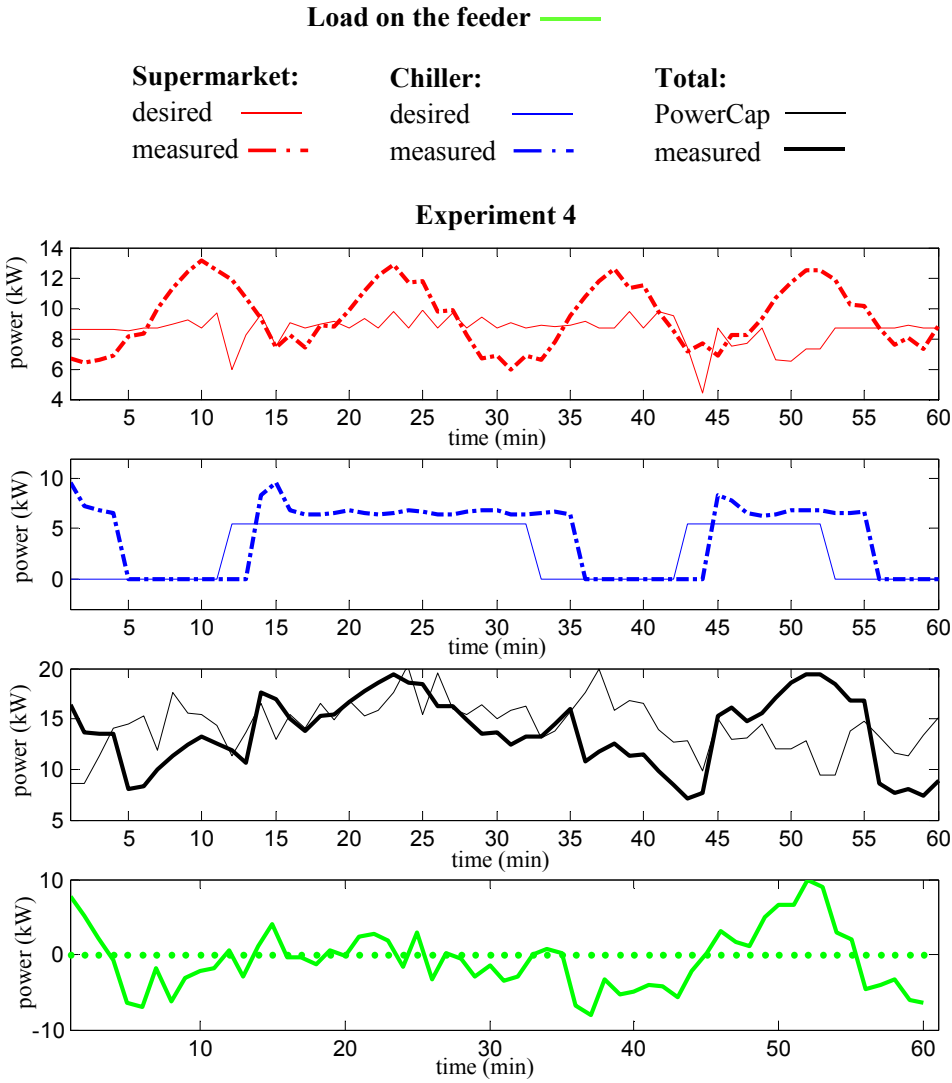


Figure 6.16: Experimental results for “PowerCap” service during the one hour activation time.

connected to the feeder, is not able to satisfy the total load at all times. Figure 6.15 and Figure 6.16 show the experimental results of the two separate tests denoted by “Experiment 3” and “Experiment 4”. Other than the supermarket, the chiller and the aggregated consumption, the load on the feeder is also shown (plots at the bottom). The following points are notable for the shown results:

- 1) As we expected, the time-varying maximum limit affects the power distribution to the supermarket system compared to the “PowerMax” service. Moreover, depending on the flexibility parameters during the experiment, the number of on/off commands and the duration can change for the chiller system as seen in “Experiment 3” and “Experiment4”.
- 2) The power consumption of the real supermarket has an almost sinusoidal form around the reference power.
- 3) Same as the “PowerMax” experiment, the total measure power violates the “Power-Cap” limit in some places, both when the chiller is turned on and when the supermarket consumes above its baseline.
- 4) The total load on the feeder is not only determined by the aggregator consumption, but also the Flexhouse consumption and the diesel generation. However, as shown, the feeder is higher loaded when the “PowerCap” limit is violated. In “Experiment 4”, the violation seems to be unacceptable around  $t = 50\text{min}$ . It should be noted that the evaluation of the service is not in the scope of this work.

## 6.8 Summary

This chapter has presented an industrial scale experimental setup to aggregate the flexibility of industrial thermal loads for ancillary services provision to the distribution grid. The experimental setup consists of an aggregator in a hierarchical framework connected via Internet to the DERS at the bottom (a laboratory refrigeration system, a real supermarket and a real HVAC chiller in conjunction with an ice storage) and the DSO on the top. The DSO provides measurements of a flexible intelligent energy laboratory, called SYSLAB, which acts as an electrical MicroGrid with our proposed aggregator as one of its consumption units. The aggregator aims to control the active power consumption of the consumers directly, such that the aggregated power consumption stays below a certain level during an activation time. This service would be of interest to the distribution system operators, since it ensures the DSO that a feeder of interest will never be higher loaded. By aggregating the flexibility of different DERs, the aggregator is able to provide the aforementioned DSO service to a satisfactory level. Results from the experiments indicate that the total power consumption exceeded the maximum limit in just a few short periods of time, which is not consequential from a DSO point of view.

## 7 | Conclusion

This thesis has addressed the demand side management in the Smart Grid context. One of the key components of the future Smart Grid is the flexible consumers, those units that can advance or postpone their power consumption in case of power surplus or power deficit in the grid. Smart Grid facilities enable the flexible consumers to become an active player in the electricity market through the ancillary services provision. Evidently, consumers cannot make bids in the market individually and new entities are required. This introduces a new actor, a so-called “Aggregator” to the future market, which is placed between a grid operator and the flexible consumers to manage the consumers’ services and their participation in the electricity market. In this work, we have investigated the aggregator design when the aim is to utilize the flexibilities of industrial thermal loads. This chapter summarizes our contributions in response to the research questions we have addressed in Chapter 1. Furthermore, our suggestions for future works are provided.

### 7.1 Concluding Remarks

We addressed three research questions for this study. In the following, the main conclusions are provided:

#### **What kind of services would be of interest to the grid operators?**

In relation to this question, we proposed a hierarchical market setup to aggregate the flexibilities of industrial thermal loads based on the direct control policy. The setup comprises three levels: a grid operator on the top, a set of competitive aggregators in the middle and a number of DERs under the jurisdiction of each aggregator in the middle. Particularly, we considered the power reference following scenario for this setup, i.e., the grid operator aims to keep the total power consumption at a specified level during a certain period of activation time. In iPower WP2, which this study is a part of, the focus is on industrial demands. Among the industrial enterprises, we chose the industrial thermal energy storages due to three reasons. Firstly, the type of flexibility in the thermal storages is suitable for the considered scenario, when the units are asked to follow a power reference in a continuous manner. Secondly, we can utilize the flexibility which is already available in the existing systems and no significant changes is needed at the consumers’ side. Thus, the consumers are encouraged to take part in the trades. Lastly, we had the opportunity to implement the proposed scenario on the real systems, since the companies involved in this work are equipped with thermal storages.

We examined how to optimize the power distributions from the grid operator to the aggregators and from each aggregator to the consumers. Keeping the active power consumption of a portfolio of consumers at a desired value can be a valuable service for any grid operators, e.g. the transmission system operator (TSO) and the distribution grid operator (DSO). The TSO ensures the stability of the transmission system by maintaining balance between the production and the consumption of electricity. Flexible consumers, who are able to increase or decrease their consumption to the extent and at any time that is needed, can help the TSO in balancing issues. The DSO is responsible for secure operation of the distribution grid. Controlling the active power consumption of the consumers will ensure the DSO that a feeder of interest will never be higher loaded than specified by the DSO. Forcing the consumers to follow a specific power reference is not a trivial task and may not even be feasible in some cases. The proposed setup is based on a contract agreement and hence, the consumers can make money from their participation in the market. However, this is not the first priority of the consumers and should not threaten their first business.

In the aggregator design, the flexibility characteristics of the consumers were taken into account with incorporating the model of consumption units in the proposed algorithms. The aggregator tries to run the consumers close to their optimal operating points as far as possible while respecting their constraints. The robust methods in Chapter 3 are also proposed in order to meet this goal, i.e., to make the setup as feasible as possible. In other words, optimal power distribution in our setup means to distribute the power in such a way that the grid operator's objective is fulfilled and at the same time, the consumers are convinced to participate.

### **What is achieved by aggregating the flexibility of heterogeneous consumers?**

Through the simulations, we showed that the heterogeneous aggregation outperforms the homogeneous one. Simulation results in Section 5.1 indicated that the flexibility can be utilized more effectively by aggregating the heterogeneous units than aggregating the units with the same flexibility characteristics, since different flexibility models matter in power distributions. Moreover, comparing the heterogeneous and homogeneous aggregation setup in Section 5.2 revealed that the heterogeneous aggregation has a lower cost and greater profit in terms of energy consumption. Likewise, the heterogeneous aggregation is more flexible than the homogeneous one in a sense that it can better handle the unpredictable situations such as unexpected initial conditions. At the end, it should be noted that, not only the power reference following, but also the exploitation of heterogeneity in consumption units require the direct control and cannot be achieved through the indirect setup as shown in Section 5.5.

### **To what extent is the proposed scenario implementable in practice?**

To answer this question, it was required to evaluate our setup, in which we utilize the simplified models of consumers, against the real complicated systems. Our case studies were the supermarket refrigeration systems and the chiller systems connected to ice storage. At first we connected the aggregator to a complex and verified model of an actual supermarket refrigeration system, that was available from another study. Simulation results in

Section 5.3 showed that there is a 11.2% difference between the estimated profit and the actual profit and also there is a delay in response to power changing at the supermarket.

In the second and more important step, we demonstrated the power reference following scenario, in an experimental setup consisted of a real supermarket, a supermarket refrigeration lab and a real chiller system that were virtually connected to the aggregator and a real electrical MicroGrid. During the several runs of experiment, we noticed the following points that had not been seen or considered through the simulations: **1)** In the demonstration scenario, the aggregator was not commanded to exactly follow the power reference, but it should keep the consumption below a maximum limit. The aggregator performance was satisfactory for this purpose as shown in Section 6.7. However, the exact power following cannot be accomplished at least with a few number of DERs (two in our setup). The DERs have delay in response to the change in power, which is not constant all the time. The power reference is also followed with some errors. For the chiller system, the error is mainly when the system is turned on. For the supermarket system, the power profile fluctuates around the desired level. **2)** Different DERs have specific requirements which leads the information exchange between the aggregator and the DERs is not exactly as we defined in Chapter 2. For instance, the supermarket in our setup required to receive the time and the duration of the first up-regulation during the activation time or the chiller system required to communicate the minimum switching time.

## 7.2 Future Work

This work has presented an aggregation framework for utilizing the flexibility of industrial thermal energy storages in the future electricity market. The work involved both theoretical and practical studies. Based on the findings in both aspects, we can improve and extend the study in several ways. Our suggestions for future work are given below:

**Consumers' model:** It is still valid that a simplified model of the consumers should be used at the aggregator. However, evaluation of the aggregator through the simulation and experiment revealed that a delay in response to the aggregator' commands is inevitable from the consumer side. One way to improve the performance of the aggregator would be to include the delay in the modeling of the consumers. Furthermore, it appears that the assumed first-order response does not match the actual power consumption profiles well, as both the supermarket and chiller exhibit significant overshoot. A second-order model may thus be more appropriate, although this comes at the expense of a higher computational burden. Thus a more thorough study of the computational complexity of the aggregator would definitely be of interest.

**Robustness:** In this work, we suggested two methods to make the proposed setup more robust. However, the robust setup does not address the probabilistic nature of some of the constraints which arises from more or less random events such as defrosting, consumer's behavior etc. The Stochastic MPC can address these concerns and would be of interest for future work.

**Data exchange:** Data exchange between the components is an essential part of the direct control policy. An elaboration on data exchange would be interesting if we

want to continue the research within the direct control framework. We have presented a standard data exchange in Chapter 2 of this thesis. However, experimental studies of the real systems revealed that each consumer type has its own specific requirements as well. Thus, the required information exchange was slightly different from our expectation as explained in Chapter 6. For the future work, consumers' specific requirements can be identified to provide a thorough information exchange framework.

**Aggregation:** In this work, we provided an aggregator design for the industrial thermal energy storage. A natural extension to this work is to consider other types of consumer with different flexibility characteristics. In Chapter 1, a taxonomy of consumers was introduced entitled “Buckets, Batteries and Bakeries” from [40]. Thermal energy storages belong to the “Buckets” model. It would be interesting if we can include the “Batteries” and the “Bakeries” model in the aggregator design. In the simulation parts, we only considered two case studies, namely the supermarket refrigeration system and the chiller system with ice storage. Even, assuming other types of thermal storages would be interesting for the future work.

**Market integration:** An interesting extension to this work would be to investigate the aggregator's integration to the market. In this work we had a top-to-bottom approach, where the aggregator was activated by the grid operator to change its consumption based on a contract agreement. There should be a bidding process before the activation process, when the aggregator submits its offer for providing the flexibility. Future work can involve the bidding process, as well as explaining the contracts between the aggregator and other components. Likewise, the evaluation of the provided service by the grid operator can be included.

**Experiment:** During the experimental verification in this work, we noticed some points that we had never realized through the simulations. Any extension to the experimental setup would be of interest for future work. As of the time of this writing, there are other types of load, e.g. electric vehicle, available at the energy laboratory, SYSLAB, that can be included in the experimental setup. Moreover, it would be interesting if we can convince other companies to take part in the experiment.

## References

- [1] G. M. Shafiullah, A. M. T. Oo, D. Jarvis, A. B. M. S. Ali and P. Wolfs, *Potential Challenges: Integrating Renewable Energy with the Smart Grid*, 20th Australasian Universities Power Engineering Conference (AUPEC), Christchurch, 2010
- [2] T. Nejsum, *Smart Grid in Denmark 2.0*, Danish Energy Association and Energinet.dk, Report, 2012.
- [3] P. B. Andersen, J. Hu and K. Heussen, *Coordination Strategies for Distribution Grid Congestion Management in a Multi-Actor, Multi-Objective Setting*, 3rd IEEE PES International Conference and Exhibition on Innovative Smart Grid Technologies (ISGT Europe), Berlin, 2012
- [4] V. C. Gungor, D. Sahin, T. Kocak, S. Ergut, C. Buccella, C. Cecati and G. P. Hancke, *Smart Grid Technologies: Communication Technologies and Standards*, IEEE Transactions on Industrial Informatics, Vol. 7, No. 4, Pages: 529-539, 2011
- [5] X. Fang, S. Misra, G. Xue and D. Yang, *Smart Grid – The New and Improved Power Grid: A Survey*, IEEE Communications Surveys & Tutorials, Vol. 14, No. 4, Pages: 944-980, 2012
- [6] P. E. Petruzzi, D. Busquets and J. Pitt, *Self Organising Flexible Demand for Smart Grid*, IEEE 7th International Conference on Self-Adaptation and Self-Organizing Systems Workshops (SASOW), Philadelphia, 2013
- [7] B. Biegel, L. H. Hansen, J. Stoustrup, P. Andersen and S. Harbo, *Adjustable Consumption Participating in the Electricity Markets*, IEEE 52th Annual Conference on Decision and Control (CDC), Florence, 2013
- [8] Y. Huang, *Market Concepts and Regulatory Bottlenecks for Smart Distribution Grids in EU Countries*, MSc Thesis, KTH Royal Institute of Technology, Stockholm, 2011
- [9] Eurelectric Paper, *Flexibility and Aggregation: Requirements for their Interaction in the Market*, 2014
- [10] G. Heffner, C. Goldman, B. Kirby and M. KintnerMeyer, *Loads Providing Ancillary Services: Review of International Experience*, Ernest Orlando Lawrence Berkeley National Laboratory Report, 2007
- [11] K. Heussen, D. E. M. Bondy, J. Hu, O. Gehrke and L. H. Hansen, *A Clearinghouse Concept for Distribution-Level Flexibility Services*, 4th IEEE/PES Innovative Smart Grid Technologies Europe (ISGT EUROPE), Lyngby, 2013



- [12] J. R. Molina, M. M. Nunez, J. Fernan Martinez and W. P. Aguiar, *Business Models in the Smart Grid: Challenges, Opportunities and Proposals for Prosumer Profitability*, Energies, Vol. 7, No. 4, Pages: 6142-6171, 2014
- [13] S. Hussain, R. Gustavsson, A. Saleem and L. Nordstrom, *Service Level Agreement: Coordination and Monitoring of Actors in Smart Grid*, 3rd IEEE PES Innovative Smart Grid Technologies Europe (ISGT Europe), Berlin, 2012
- [14] J. Medina, N. Muller and I. Roytelman, *Demand Response and Distribution Grid Operations: Opportunities and Challenges*, IEEE Transactions on Smart Grid, Vol. 1, No. 2, 2010
- [15] Q. Lambert, *Business Models for an Aggregator: Is an Aggregator Economically Sustainable on Gotland?*, MSc Thesis, KTH Royal Institute of Technology, Stockholm, 2012
- [16] D. York and M. Kushler, *Exploring the Relationship Between Demand Response and Energy Efficiency: A Review of Experience and Discussion of Key Issues*, American Council for an Energy-Efficient Economy Report, 2005
- [17] A. M. Kosek, G. T. Costanzo, H. W. Bindner and O. Gehrke, *An Overview of Demand Side Management Control Schemes for Buildings in Smart Grids*, IEEE International Conference on Smart Energy Grid Engineering (SEGE'13), Portland, Oregon, 2013.
- [18] M. Ifland, N. Exner and D. Westermann, *Appliance of Direct and Indirect Demand Side Management*, IEEE Energytech, Cleveland, OH, 2011
- [19] O. Corradi, H. Ochsenfeld, H. Madsen and P. Pinson, *Controlling Electricity Consumption by Forecasting its Response to Varying Prices*, IEEE Transactions on Power Systems, Vol. 28, No. 1, Pages: 421 - 429, 2013
- [20] M. Juelsgaard, P. Andersen and R. Wisniewski, *Stability Concerns for Indirect Consumer Control in Smart Grids*, European Control Conference (ECC), Zurich, 2013
- [21] H. Farhangi, *The path of the smart grid*, IEEE Power Energy Magazine, Vol. 8, No. 1, Pages 1828, 2010.
- [22] S. You, *Developing Virtual Power Plant for Optimized Distributed Energy Resources Operation and Integration*, PhD Thesis, Technical University of Denmark, 2010
- [23] S. Kishore and L. Snyder, *Control Mechanisms for Residential Electricity Demand in Smart Grids*, 1st IEEE International Conference on Smart Grid Communications, Gaithersburg, 2010
- [24] B. Dupont, J. Tant and R. Belmans, *Automated Residential Demand Response Based on Dynamic Pricing*, 3rd IEEE PES Innovative Smart Grid Technologies Europe (ISGT Europe), Berlin, 2010

- 
- [25] A. H. Mohsenian-Rad, V. W. S. Wong, J. Jatskevich, R. Schober and A. Leon-Garcia, *Autonomous Demand-Side Management Based on Game-Theoretic Energy Consumption Scheduling for the Future Smart Grid*, IEEE Transactions on Smart Grid, Vol. 1, No. 3, Pages: 320 - 331, 2010
  - [26] Z. Md. Fadlullah, Y. Nozaki, A. Takeuchi and N. Kato, *A Survey of Game Theoretic Approaches in Smart Grid*, International Conference on Wireless Communications and Signal Processing (WCSP), Nanjing, 2011
  - [27] C. O. Adika and L. Wang, *Non-Cooperative Decentralized Charging of Homogeneous Households Batteries in a Smart Grid*, IEEE Transactions on Smart Grid, Vol. 5, No. 4, Pages: 1855 - 1863, 2014
  - [28] O. Erdinc, N. G. Paterakis, T. D. P. Mendes, A. G. Bakirtzis and J. P. S. Catalao, *Smart Household Operation Considering Bi-Directional EV and ESS Utilization by Real-Time Pricing-Based DR*, IEEE Transactions on Smart Grid, Vol. 6, No. 3, Pages: 1281 - 1291, 2015
  - [29] A. Joseph and M. Shahidehpour, *Battery Storage Systems in Electric Power Systems*, IEEE Power Engineering Society General Meeting, 2006
  - [30] A. Hajiah, M. Krarti, *Optimal control of building storage systems using both ice storage and thermal mass Part I: Simulation environment*, Energy Conversion and Management 64, Pages: 499508, 2012
  - [31] H. Hao, Y. Lin, A. S. Kowli, P. Barooah and S. Meyn, *Ancillary Service to the Grid Through Control of Fans in Commercial Building HVAC Systems*, IEEE Transactions on Smart Grid, Vol. 5, No. 4, Pages: 2066 - 2074, 2014
  - [32] M. Maasoumy, B. M. Sanandaji, A. Sangiovanni-Vincentelli and K. Poolla, *Model Predictive Control of Regulation Services from Commercial Buildings to the Smart Grid*, American Control Conference (ACC), Portland, Oregon, 2014
  - [33] M. A. A. Pedrasa, M. M. Oro, N. C. R. Reyes and J. R. I. Pedrasa, *Demonstration of Direct Load Control of Air Conditioners in High Density Residential Buildings*, IEEE Innovative Smart Grid Technologies (ISGT Asia), Kuala Lumpur, 2014
  - [34] J. Kondoh, N. Lu and D. J. Hammerstrom, *An Evaluation of the Water Heater Load Potential for Providing Regulation Service*, IEEE Transactions on Power Systems, Vol. 26, No. 3, Pages: 1309 - 1316, 2010
  - [35] S. Pfaffen, K. Werlen and S. Koch, *Evaluation of Business Models for the Economic Exploitation of Flexible Thermal Loads*, 39th Annual Conference of the IEEE Industrial Electronics Society, IECON, Vienna, 2013
  - [36] D. I. Mendoza-Serrano and D. J. Chmielewski, *Demand Response for Chemical Manufacturing using Economic MPC*, American Control Conference (ACC) Washington, DC, 2013
  - [37] A. Gholian, H. Mohsenian-Rad, Y. Hua and J. Qin, *Optimal Industrial Load Control in Smart Grid: A Case Study for Oil Refineries*, 2013 IEEE Power and Energy Society General Meeting (PES), Vancouver, BC, 2013
-

- [38] Y. M. Ding, S. H. Hong and X. H. Li, *A Demand Response Energy Management Scheme for Industrial Facilities in Smart Grid*, IEEE Transactions on Industrial Informatics, Vol. 10, No. 4, Pages: 2257 - 2269, 2014
- [39] T. G. Hovgaard, L. F. S. Larsen and J. B. Jorgensen, *Flexible and Cost Efficient Power Consumption using Economic MPC A Supermarket Refrigeration Benchmark*, 50th IEEE Conference on Decision and Control and European Control Conference (CDC-ECC), Orlando, FL, 2011
- [40] S. Ehsan Shafiei, J. Stoustrup and H. Rasmussen, *Model predictive control for flexible power consumption of large-scale refrigeration systems*, American Control Conference (ACC), Portland, 2014
- [41] M. K. Petersen, K. Edlund, L. H. Hansen, J. Bendtsen and J. Stoustrup, *A Taxonomy for Modeling Flexibility and a Computationally Efficient Algorithm for Dispatch in Smart Grids*, American Control Conference (ACC) Washington, DC, 2013
- [42] S. You, C. Traeholt, and B. Poulsen, *Generic virtual power plants: Management of distributed energy resources under liberalized electricity market*, 8th International Conference on Advances in Power System Control, Operation and Management, Hong Kong, 2009.
- [43] L. Gkatzikis, I. Koutsopoulos and T. Salonidis, *The Role of Aggregators in Smart Grid Demand Response Markets*, IEEE Journal on Selected Areas in Communications, Vol. 37, No. 7, Pages 1247-1257, 2013
- [44] M. Parvania, M. Fotuhi-Firuzabad and M. Shahidehpour, *Optimal Demand Response Aggregation in Wholesale Electricity Markets*, IEEE Transactions on Smart Grid, Vol. 4, No. 4, Pages: 1957-1965, 2013
- [45] A. Koto, S. Lu, T. Valavaara, A. Rautiainen and S. Repo, *Aggregation of Small-Scale Active Resources for Smart Grid Management*, 2nd IEEE PES International Conference and Exhibition on Innovative Smart Grid Technologies (ISGT Europe), Manchester, 2011
- [46] S. Han and K. Sezaki, *Development of an Optimal Vehicle-to-Grid Aggregator for Frequency Regulation*, IEEE Transactions on Smart Grid, Vol. 1, No. 1, Pages 65-72, 2010
- [47] B. G. Kim, S. Ren, M. v. d. Schaar and J. W. Lee, *Bidirectional Energy Trading and Residential Load Scheduling with Electric Vehicles in the Smart Grid*, IEEE Journal on Selected Areas in Communications, Vol. 31, No. 7, Pages: 1219-1234, 2013
- [48] G. D. Bella, L. Giarre, M. Ippolito, A. Jean-Marie, G. Neglia and I. Tinnirello, *Modeling Energy Demand Aggregators for Residential Consumers*, 52nd IEEE Conference on Decision and Control, Florence, 2013
- [49] A. Mondal and S. Misra, *Dynamic Data Aggregator Unit Selection in Smart Grid: An Evolutionary Game Theoretic Approach*, 2014 Annual IEEE India Conference (INDICON)

- 
- [50] M. A. Lopez, J. A. Aguado, S. d. I. Torre and M. Figueroa, *Optimization-Based Market-Clearing Procedure with EVs Aggregator Participation*, 4th IEEE PES Innovative Smart Grid Technologies Europe (ISGT Europe), Copenhagen, 2013
- [51] P. O. Andreasen and L. Aagaard, *Smart Grid in Denmark*, Energinet.dk and Dansk Energi Report, 2010.
- [52] *Ancillary Services to be Delivered in Denmark: Tender Conditions*, Energinet.dk Report, 2011
- [53] P. Nyeng, K. O. H. Pedersen and J. Ostergaard, *Ancillary Services from Distributed Energy Resources Perspectives for the Danish Power System*, IYCE Conference, 2007
- [54] P. Sorknaes, H. Maeng, T. Weiss and A. N. Andersen, *Overview of the Danish Power System and RES Integration*, Intelligent Energy Europe Programme of the European Union Report, 2013
- [55] [www.ipower-net.dk](http://www.ipower-net.dk)
- [56] C. Bang, F. Fock and M. Togeby, *The Existing Nordic Regulating Power Market*, FlexPower Project Report, 2012
- [57] A. Bemporad and M. Morari, *Control of Systems Integrating Logic, Dynamics, and Constraints*, Automatica, Vol. 35, Pages: 407-427, 1999
- [58] P. Niemczyk, *Model-based Fuel Flow Control for Fossil-fired Power Plants*, PhD Thesis, Aalborg University, Denmark, 2011
- [59] J. M. Maciejowski, *Predictive Control with Constraints*, Pearson Education Limited, Prentice Hall, 2002
- [60] A. Bemporad, *Model Predictive Control: Basic Concepts*, Lecture Notes, Controllo di Processo e dei Sistemi di Produzione, 2009.
- [61] L. F. S. Larsen, *Model Based Control of Refrigeration Systems*, PhD Thesis, Aalborg University, Denmark, 2005
- [62] M. J. Skovrup, *Thermodynamic and Thermophysical Properties of Refrigerants - Software Package in Borland Delphi*, Department of Energy Engineering, Technical University of Denmark, 2000.
- [63] T. B. Jekel, *Modeling of Ice-storage Systems*, MSc Thesis, University of Wisconsin, Madison, 1991
- [64] J. M. Bailey, *Modelling Phase Change Material Thermal Storage Systems*, Msc Thesis, McMaster University, Canada, 2010
- [65] D.R. Wulfinhoff, *Measure 2.11.1 Install Cooling Thermal Storage*, Technical Report, Energy Efficiency Manual-Chapter 2 Chiller Plant, 1999.
- [66] S. E. Shafiei, H. Rasmussen and J. Stoustrup, *Modeling Supermarket Refrigeration Systems for Demand-Side Management*, Energies, 6(2):900-920, 2013

## REFERENCES

---

- [67] S. E. Shafiei, J. Stoustrup and H. Rasmussen, *Model Predictive Control for Flexible Power Consumption of Large-scale Refrigeration Systems*, American Control Conference, Portland, Oregon, 2014.
- [68] M.J. Willis, *Proportional-Integral-Derivative Control*, Dept. of Chemical and Process Engineering, University of Newcastle, 1999
- [69] Y. Ding, L.H. Hansen, P.D. Cajar, P. Brath, H.W. Bindner, C. Zhang and N.C. Nordentoft, *Development of a DSO-Market on Flexibility Services*, [www.iPower-net.dk/publications](http://www.iPower-net.dk/publications), 18-03-2013.
- [70] [www.powerlab.dk/facilities/syslab.aspx](http://www.powerlab.dk/facilities/syslab.aspx)